การสังเคราะห์แกมมาอะลูมินาที่มีรูพรุนจากแม่แบบเรโซซินอล-ฟอร์มัลดีไฮด์เจล

ผ่านกระบวนการอบแห้งแบบพ่นฝอย

นางสาวสุขฤทัย ทรัพย์นิวัตต์

วิทยานิพนธ์นี้เป็นส่วนหนึ่งของการศึกษาตามหลักสูตรปริญญาวิศวกรรมศาสตรมหาบัณฑิต

สาขาวิชาวิศวกรรมเคมี ภาควิชาวิศวกรรมเคมี

คณะวิศวกรรมศาสตร์ จุฬาลงกรณ์มหาวิทยาลัย

ปีการศึกษา 2554

SYNTHESIS OF POROUS γ-ALUMINA WITH RESORCINOL-
FORMALDEHYDE GEL TEMPLATE VIA SPRAY DRYING

Miss Sukruthai Sapniwat

A Thesis Submitted in Partial Fulfillment of the Requirements

for the Degree of Master of Engineering Program in Chemical Engineering

Department of Chemical Engineering

Faculty of Engineering

Chulalongkorn University

Academic Year 2011

Thesis Title	SYNTHESIS OF POROUS γ-ALUMINA WITH RESORCINOL-FORMALDEHYDE GEL TEMPLATE VIA SPRAY DRYING
By	Miss Sukruthai Sapniwat
Field of Study	Chemical Engineering
Thesis Advisor	Assistant Professor Apinan Soottitantawat, D.Eng.
Thesis Co-advisor	Assistant Professor Varong Pavarajarn, Ph.D.
	Wiyong Kangwansupamonkon, Ph.D.

Accepted by the Faculty of Engineering, Chulalongkorn University in Partial Fulfillment of the Requirements for the Master's Degree

………………………………… Dean of the Faculty of Engineering
(Associate Professor Boonsom Lerdhirunwong, Dr.Ing.)

THESIS COMMITTEE

………………………………… Chairman
(Associate Professor Tawatchai Charinpanitkul, D.Eng.)

………………………………….. Thesis Advisor
(Assistant Professor Apinan Soottitantawat, D.Eng.)

………………………………….. Thesis Co-advisor
(Assistant Professor Varong Pavarajarn, Ph.D.)

………………………………….. Thesis Co-advisor
(Wiyong Kangwansupamonkon, Ph.D.)

………………………………… Examiner
(Associate Professor Prasert Pavasant, Ph.D.)

………………………………… External Examiner
(Apiluck Eiad-ua, D.Eng.)

สุขฤทัย ทรัพย์นิวัตต์: การสังเคราะห์แกมมาอะลูมินาที่มีรูพรุนจากแม่แบบเรโซซินอล-ฟอร์มัลดีไฮด์เจล ผ่านกระบวนการอบแห้งแบบพ่นฝอย (SYNTHESIS OF POROUS γ-ALUMINA WITH RESORCINOL-FORMALDEHYDE GEL TEMPLATE VIA SPRAY DRYING) อ.ที่ปรึกษาวิทยานิพนธ์หลัก: ผศ.ดร. อภินันท์ สุทธิธารธวัช, อ.ที่ปรึกษาวิทยานิพนธ์ร่วม: ผศ.ดร. วรงค์ ปวราจารย์, ดร. วิยงค์ กังวานศุภมงคล, 90 หน้า.

อะลูมินาที่มีรูพรุนถูกสังเคราะห์ขึ้นโดยอะลูมินิเนียมโซลและใช้คาร์บอนสังเคราะห์เป็นแม่แบบสำหรับ ควบคุมคุณสมบัติรูพรุนของผลิตภัณฑ์ สารละลายเรโซซินอล-ฟอร์มัลดีไฮด์เจล (อาร์เอฟเจล) ถูกเตรียมขึ้นด้วย วิธีโซล-เจล เพื่อใช้เป็นแม่แบบสังเคราะห์ช่วยเสริมความเป็นรูพรุนของอะลูมินาให้สูงขึ้น สภาวะในการเตรียม สารถูกศึกษาจากระยะเวลาการบ่มอะลูมิเนียมโซลและอาร์เอฟเจล นอกจากนี้ยังศึกษาสัดส่วนโมลของอะลูมิเนียม อะซิติลอะซิโตเนตต่อฟอร์มัลดีไฮด์และเรโซซินอล อะลูมิเนียมโซลถูกใส่ลงในสารละลายอาร์เอฟและใช้ เอธานอลเป็นตัวทำละลายของเจลผสม เจลผสมจะถูกทำให้แห้งผ่านเครื่องอบแห้งแบบพ่นฝอยเปรียบเทียบกับ การอบแห้งแบบธรรมดาเพื่อให้ได้ผงประกอบอะลูมิเนียม/อาร์เอฟเจล ผงประกอบอะลูมิเนียม/อาร์เอฟเจลจะถูก ทำไปเผาที่อุณหภูมิ 800 องศาเซลเซียส เพื่อให้ได้แกมมาอะลูมินา ผลการทดลองพบว่าอะลูมินาที่ผ่านการอบแห้ง แบบธรรมดามีพื้นที่ผิวสูงสุด 327 ตารางเมตรต่อกรัม ในขณะที่อะลูมินาที่ผ่านการอบแห้งแบบพ่นฝอยมีพื้นที่ผิว สูงสุด 209 ตารางเมตรต่อกรัม แม้ว่าอนุภาคอะลูมินาจากการอบแห้งแบบพ่นฝอยจะมีพื้นที่ผิวน้อยกว่าอนุภาค จากการอบแห้งแบบธรรมดา แต่ผลิตภัณฑ์จากการอบแห้งแบบพ่นฝอยมีรูพรุนขนาดใกล้เคียงกัน

ภาควิชา.........วิศวกรรมเคมี......... ลายมือชื่อนิสิต...

สาขาวิชา.........วิศวกรรมเคมี......... ลายมือชื่อ อ.ที่ปรึกษาวิทยานิพนธ์หลัก...

ปีการศึกษา.............2554............ ลายมือชื่อ อ.ที่ปรึกษาวิทยานิพนธ์ร่วม...

ลายมือชื่อ อ.ที่ปรึกษาวิทยานิพนธ์ร่วม...

5370505821: MAJOR CHEMICAL ENGINEERING
KEYWORDS: POROUS ALUMINA/ RESORCINOL FORMALDEHYDE GEL/ MESOPOROUS MATERIALS/ SPRAY DRYING

SUKRUTHAI SAPNIWAT: SYNTHESIS OF POROUS γ-ALUMINA WITH RESORCINOL-FORMALDEHYDE GEL TEMPLATE VIA SPRAY DRYING. ADVISOR: ASST. PROF. APINAN SOOTTITANTAWAT, D.Eng., CO-ADVISOR: ASST. PROF. VARONG PAVARAJARN, Ph.D., WIYONG KANGWANSUPAMONKON, Ph.D., 90 pp.

The synthesis of porous alumina powder by aluminium preformed sol and the controlling textural properties of alumina by using synthesized carbon template via spray drying process have been studied. Firstly, aluminium acetylacetonate (A) has been dissolved with formaldehyde solution (F) to form aluminium preformed sol. Resorcinol-formaldehyde solution has been also prepared by sol-gel processing as assisted-template to obtain high porosity alumina. The conditions to prepare the preformed aluminium sol and RF-gel were studied in the different aging time. In addition, the sol-gel reaction was studied with the different aluminium acetylacetonate to formaldehyde (A/F) molar ratio and resorcinol (A/R) molar ratio. The preformed aluminium sol was added into RF solution and use ethanol as solvent of the mixed gel. To obtain the powder of aluminium/RF-gel composite, the mixed gel was dried via spray dryer. The powder was further calcined to obtain porous γ-alumina at 800°C. The results show the maximum surface area of conventional dried alumina is 327 m^2/g while the maximum surface area of spray dried alumina is 209 m^2/g. Although the alumina particle from spray dryer is lower surface area than the particle from conventional drying, the spray dried products has uniform mesopore size.

Department: ....Chemical Engineering.............   Student's Signature …..……..………………

Field of Study: ....Chemical Engineering.....   Advisor's Signature ………….……………….

Academic Year: ………….2011……………   Co-advisor's Signature……………….…….....

Co-advisor's Signature…………………..…...

ACKNOWLEDGEMENTS

CONTENTS

LIST OF TABLES

LIST OF FIGURES

Figure   **page**

Figure page

CHAPTER I

INTRODUCTION

1.1 MOTIVATION

Porous ceramics are most widely used as catalyst supports because of their various excellent properties such as large surface area and high resistance to chemical agents and heat [1]. There are many applications of alumina such as catalyst, catalyst support, adsorbents and insulator etc. Specially, alumina with gamma (γ) metastable phase is always used as catalytic supports in automotive and petrochemical industries. Many works always produce alumina with high surface area to improve catalyst loading performance.

There are many methods to synthesis alumina such as precipitation, sol-gel processing and thermal decomposition method etc. The difference of three aforementioned methods is using the different substrate: thermal decomposition uses downstream materials like boehmite with heating to obtain alumina while the others use aluminium precursor to obtain the intermediate first [2]. In industrial field, precipitation is mostly use for synthesis alumina because of its ease to produce alumina and less time consuming [3]. Precipitation is the formation of a solid in a solution. When the reaction occurs in a liquid, the solid formed is called the precipitate. This process usually requires precursor and reducing agent. The limit of precipitation depends on rapid quenching or ion implantation, and the temperature is high enough that diffusion can lead to segregation into precipitates. To synthesis alumina by precipitation, many reviewed works always use aluminium nitrate as precursor as followed: the achievement work of Liu et al. (2008) described synthesis of mesoporous alumina, with highest surface area 604 m^2/g, by using this method with surfactant assist [4]. Parida et al. (2009) studied the effect of different precipitating agent with using aluminium nitrate as precursor. Although the work can synthesize γ–alumina with uniform nanoparticles, the surface area of alumina is quietly low about 140-190 m^2/g [5]. Zhang et al. (2002) produced alumina with surface area up to 346 m^2/g. Unfortunately, there was warning in the washing procedure that eliminating total of ammonium nitrate because explosion is occurred between calcination [6]. Although, precipitation occur alumina with high surface area, there is the mainly disadvantage of alumina synthesis by this method. When synthesized alumina with precipitation and using aluminium oxide-hydroxide precursor, the broad pore size distribution

and the surface area lower than 350 m^2/g was occurred [7]. In addition, this method has more complicated steps when washing than sol-gel processing has [3]. In this work, the sol-gel processing will be considered.

According to sol-gel processing, this process involves the hydrolysis and condensation reactions of alkoxide or salts dissolved in organic solvents. In synthesis of alumina, there are three steps these are provided: hydrolysis of aluminium alkoxide, formation of gel and finally calcination of alumina [8]. The sol-gel processing often uses aluminium nitrate nonahydrate as precursor because of low prices. However, aluminium nitrate is reactive substance which highly exothermic when react in alkali containing process. Recently, Sharbatdaran et al. (2010) synthesized alumina with a novel precursor, aluminium 2-methoxyethoxyethoxide. Unfortunately, this aluminium alkoxide produced alumina with lower surface area 78 m^2/g comparing with aluminium 2-butoxide which is a raw material for aluminium 2-methoxyethoxyethoxide synthesis [9].

There are many parameters controlling morphology of pore such as reactant concentration, aging time in sol-gel processing, pH value. The mostly used way to raise the surface area of alumina is using assisted template especially surfactant. The word of surfactant is standing for surface-active agent. Surfactant, is usually organic compound, consists of two parts: hydrophobic and hydrophilic groups. Many surfactants can also assemble in the bulk solution into aggregates as micelle. In the present, the surfactants are classified into five primary groups; anionic, cationic, non-ionic, zwitterionic and polymeric surfactant. Surfactants are usually used as template including P123 and Brij30 (both are non-ionic surfactant), SDS and AOT (both are anionic surfactant) and CTAB (cationic surfactant). Non-ionic surfactants triblock copolymer like $EO_{20}PO_{70}EO_{20}$ (P123) could synthesize mesoporous alumina with high surface area 604 m^2/g with using in precipitation reaction of aluminium nitrate [4]. Nevertheless, surfactant is only activated with appropriated condition and can not control textural properties of the main product. In recent decade, the invented template e.g. carbon gel is considered to produce porous materials. The strength of using invented template is flexible. The main materials also are high porosity materials by condition controllable template. Resorcinol-formaldehyde is one of organic and carbon gel which has high porosity because of their three dimensional crosslink [10]. There are many criterions to control morphology of resorcinol-formaldehyde gel such as substrate concentration, pH value, quantities of catalyst, aging condition and type of drying. Ritter et al. (2003) summarized that raw material concentration affects both particle and pore size and surface area. Moreover, they described other parameter for instance gelation condition effects on crosslink of the gel

[10]. In this work, there is a motivation to present an invented template like resorcinol-formaldehyde gel. The assumption is to synthesis porous alumina with studying the reactants concentration.

According Prathap et al. (2011) synthesized cerium oxide using surfactant-carbon aero gel as template. They used phloroglucinol-formaldehyde gel with triblock copolymer assist as template. As the results, the surface area of cerium oxide is higher than commercial's [11].

The important step of above methods is drying. The goal of drying is removal the solvent from the bulk gel or solid. Conventional drying is always used in the processing. Despite its simple, conventional drying is not easy to reach industrial scale because it is batch operating. Spray drying processing industrial continuous was used in this work. Moreover, the spherical porous alumina can be made with the surfactants as the template. According to two-feed-nozzle spray drying, the viscosities of samples affects on particle diameters and compatibility of spraying [12].

The significant factor of spray drying is viscosity. Generally, viscosity of RF-gel has an impact on aging time which directly affect on textural properties of particle. The high surface area of particle occurs when the high viscosity is reached. However, high viscosity solution is not suitable for spray drying process. Using ethanol as solvent instead of water in the sol-gel process of RF-gel can highly extend the gelation time of the RF-gel [13].

In summary, this work, a new non-reactive precursor, aluminium acetylacetonate, was used to produce porous alumina by preparing preformed sol. Assisted-template likes resorcinol-formaldehyde gel which proposed by Pekala et al. (1989) occurred high surface area alumina from their high porosity [14]. Both of the aluminium sol and resorcinol-formaldehyde gel were studied investigating particle-forming mechanism by Fourier Transform Infrared Spectroscopy (FTIR) investigating with different aging time. Moreover, variable aluminium alkoxide to formaldehyde (A/F) molar ratio and aluminium alkoxide to resorcinol (A/R) molar ratio were studied. The mixed gel was dried by comparing between conventional dryer at 110°C and spray dryer with inlet temperature at 220°C which has been operated in Bertrand et al. works' (2003) [15]. The dried gel was calcined to obtain porous alumina at 800°C. Finally, the particles were characterized morphology of the particles by X-ray diffraction (XRD), scanning electron microscopy (SEM) and surface area and porosity measurement via nitrogen adsorption-desorption analyzer with Brunauer-Emmett-Teller (BET) and Barrett, Joyner and Halenda (BJH) equation.

1.2 OBJECTIVE OF THE RESEARCH

The aim of this thesis is to synthesize porous γ-alumina with studying varied quantity of raw materials and to compare results between using conventional drying and spray drying that affect the textural properties of products; alumina and its porosity.

CHAPTER II

BACKGROUND AND LITERATURE REVIEWS

The theory relating to synthesis and properties of alumina and principle of spray drying will be explained in this chapter.

2.1 ALUMINA

Aluminum oxide, commonly referred to as alumina, normally appears as white crystalline powder in various mesh sizes. Aluminium oxide appear in natural form as corundum (α-Al$_2$O$_3$). Alumina is one of the most important ceramics because of their high specific surface area, excellent physical strength, resistance chemical agents at elevated temperature and high hardness. There are many fields of alumina application such as catalyst and catalyst support, adsorbent and insulator [16-19].

There are many metastable phases of alumina including γ-, η-, δ-, θ-, κ-and χ-alumina. The phase will be changed into the other phase with many factors such as synthesized procedure, raw material and calcination. The important factor is calcination temperature which can be illustrated from boehmite as raw material in Figure 2.1. At 1000°C, the stable phase, α-alumina can be obtained [20]. However, α-alumina has lower surface area than other metastable phase has because calcination in the high temperature makes pores in the alumina collapse.
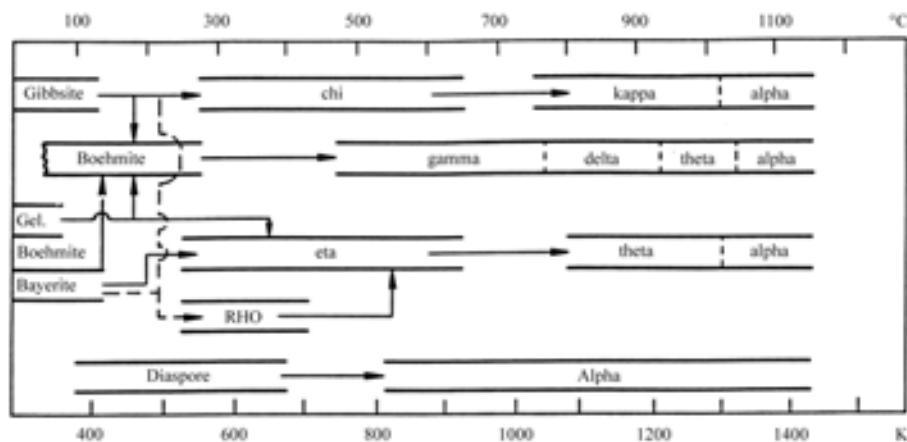
Figure 2.1 Phase transformation of alumina [21].

For γ-alumina, this is one kind of extremely important materials. It is mostly used as a catalyst and catalyst substrate in automotive and petroleum industries, structural composites for abrasive and thermal wear coatings [22].Although it is hard to obtain single γ-alumina phase, Wang et al.(2008) have been produced γ-alumina which directly transformed stable phase by sol-gel precipitation in ethanol [23, 24]. As the results, range of γ metastable phase in phase transformation is wider than other work.

2.2 SYNTHESIS OF ALUMINA PARTICLES

There are many methods to produce alumina from aluminium precursor. This section summarized methods as follow:

2.2.1 PRECIPITATION

Precipitation is the formation of a solid in a solution. When the reaction occurs in a liquid, the solid formed is called the precipitate. Then, it causes settling or sedimentation. The solid (insoluble) falls down due to ambient forces like gravity or centrifugation. In solids, precipitation occurs if the concentration of one solid is above the solubility limit in the host solid, due to e.g. rapid quenching or ion implantation, and the temperature is high enough that diffusion can lead to segregation into precipitates. Precipitation in solids is routinely used to synthesize clusters.

This process usually requires precursor and reducing agent. The limit of precipitation depends on rapid quenching or ion implantation, and the temperature is high enough that diffusion can lead to segregation into precipitates.

2.2.2 HYDROTHERMAL SYNTHESIS

Hydrothermal synthesis includes the various techniques of crystallizing substances from high-temperature aqueous solutions at high vapor pressures. Hydrothermal synthesis can be defined as a method of synthesis of single crystals that depends on the solubility of minerals in hot water under high pressure. The crystal growth is performed in an apparatus consisting of a steel pressure vessel called autoclave, in which a nutrient is supplied along with water. A gradient of temperature is maintained at the opposite ends of the growth chamber so that the hotter end dissolves the nutrient and the cooler end causes seeds to take

additional growth. Disadvantages of the method include the need of expensive autoclaves, and the impossibility of observing the crystal as it grows [25].

2.2.3 SOL-GEL PROCESSING

The sol-gel process involves the hydrolysis and condensation reactions of alkoxide or salts dissolved in water or organic solvents. When the extent of polymerization and cross-linking of polymeric molecules become extensive, the entire solution becomes rigid and a solid gel is formed.

The size and the degree of branching of the inorganic polymer, and the extent of cross-linking have strong influence on porosity of this gel, and later, the surface area, pore volume, pore size distribution, and thermal stability of the final oxide after calcination.

In general, if the gel contains polymeric chains with significant branching and cross-linking (as shown in Figure 2.2a), the gel is structurally quite rigid with large void regions and the resulting oxide after calcination has mostly macropores and mesopores. If the gel contains polymeric chains with little branching and cross-linking (as shown in Figure 2.2b), the gel has structurally weak with smaller void regions. The resulting oxide has mostly micropores and low surface area because of pores collapse [26].
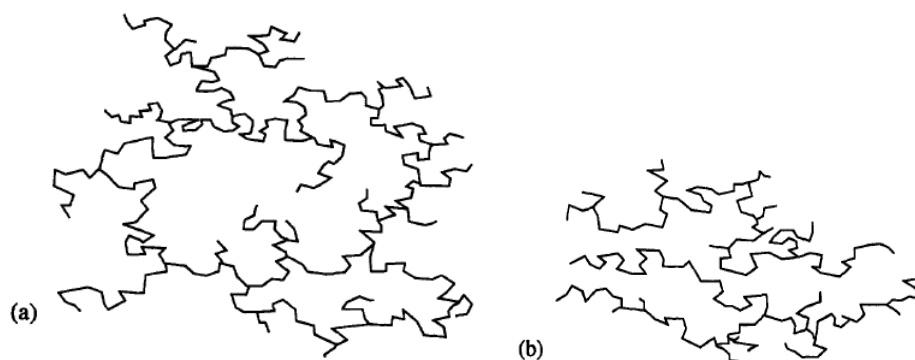
Figure 2.2 Differences between gels of polymers with (a) significant branching and cross-linking and (b) little branching and cross-linking [26].

Morphology of particles is functions of many parameters such as pH, temperature, nature and concentration of the metal ion precursors and water, the aging, drying technique, and calcination conditions [26].

For synthesis of alumina via sol-gel technique, the process which is proposed by Maria et al. (2004) used aluminium nitrate nonahydrate as precursor with hydrolysis control

performed by urea. After heating at 300°C, the gel transformed to γ –alumina without the other metastable phases and obtaining high surface area 429 m^2/g [23]. While Sharbatdaran et al. (2010) produced γ –alumina with lower surface area, 78 m^2/g, than previous work. This work investigates with aluminium 2-methoxyethoxyethoxide as novel precursor comparing with aluminium 2-butoxide [9]. Recently, Keshavarz et al. (2011) synthesized γ –alumina with many methods. One of the methods is sol-gel processing with aluminium isopropoxide and two different template sources, which are sucrose and hexadecyltrimethyl ammonium bromide (CTAB). As the results, the addition of both surfactants decreased the crystallite size and increased the surface area [2].

Some others work' applied sol-gel precipitation. Wang et al. (2008) obtained alumina beginning with precipitation of white gel aluminium hydroxide, thus filtration and washing were operated to get the gel [24].

2.3 USING RESORCINOL-FORMALDEHYDE GEL AS TEMPLATE TO INCREASE THE SURFACE AREA OF PARTICLES

According Pekala et al. works (1989), resorcinol-formaldehyde gel was synthesized which high surface area and porosity [14].

The first resorcinol-formaldehyde (RF) gel was produced via the sol-gel polycondensation of resorcinol (R) and formaldehyde (F) with sodium carbonate (C) as basic catalyst [14]. The intermediates formed during the reactions further react to form a cross-linked polymer network (a three-dimentional network) [27].

The two major reactions as shown in Figure 2.3 include the formation of hydroxymethyl (-CH$_2$OH) derivatives of resorcinol and the condensation of hydroxymethyl derivatives to form methylene (-CH$_2$-) and methylene ether (-CH$_2$OCH$_2$-) bridged compounds [10].

Addition reaction:
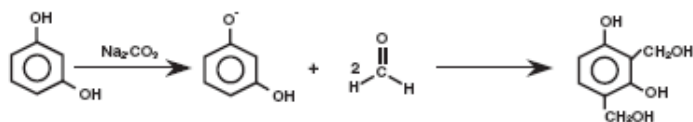
Condensation reaction:
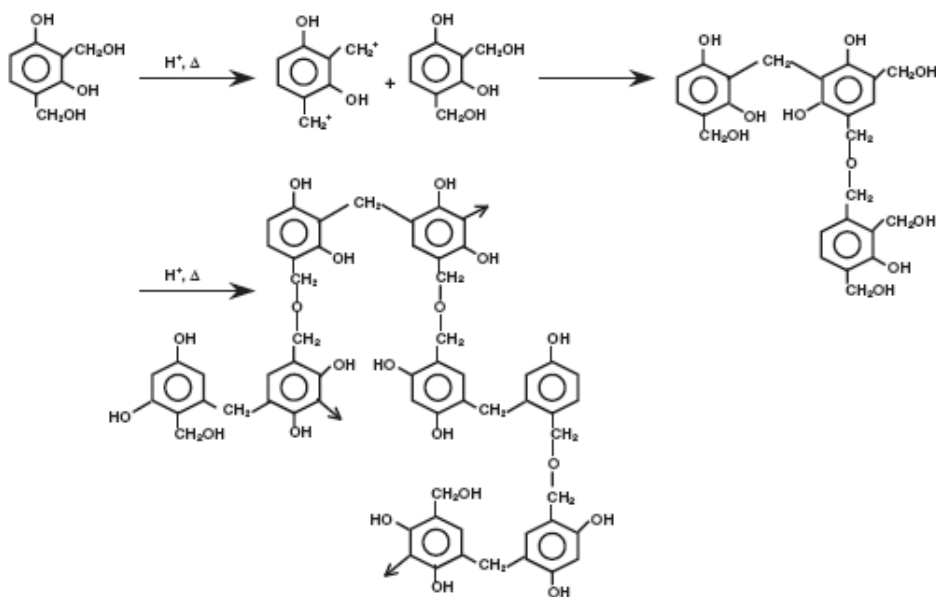
Figure 2.3 Molecular presentation of the polymerization mechanism of resorcinol with formaldehyde [28].

There are many variables effect on morphology of carbon particle synthesized by resorcinol-formaldehyde gel such as reactant concentration, pH value, kinds of catalyst, gelation and curing, solvent exchanging, drying method and calcination temperature [10].

According Prathap et al. (2011) synthesized cerium oxide using surfactant-carbon aero gel as template. They used phloroglucinol-formaldehyde gel with triblock copolymer assist as template. As the results, the surface area of cerium oxide is higher than commercial's [11].

2.4 PRINCIPLE OF DRYING

Drying is an essential operation in the industrial field such as chemical, food, polymer, mineral processing. There are many reasons for using drying process: need for easy-to-handle free-flowing solids, preservation and storage, reduction in cost of transportation,

achieving desired quality of product, etc. In many processes, improper drying may lead to irreversible damage to product quality and hence a non-salable product.

Drying is a complex operation involving transient transfer of heat by convection, conduction and radiation depending on heating source and mass transferring. Physical changes that may occur include: shrinkage, puffing, crystallization, glass transitions. In some cases, desirable or undesirable chemical or biochemical reactions may occur leading to changes in color, texture, odor or other properties of the solid product. In the manufacture of catalysts, for example, drying conditions can yield significant differences in the activity of the catalyst by changing the internal surface area.

Drying occurs by effecting vaporization of the liquid by supplying heat to the wet bulk solid. The heat diffuses into the solid primarily by conduction. The liquid must travel to the boundary of the material before it is transported away by the carrier gas. While moisture transportation within the solid may occur by any one or more of the following mechanisms of mass transfer:

- Liquid diffusion when the wet solid is at a temperature below the boiling point of the liquid
- Vapor diffusion when the liquid vaporizes within material
- Knudsen diffusion when drying takes place at very low temperatures and pressures, especially in freeze drying
- Surface diffusion
- Hydrostatic pressure differences, when internal vaporization rates exceed the rate of vapor transport through the solid to the surroundings

The criteria of drying are included humidity, temperature (dew point), moisture in materials. In Figure 2.4, step of drying can be described.
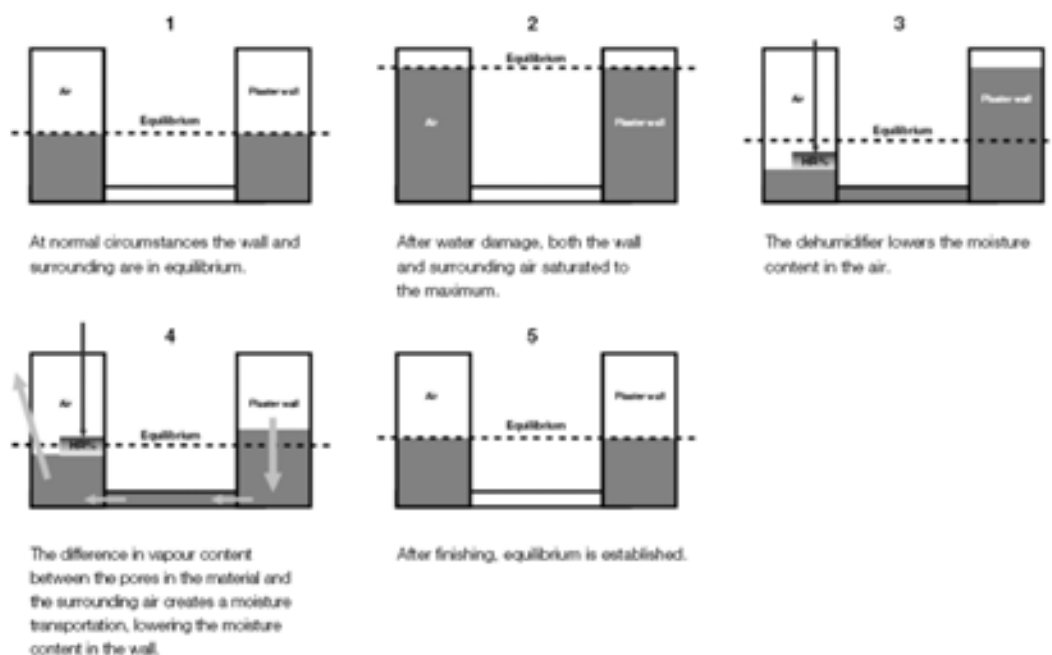
Figure 2.4 Principle for drying construction (Munters: Drying Fundamental).

In general, many types of drying are available such as freeze drying, vacuum drying, superheated steam drying and spray drying. This section describes only related type: spray drying.

2.5 SPRAY DRYING

Spray drying is a very fast method of drying due to the very large surface area created by the atomization of the liquid feed. As a consequence, high heat transfer coefficients are generated and the fast stabilization of the feed at moderate temperatures makes this method very attractive for heat sensitive materials. A spray dryer mixes a heated gas with an atomized liquid stream within a drying chamber to accomplish evaporation and produce a free flowing dry powder. Spray drying consists of the following phases [29]:

▪ Feed preparation: solution or suspension is fed into the atomizer
▪ Atomization (transforming the feed into droplets): Most critical step in the process. The degree of atomization controls the drying rate and therefore the dryer size. The most commonly used atomization techniques are:

Pressure nozzle atomization: Spray created by forcing the fluid through an orifice. This is an energy efficient method which also offers the narrowest particle size distribution.

Two-fluid nozzle atomization: Spray created by mixing the feed with a compressed gas. This is appropriate to make extremely fine particles.

Centrifugal atomization: Spray created by passing the feed through or across a rotating disk. Most resistant to wear and can generally be run for longer periods of time.

- For two fluid nozzle-spray drying in Figure 2.5, there are 2 steps of drying: the first called "droplet-air contact", atomized liquid is brought into contact with hot gas, resulting in the evaporation of 95% of the water contained in the droplets in a matter of a few seconds. Secondly, "droplet drying": a constant rate phase ensures moisture evaporates rapidly from the surface of the particle. This is followed by a falling rate period where the drying is controlled by diffusion of water to the surface of the particle.
- Separation: cyclones and bag filters are used for solid-gas separation. Wet scrubbers are often used to purify and cool the air so that it can be released to atmosphere or recirculated.

① Air inlet (optional with attached inlet filter)
② Electric heater
③ Concentric inlet of the hot air around the spray nozzle
④ Spray cylinder
⑤ Cyclone to separate particles from gas stream
⑥ Product collection vessel
⑦ Outlet filter
⑧ Aspirator to pump air through system
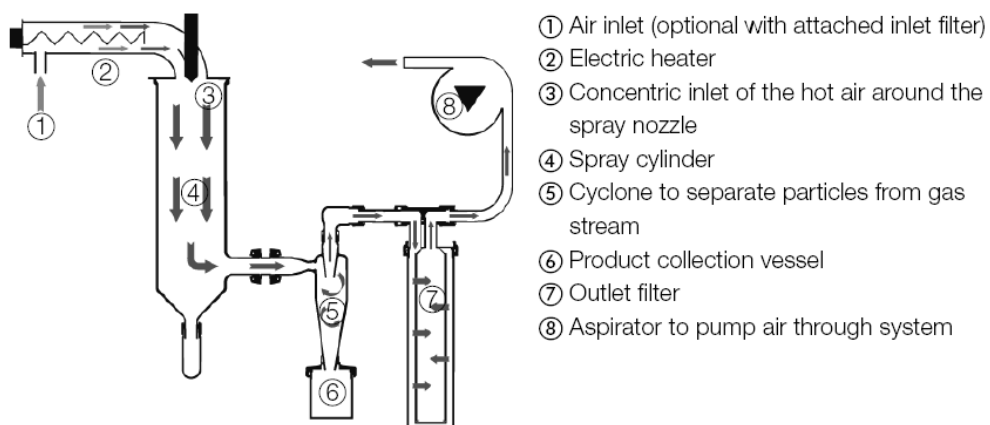
Figure 2.5 Functional principle of the drying air (From Büchi$^{©}$ manual).

There are many advantages obtaining from spray drying include designing to industrial scale, operation is continuous, using with heat sensitive products and spherical particles can be produced.

As spray drying application, Kimura et al. (2010) synthesize spherical alumina particle using aluminium chloride as precursor in preformed sol. Moreover, three different

surfactants including $EO_{106}PO_{70}EO_{106}$ (F127) 1,3,5-trimethylbenzene (TMB) and 1,3,5-triisopropylbenzene (TIPBz) was used with drying at low inlet temperature 110°C. As the results, highest surface area, 315 m^2/g was obtained by using 1,3,5-trimethylbenzene as surfactant [30]. Pitchumani et al. (2009) focused on outlet temperature of spray dryer to produced silica and silica-alumina catalyst with evaporation-induced self-assembly (EISA) [31].

2.6 N₂ ADSORPTION ISOTHERM
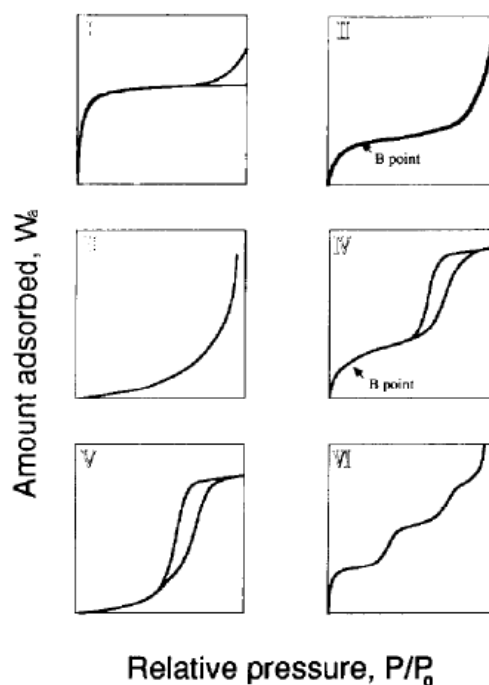
Figure 2.6   IUPAC classification of adsorption isotherms [32].

The IUPAC recommended the following six types of the adsorption isotherms as shown in Figure 2.6. The type I isotherm corresponds to the so-called Langmuir isotherm. In the case of physical adsorption, the type I isotherm represents presence of micropores where molecules are adsorbed by micropore filling which has been actively studied in adsorption science. The type II isotherm is the most familiar; the multilayer adsorption theory by Brunauer, Emmett, and Teller was originally developed for this type of adsorption. Hence, this isotherm is indicative of the multilayer adsorption process, suggesting the presence of nonporous or macroporous surfaces. Although the adsorption isotherm near $P/P_0= 1$ gives important information on macropores, such an analysis is not practical for accurate

measurement. This is because serious condensation on the apparatus walls begins near the saturated vapor pressure. Adsorption from solution using macromolecules has been applied to macropore analysis, but we still need more examinations. Consequently, only macropore analysis with mercury porosimetry is described in this review. The type III isotherm arises from nonporous or macroporous surfaces which interact very weakly with the adsorbent molecules. The type IV isotherm gives useful information on the mesopore structure through its hysteresis loop that is non-overlapping of the adsorption and desorption branches. In the mesopores, molecules form a liquid-like adsorbed phase having a meniscus of which curvature is associated with the Kelvin equation, providing the pore size distribution. The type V isotherm is closed to the type IV isotherm instead of very weak adsorbent-adsorbate interaction. The type VI isotherm is the stepped adsorption isotherm which comes from phase transition of the adsorbed molecular layer or adsorption on the different faces of crystalline solids. In the following description, mainly type I and IV isotherms will appear in relation to the micropore and mesopore analyses, respectively.
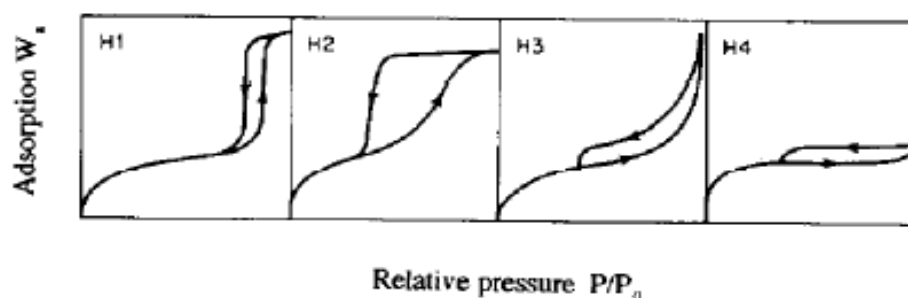
Figure 2.7   IUPAC classification of adsorption hysteresis [32].

The IUPAC classification uses the symbols H1, H2, H3 and H4. The type H1 is observed in the case of mesopores having geometries, for example, tubular capillary open at both ends, tubular capillaries with cross sections of two different main dimensions, and narrow-necked ink bottle. The H2 type is often observed in the adsorption isotherm of silica gel or cracking catalysts, although the pore geometry is not sufficiently fixed. Fundamentally the pore of this type may have the structure similar to the H1 type, in which there is some size distribution in the narrowed part [32].

2.7 SUMMARIZE THE LITERATURE SURVEYS OF SYNTHESIZED ALUMINA

The other works can be summarized are tables as follow:

Table 2.1 The literatures reviewed of synthesized alumina.

Authors	Year	Synthesized method	Product	Precursor	Assist	Surface area (m^2/g)	Remarks
Zhang et al.	2002	Precipitation	γ-alumina	Aluminium nitrate	Di- and triblock copolymer as surfactant	346	eliminating ammonium nitrate avoid explosion
Xu et al.	2006	Precipitation	γ-alumina	aluminium isopropoxide	-	350	broad pore size distribution
Liu et al.	2008	Precipitation	γ-alumina	Aluminium nitrate	P123 as surfactant	604	-
Parida et al.	2009	Precipitation	γ-alumina	Aluminium nitrate	-	190	-
Wang et al.	2008	Precipitation	γ-alumina	Aluminium chloride	-	313	-
Maria et al.	2004	Sol-gel processing	γ-alumina	aluminium nitrate	Urea hydrolysis	425	-
Sharbatdaran et al.	2010	Sol-gel processing	γ-alumina	aluminium 2-methoxyethoxyethoxide	-	78	-
Keshavarz et al.	2011	Sol-gel processing	γ-alumina	aluminium isopropoxide	CTAB as surfactant	375	-

Table 2.1 (continued).

Authors	Year	Synthesized method	Product	Precursor	Assist	Surface area (m^2/g)	Remarks
Kimura et al.	2010	Sol preforming	alumina	Aluminium chloride	F127, TMB and TIPBz as surfactant	315	Operating with spray drying
De Feria Jr et al.	2009	Ball milling	alumina	alumina	-	-	Obtained macropore alumina
Frey et al.	1984	Alumina slurry	alumina	α- and γ-alumina	-	-	Operating with spray drying [33]
Bertrand et al.	2003	Alumina slurry	α-alumina	α-alumina dispersed in ammonium polyacrylate	-	-	Operating with spray drying and T_{inlet} 220°C

Table 2.2 The literatures reviewed of other products.

Authors	Year	Synthesized method	Product	Precursor	Assist	Surface area (m^2/g)	Remarks
Ritter et al.	2003	Sol-gel processing	RF-gel	Resorcinol and formaldehyde	-	-	-
Qin et al.	2001	Sol-gel processing	RF-gel	Resorcinol and formaldehyde	-	-	Using Alcoholic sol-gel process
Bruinsma et al.	1997	-	Silica	tetraethoxysilane	cetyltrimethylammonium chloride as sufactant	1770	Operating with spray drying and obtained hollow sphere particles [34]
Lind et al.	2003	-	Silica	tetraethyl orthosilicate	hexadecyltrimethylammonium bromide as surfactant	1588	Operating with spray drying [35]
Pitchumani et al.	2009	-	Silica-alumina	boehmite	P123 as surfactant	284	Controlled outlet temperature at 110℃
Prathap et al.	2011	Sol-gel processing	Cerium oxide	Cerium nitrate hexahydrate	Phloroglucinol-formaldehyde solution as template and F127 as surfactant	140	The surface area is higher than area of commercial grade

CHAPTER III

EXPERIMENTAL

This chapter describes the experimental procedures to obtain alumina particles. It is divided into two parts: materials information, experimental procedures.

3.1 MATERIALS
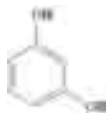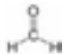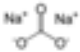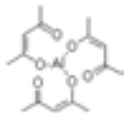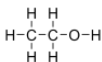
Aluminium acetylacetonate and resorcinol with purity 95% and 99% respectively were purchased from Sigma. Formaldehyde solution with 36.5-38.0 percent by weight and Sodium carbonate with purity 99% were purchased Ajax Fine Chemical. Ethanol absolute 99.9% was purchased VWR International S.A.S.

List of the chemicals employed in this work their structures are illustrated in Table 3.1 and Table 3.2, respectively.

Table 3.1 List of chemical agents used in the research.

Chemical agents	Using for
Resorcinol $(C_6H_4(OH)_2)$	Synthesis of Resorcinol-Formaldehyde solution
Formaldehyde (HCOH)	Synthesis of Resorcinol-Formaldehyde solution and Aluminium Formaldehyde sol (AF sol)
Sodium carbonate (Na_2CO_3)	Synthesis of Resorcinol-Formaldehyde solution
Deionized water (H_2O)	Synthesis of Resorcinol-Formaldehyde solution
Aluminum acetylacetonate $(C_{15}H_{21}AlO_6)$	Synthesis of Alumina / Resorcinol-Formaldehyde (RF)gel
Ethanol Absolute (C_2H_5OH)	Synthesis of Alumina / Resorcinol-Formaldehyde (RF)gel

Table 3.2 Chemical structure of these work reactants.

Chemical name	Designation	Chemical structure
Resorcinol	R	
Formaldehyde	F	
Sodium carbonate	C	
Aluminum acetylacetonate	A	
Ethanol	E	

3.2 EXPERIMENTAL PROCEDURES

3.2.1 PREPARATION OF ALUMINIUM FORMALDEHYDE PREFORMED SOL (AF SOL)

Aluminium acetylacetonate (A) was dissolved by Formaldehyde (F) solution at 60°C. The ratio of Aluminium acetylacetonate to Formaldehyde (A/F) was changed from 0.01 to 0.13. The sol was aged at room temperature with investigating aging time from 0 to 72 hours.

3.2.2 PREPARATION OF RESORCINOL-FORMALDEHYDE GEL (RF-GEL)

According method proposed by Pekala et al., Resorcinol (R) was dissolved by deionization water (W) while Sodium Carbonate (C) which used as catalyst was dissolved with concentration of 0.1 g in 10 ml water. After stirred the solution about 10 minutes, sodium carbonate solution was added into the solution and stirred 15 minutes. Finally, formaldehyde solution was added into the solution. These above steps was run at room temperature with fixed molar ratio of resorcinol to water (R/W), resorcinol to catalyst and resorcinol to formaldehyde were 0.15, 86.67 and 0.5 respectively. The difference of aging time was studied from 0 to 21 hours.

3.2.3 PREPARATION OF ALUMINA PARTICLES

The aged resorcinol-formaldehyde gel was added into the aged preformed sol with stirring 10 minutes with investigating varied molar ratio of aluminium precursor to resorcinol between 0.05 and 6.73. After that, ethanol was added into the mixed solution with molar ratio of ethanol to resorcinol (E/R) is 5.67, 28.34. The sample was dried via conventional dry at 110°C overnight, so this sample was called "bulk sample". While "spray dried sample" was dried via spray dried: Büchi© B290 with fixed feed flow rate and inlet temperature.

The both of samples were calcined at 800°C to remove carbon template obtained from resorcinol-formaldehyde gel and to obtain porous gamma alumina. The calcination held for 4 hours with heating rate 5°C/min.

3.2.4 CHARACTERIZATION

3.2.4.1   FOURIER TRANSFORM INFRARED SPECTROSCOPY (FTIR)

Functional groups of the aged gels were identified by Nicolet 6700, Thermo Scientific Fourier transform infrared (FTIR) spectrometer at Center of Excellence in Particle and Technology Engineering laboratory, Chulalongkorn University. Infrared spectra were recorded between wavenumber of 400 and 4000 cm^{-1}. The number of scans is 200 and resolution is 2. The results show in absorbance bands between wavenumber of 400 and 2000 cm^{-1} with automatic baseline collect and normalize absorbance (y-axis) scale.

3.2.4.2   X-RAY DIFFRACTION (XRD)

The crystalline phases of Al_2O_3 were identified by using a Bruker D8 Advance equipped with a CuKα radiation source (λ = 0.15406 nm) and operated at 40 kV and 40 mA at National Nanotechnology Center (NANOTEC). The measurements were carried out in the *2θ* range of 20-80 degree at the scan step of 0.04 degree. The crystallite size calculated from the half-height width of the diffraction peak of XRD pattern using Scherrer's equation[36].

$$D = \frac{0.9\lambda}{\beta\cos\theta} \qquad (1)$$

Where *D* is crystal size, λ is wavelength of X-ray, β is full width at half maximum, θ is diffraction angle.

3.2.4.3 SCANNING ELECTRON MICROSCOPY (SEM)

Morphology of the obtained products was studied by using a scanning electron microscope (JSM-6400, JEOL Co., Ltd.) and size of the products was then measured from the micrographs, using image processing software (JEOL Semafore 5.0) at the Scientific and Technological Research Equipment Center (STREC), Chulalongkorn University.

3.2.4.4 NITROGEN ADSORPTION-DESORPTION ANALYSIS

The specific surface area of products was determined via nitrogen adsorption/desorption analysis using the Brunauer-Emmett-Teller (BET) model with pore size distribution analysis using Barrett Joyner and Halenda (BJH) method, by Belsorp mini II BEL, Japan at Center of Excellence in Particle and Technology Engineering laboratory, Chulalongkorn University.

3.2.4.5 APPARENT VISCOSITY

Viscosity of the mixed gel was measured using a BROOKFIELD Programmable DV II+ viscometer at Center of Excellence in Particle and Technology Engineering laboratory, Chulalongkorn University.

3.2.4.6 THERMAL DECOMPOSITION

Thermal decomposition of the particles was studied using METTLER TOLEDO thermal gravimetric analyzer at Center of Excellence in Particle and Technology Engineering laboratory, Chulalongkorn University. The operating condition is heating rate of 10°C/min from room temperature to 800°C in oxygen gas.

The synthesized products of this work can be summarized in the table as shown below:

Table 3.3 List of samples was synthesized in this work.

Section	A/R	A/F	E/R	Aging time of RF-gel (h)	Aging time of AF sol (h)	Drying process
1	0.05	0.10	0	0	72	Conventional drying
	0.05	0.10	0	7	72	Conventional drying
	0.05	0.10	0	14	72	Conventional drying
	0.05	0.10	0	21	72	Conventional drying
2	0.05	0.10	0	21	0	Conventional drying
	0.05	0.10	0	21	24	Conventional drying
	0.05	0.10	0	21	48	Conventional drying
	0.05	0.10	0	21	72	Conventional drying
3	0.05	0.10	0	21	72	Conventional drying
	0.9	0.10	0	21	72	Conventional drying
	0.18	0.10	0	21	72	Conventional drying
	1.38	0.10	0	21	72	Conventional drying
	13.75	0.10	0	21	72	Conventional drying
4	0.18	0.01	0	21	72	Conventional drying
	0.18	0.02	0	21	72	Conventional drying
	0.18	0.03	0	21	72	Conventional drying
	0.18	0.06	0	21	72	Conventional drying
	0.18	0.10	0	21	72	Conventional drying
	0.18	0.13	0	21	72	Conventional drying
5	0.18	0.01	5.67	21	72	Conventional drying
	0.18	0.02	5.67	21	72	Conventional drying
	0.18	0.03	5.67	21	72	Conventional drying
	0.18	0.06	5.67	21	72	Conventional drying
	0.18	0.10	5.67	21	72	Conventional drying
	0.18	0.13	5.67	21	72	Conventional drying

Table 3.3 (continued).

Section	A/R	A/F	E/R	Aging time of RF-gel (h)	Aging time of AF sol (h)	Drying process
	0.18	0.01	28.34	21	72	Conventional drying
	0.18	0.02	28.34	21	72	Conventional drying
6	0.18	0.03	28.34	21	72	Conventional drying
	0.18	0.06	28.34	21	72	Conventional drying
	0.18	0.10	28.34	21	72	Conventional drying
	0.18	0.13	28.34	21	72	Conventional drying
	0.18	0.03	5.67	21	72	Spray drying
7	0.18	0.06	5.67	21	72	Spray drying
	0.18	0.10	5.67	21	72	Spray drying
	0.18	0.01	28.34	21	72	Spray drying
	0.18	0.02	28.34	21	72	Spray drying
8	0.18	0.03	28.34	21	72	Spray drying
	0.18	0.06	28.34	21	72	Spray drying
	0.18	0.10	28.34	21	72	Spray drying
	-	0.03	0	21	72	Conventional drying
9	-	0.03	0	21	72	Spray drying
	-	0.03	5.67	21	72	Spray drying

CHAPTER IV

RESULTS AND DISCUSSION

In this chapter, alumina which synthesized from aluminium preformed sol/RF-gel composite was investigated in detail. Effects of aging time, concentration of chemicals and drying techniques on properties of the particles were also studied.

4.1 EFFECTS OF AF SOL ON VISCOSITY OF THE MIXED GEL

The effect of aluminium preformed sol on RF-gel was investigated as apparent viscosity of the mixed gel. The viscosity was measured by Brookfield Programmable DV II+ viscometer. The mixed gel was sampled after aging in a period of time. From Figure 4.1, the gelation time of RF-gel mixed with Aluminium preformed sol (AF sol) and pure RF-gel are 21.5 and 39 hours, respectively. Obviously, pure RF solution is gelled slower than the mixed solution is. These results indicate that the aluminium preformed sol can react with RF-gel and accelerate the gelation of the mixed solution.
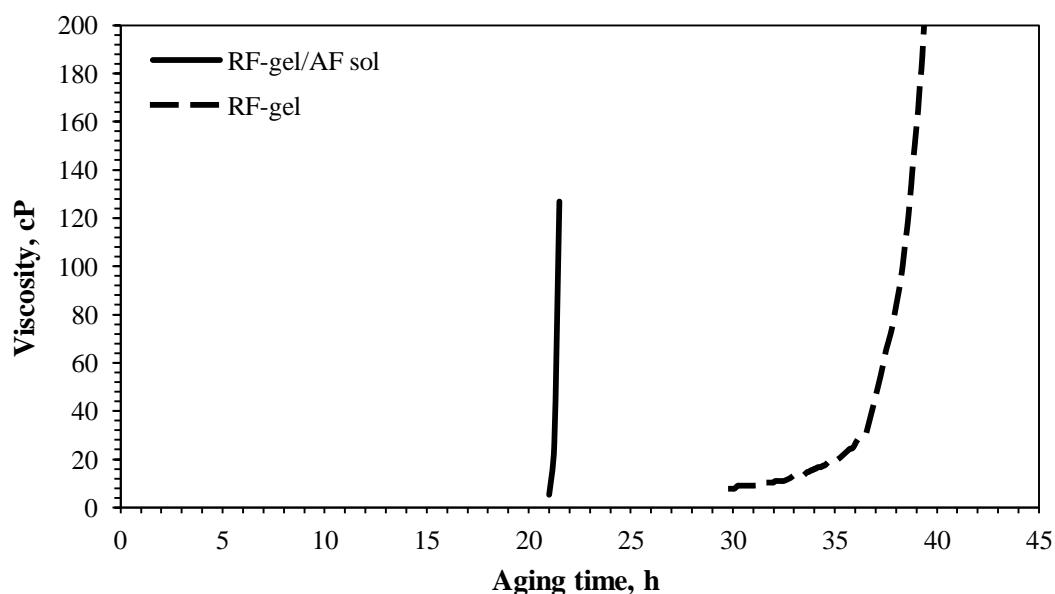
Figure 4.1 Apparent viscosity of the gels**.**

4.2 EFFECTS OF AGING TIME OF AF SOL AND RF-GEL

The aged RF-gel was added into the aged AF sol with investigating the different aging time of both solutions. The gel was sampled before mixed together and after mixed with different aging time until the mixed gel aged for 3 days. Functional groups of the aged gels were identified by Fourier transform infrared spectroscopy (FTIR). The textural properties of products which are N_2 adsorption-desorption isotherm, surface area of products, pore size distribution of products and total pore volume of particles were studied.

4.2.1 VARYING AGING TIME OF RF-GEL WITH FIXED AGING TIME OF AF SOL AT 3 DAYS

In Figure 4.2, FTIR spectra of RF-gel aged for various periods of time are considered. The assignment of characteristic absorption bands was done according to the values reported in literatures [14, 37-39]. The bands at wavenumber of 1612 cm^{-1} corresponding to C=C aromatic ring stretching vibration, at 1298 and 1175 cm^{-1} respectively corresponding to C-O stretching and CH aromatic stretch vibrations, and at 1477 cm^{-1} for -CH$_2$- scissor vibration were observed. It should be noted that the -CH$_2$- bonding is a result from a cross-linking bridge formed from the condensation of hydroxymethyl derivatives. Furthermore, absorption bands corresponding to methylene ether (-CH$_2$-O-CH$_2$-) were also detected at wavenumber of 1220 and 1092 cm^{-1}. The -CH$_2$-O-CH$_2$- bridges were a cross-linking bond formed between aromatic rings due to polycondensation of resorcinol by formaldehyde.

For FTIR spectra in Figure 4.2a-f, the interesting peaks which indicate methylene, methylene ether bridges and C=C aromatic ring stretching vibration are quite shifted. This means there are interaction between RF-gel and AF sol in the beginning of aging. The cluster of RF-gel and AF-sol are cross-linking. After that, the g-j spectra are similar. This indicated that the mixed gel finishes cross-linking and forms to be colloidal particles after the mixed gel is aged about 40 hours.

Table 4.1 summarizes identifications of the bands that have been proposed to associate with functional groups of the RF solution. Furthermore, Fourier self-deconvolution (FSD) method was used to determine integrated intensities of the absorption bands. This procedure requires input data such as the form of the apodization function, band width and enhancement [40].

Figure 4.2 FTIR spectra of the 0-hour-aged RF-gel combined with 3-day-aged AF sol (a) before mixing (b) after mixing and aged for (c) 4 h, (d) 7 h, (e) 15 h, (f) 25 h, (g) 40 h, (h) 50 h, (i) 60 h and (j) 72 h.

Table 4.1 Assignments of FTIR absorption bands of RF-gel.

IR bands (cm^{-1})	Function groups
1612	C=C aromatic ring [41]
1477	-CH$_2$- methylene bridges between resorcinol molecules [14]
1298	C-O stretching [41]
1220	C-O-C stretching vibrations of methylene ether bridges between resorcinol molecules [14]
1175	CH aromatic, in plane [41]
1092	C-O-C stretching vibrations of methylene ether bridges between resorcinol molecules [14]

In Figure 4.3, similarly with Figure 4.2, for a-c FTIR spectra in Figure 4.2, the interesting peaks are quite shifted because interaction between RF-gel and AF sol occurred in the beginning of aging. After that, the d-g spectra are similar. This indicates that the mixed gel was stable after the mixed gel was aged about 40 hours.

Figure 4.3 FTIR spectra of the 21-hour-aged RF-gel combined with 3-day-aged AF sol (a) before mixing (b) after mixing and aged for (c) 25 h, (d) 40 h, (e) 50 h, (f) 60 h and (g) 72 h.

To confirm the result which is shown in figure above, the ratios of methylene and methylene ether bridges of the mixed gel in different sampled time were calculated. These ratios can be calculated by the absorbance quantities of methylene and methylene ether bridges which are at wavenumber of 1477, 1092 cm^{-1} comparing with the constant quantities

of C=C aromatic ring in the gel at 1612 cm^{-1}. The ratios of the mixed gel with investigating difference aging time of RF-gel were shown in Figure 4.4 below.

Comparing between the methylene and methylene ether bridges of pure RF-gel and mixed gel, the bridges increase in the beginning of mixing (as shown in Figure 4.4a-d). The result indicates that adding AF sol accelerates condensation reaction of RF-gel process. When the mixed gel was aged, increasing in aging time of the mixed gel increases methylene and methylene ether bridges until 40 hours. After that, the ratios are constant. This means the mixed gel is completely cross-linking.

(a)

(b)

(c)

(d)
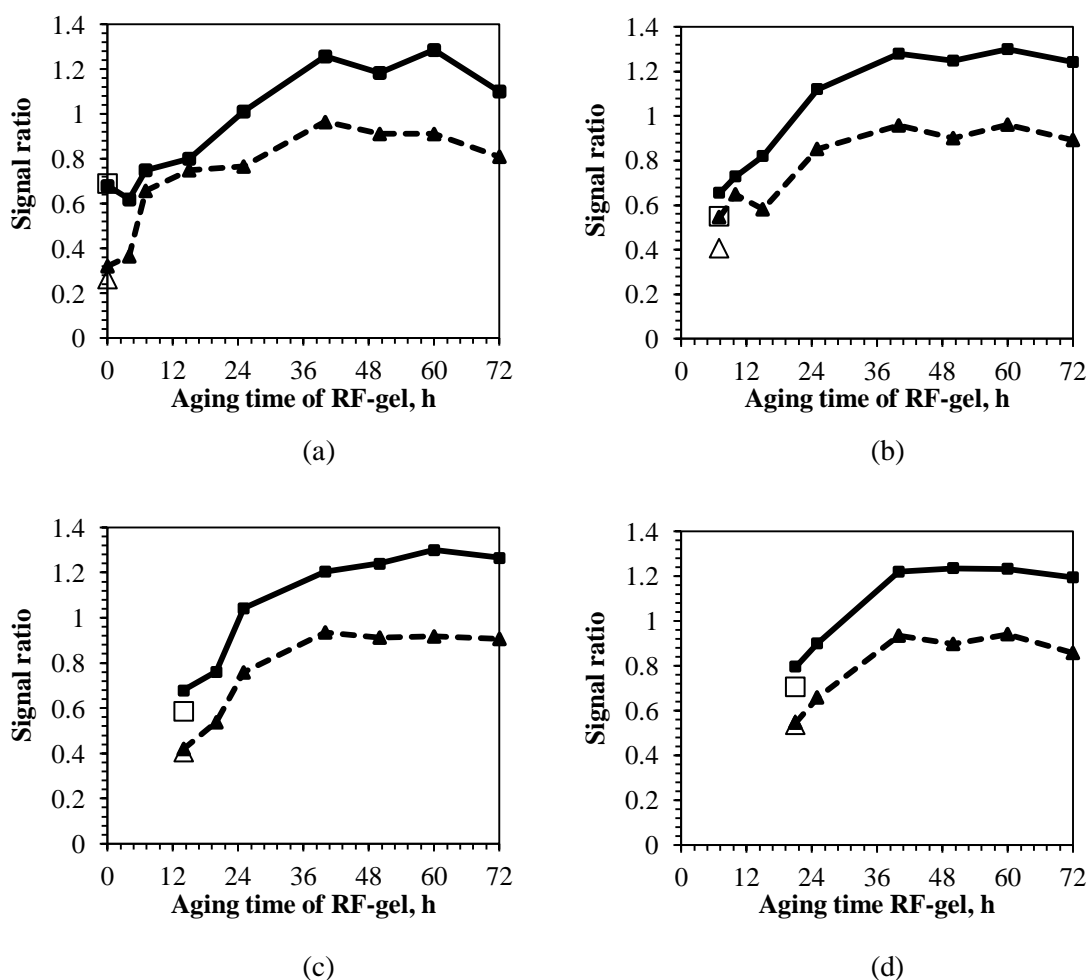
Figure 4.4 FTIR signals ratio of (■) methylene and (▲) methylene ether bridges of the mixed gel comparing with (□) methylene and (△) methylene ether bridges of RF-gel with respect to aromatic rings in the gel. The gels mixed when aged RF-gel for (a) 0 h, (b) 7 h, (c) 14 h and (d) 21 h.

4.2.2 *VARYING AGING TIME OF AF SOL WITH FIXED AGING TIME OF RF-GEL AT 21 HOURS*

From Figure 4.5, FTIR spectra change when aging time of the mixed gel changes. The partern of spectra is similar with Figure 4.2 and Figure 4.3 which are ahown aboved. the spectra as shown in Figure 4.5a and b, some peaks are shifted in the beginning of mixing. After that, the interesting peaks which are methylene and methylene ether bridge (1477 and 1092 cm^{-1}, respectively) are not shifted during the mixed gel was aged.
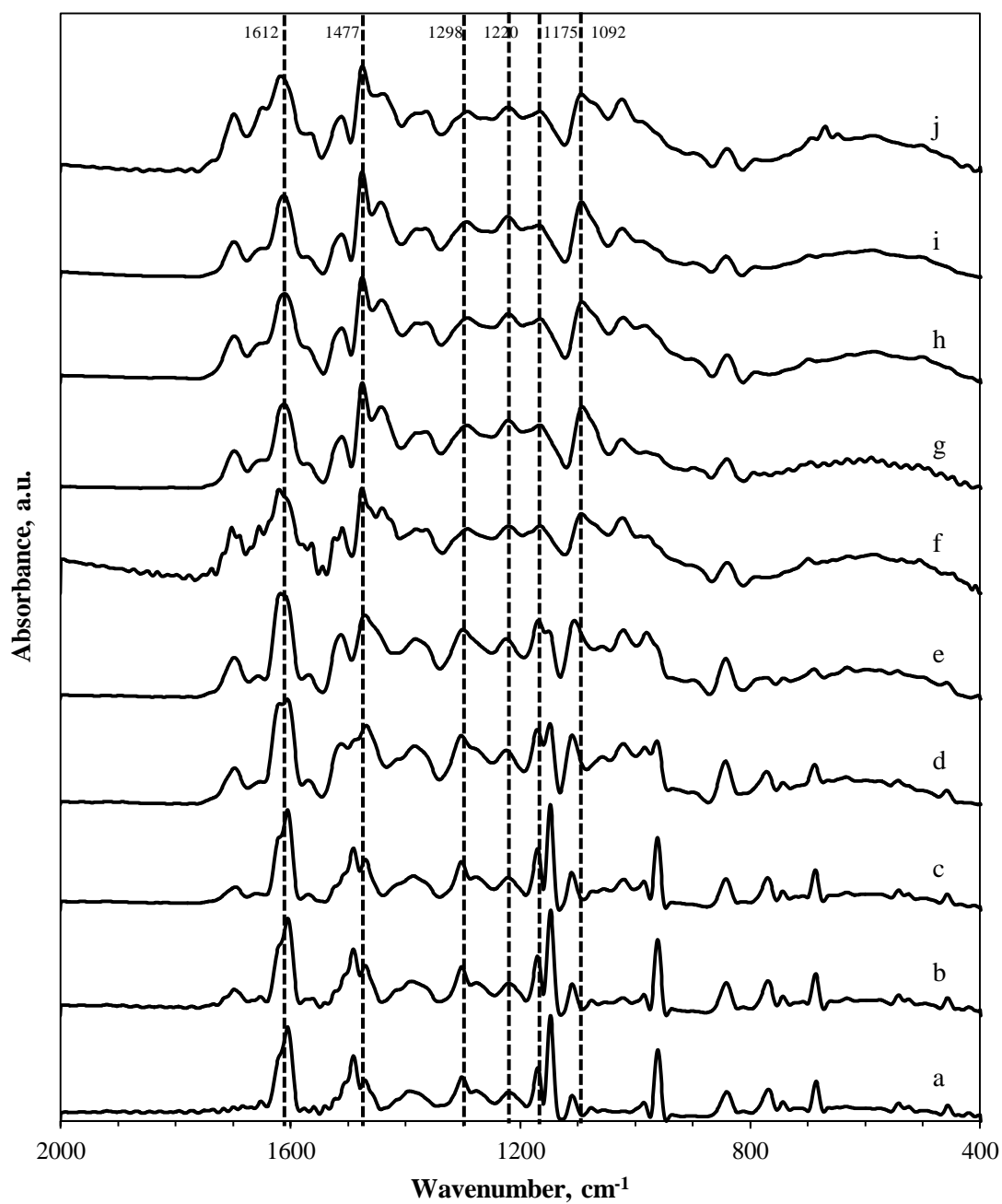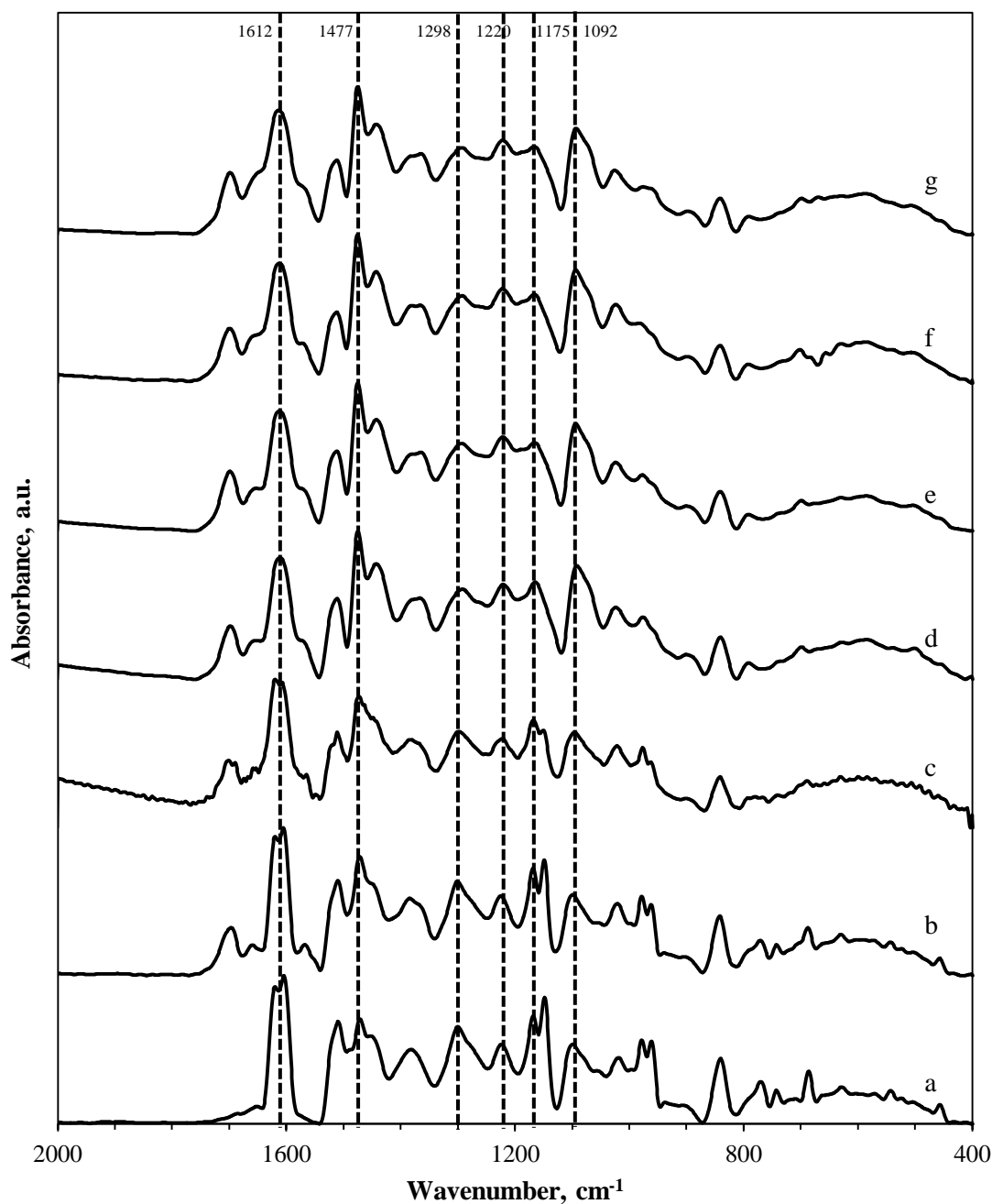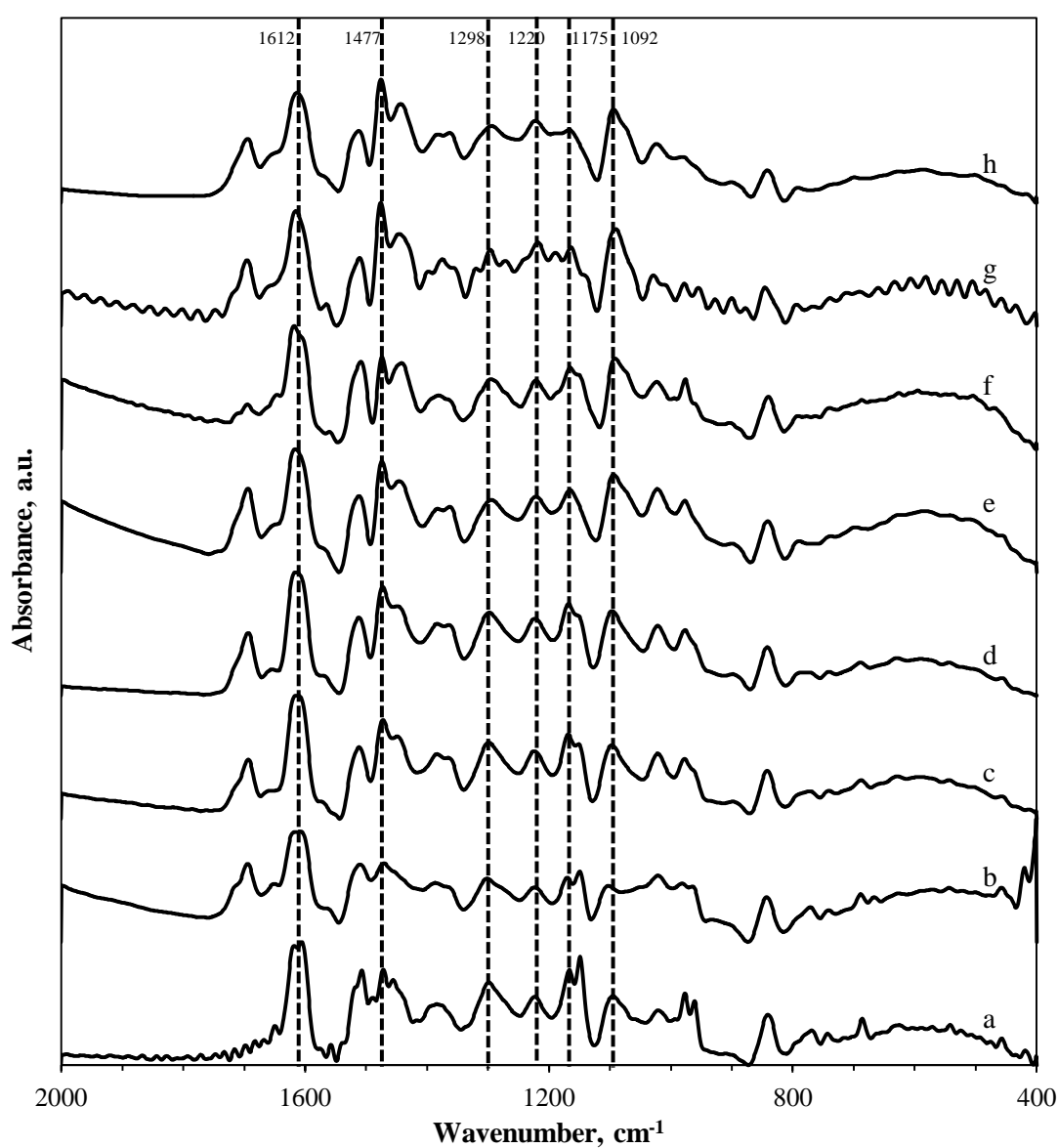

Figure 4.5 FTIR spectra of the 21-hour-aged RF-gel combined with 1-day-aged AF sol (a) before mixing (b) after mixing and aged for (c) 25 h, (d) 30 h, (e) 36 h, (f) 48 h, (g) 60 h and (h) 72 h.

The ratio of methylene and methylene ether bridges comparing with aromatic ring was calculated as shown in Figure 4.6. When RF-gel is mixed with AF sol which is aged for 0 and 1 day, the methylene and methylene ether bridges start decreasing. The result indicates that the remaining aluminium acetylacetonate from the AF sol reacts with RF-gel. The aluminium atom form complex with methylene and methylene ether bridges of RF-gel. This result also affects on the ratios of the bridges until age the mixed gel for 3 days. The ratios are not stable. While aging AF sol for 2 days over, the AF sol can react with RF-gel to form methylene and methylene ether bridges. Moreover, the increase in aging time of the mixed gel is conformed to the increase in methylene and methylene ether bridges formed.

(a)

(b)

(c)

(d)
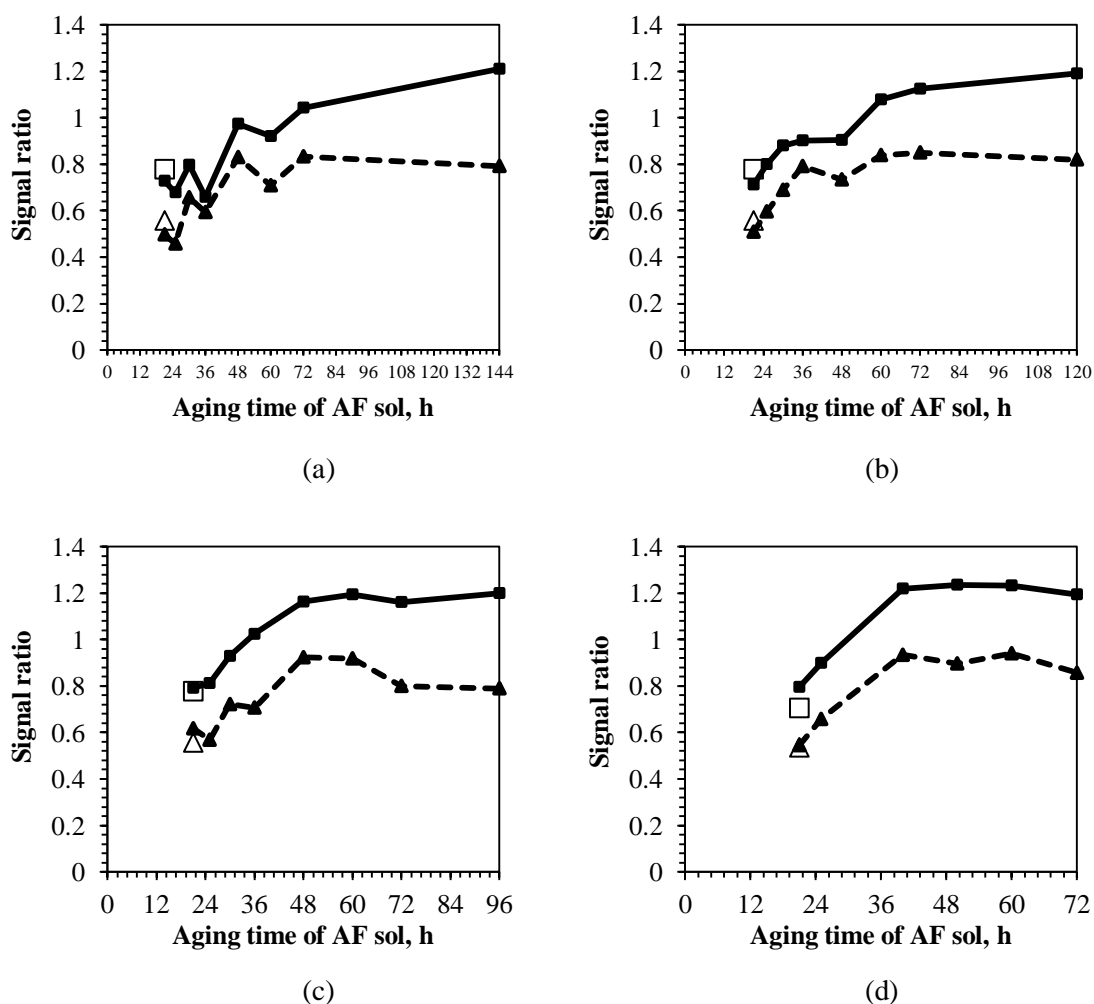
Figure 4.6 FTIR signals ratio of (■) methylene and (▲) methylene ether bridges of the mixed gel comparing with (□) methylene and (△) methylene ether bridges of RF-gel with respect to aromatic rings in the gel. The gels mixed when aged AF sol for (a) 0 h, (b) 24 h, (c) 36 h and (d) 72 h.

In part of 4.2.1 and 4.2.2, there is interesting peak at wavenumber around 1700 cm^{-1} occured after the AF sol was mixed with RF-gel. This peak also occurred in AF sol (as show in Figure 4.7 below). In addition, this interesting peak did not occur in aluminium acetylacetonate and formaldehyde (as show in Figure 4.8 below). These results show that aluminium acetylacetonate can react with formaldehyde when the both reactants are mixed together. The structure of aluminium acetylacetonate and formaldehyde were considered. The bands at wavenumber of 1700 cm^{-1} corresponding to -C=O- in functional group of ketone vibration was observed [42]. In Figure 4.9, it should be noted that the -C=O- bonding is a result from aluminum acetylacetonate reacting formaldehyde which are consist of C=O function.
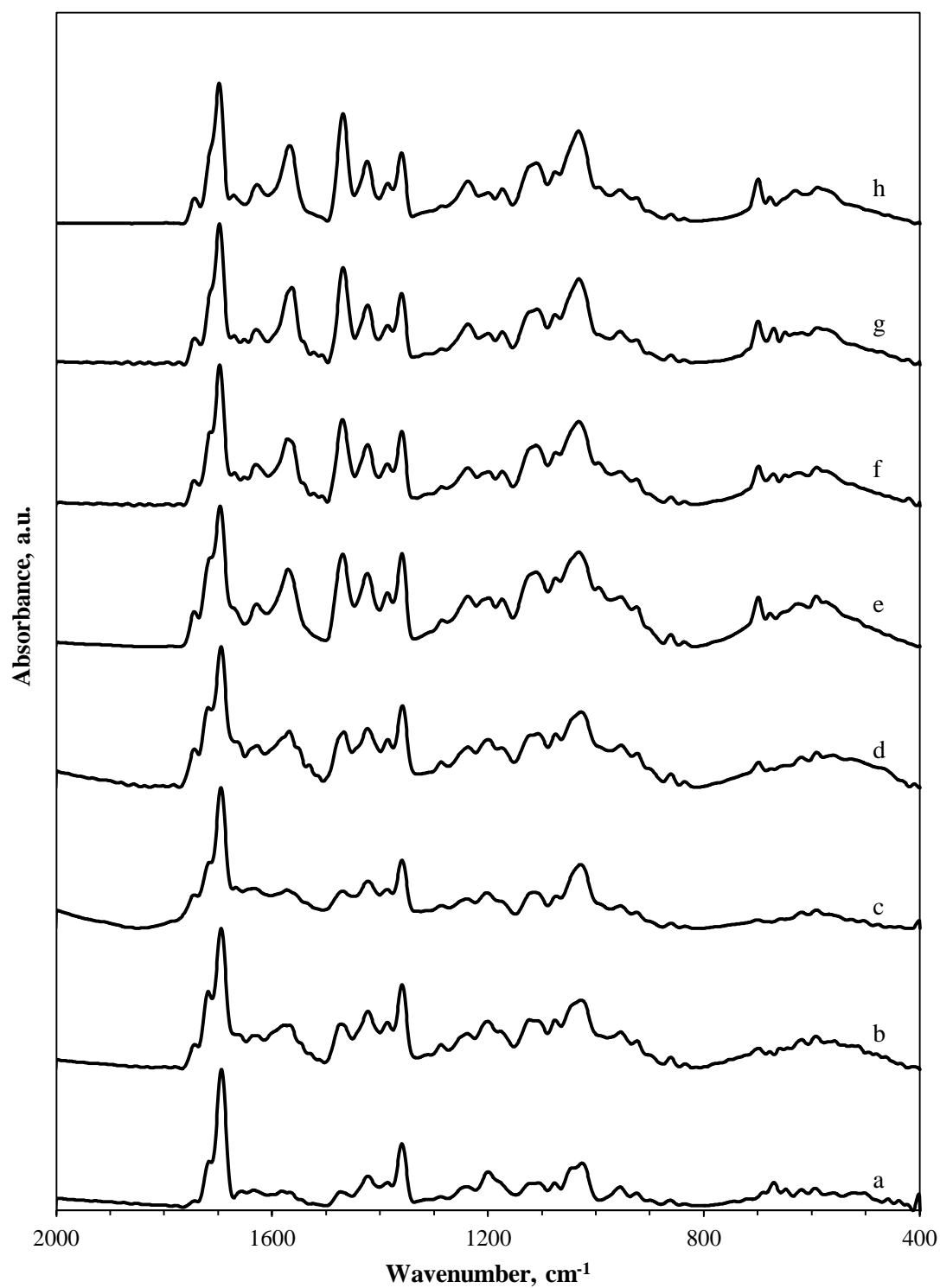
Figure 4.7   FTIR spectra of the AF sol aged for (a) 0 h, (b) 6 h, (c) 12 h, (d) 20 h, (e) 36 h, (f) 48 h, (g) 60 h and (h) 72 h.
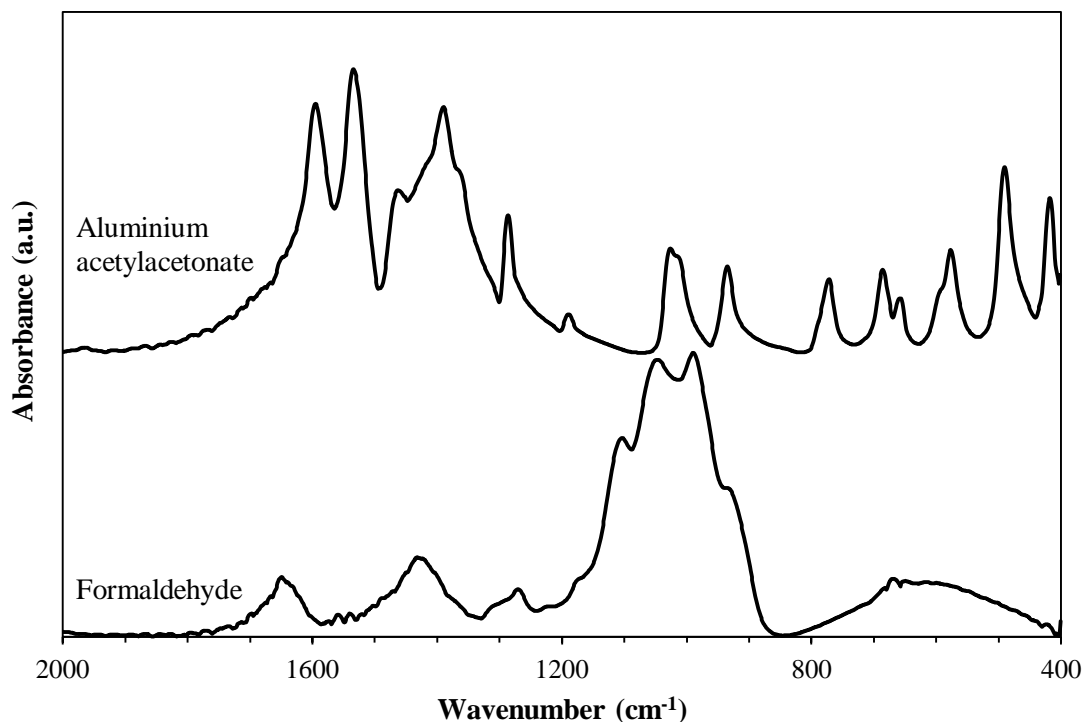
Figure 4.8 FTIR spectra of aluminium acetylacetonate and formaldehyde.
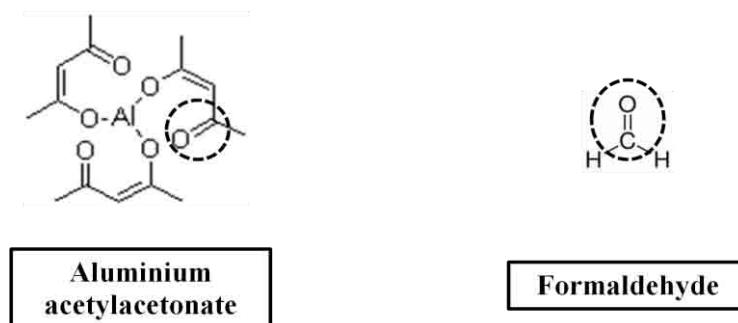
Figure 4.9 Structure of aluminium acetylacetonate and formaldehyde.

4.2.3 EFFECTS AGING TIME OF AF SOL AND RF-GEL ON TEXTURAL PROPERTIES
OF PRODUCTS

Varying aging time was splited into two cases. The first one is the mixed gel combine from RF-gel with varying aging time and AF sol with fixed aging time at 3 days. Secondly, the mixed gel combine from RF-gel with fixed aging time at 21 hours and AF sol with varying aging time.

Textural properties in Figure 4.10 which is shown the N_2 adsorption-desorption isotherms of several different aging time of RF-gel are considered, the maximum volume of

N₂ gas that was adsorbed with different aging time of RF-gel is similar. The pattern of isotherms is same as well. This means varying aging time of RF-gel has not an effect on textural properties of the particle. Obviously, all isotherms are type IV with hysteresis loop which indicate the particle with mesoporous structure. From the IUPAC classification of pore structure, this hysteresis loop indicates geometry pore shapes like tubular [32].
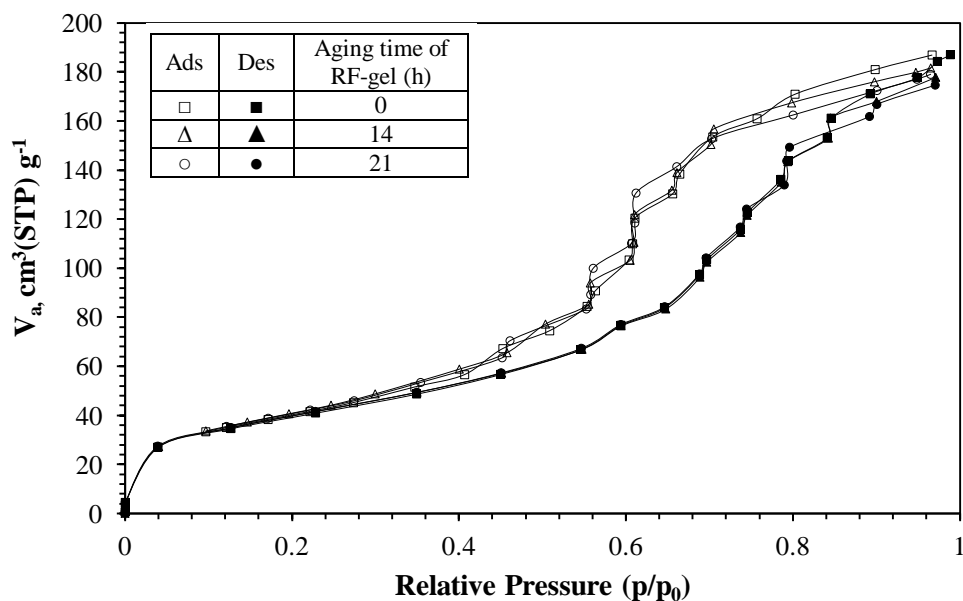
Figure 4.10 N₂ adsorption-desorption isotherm of synthesized alumina with varying aging time of RF-gel with aged AF sol for 3 days.

N₂ adsorption-desorption isotherms of synthesized alumina with varying aging time of AF sol with aged AF sol at 3 days (as shown in Figure 4.11) are considered. The maximum N₂ adsorbed volume decrease when aging time of AF sol increase. The isotherms are type IV with hysteresis loop which indicates the particle with mesoporous structure. From the IUPAC classification of pore structure, this hysteresis loop indicates geometry pore shapes like tubular [32].
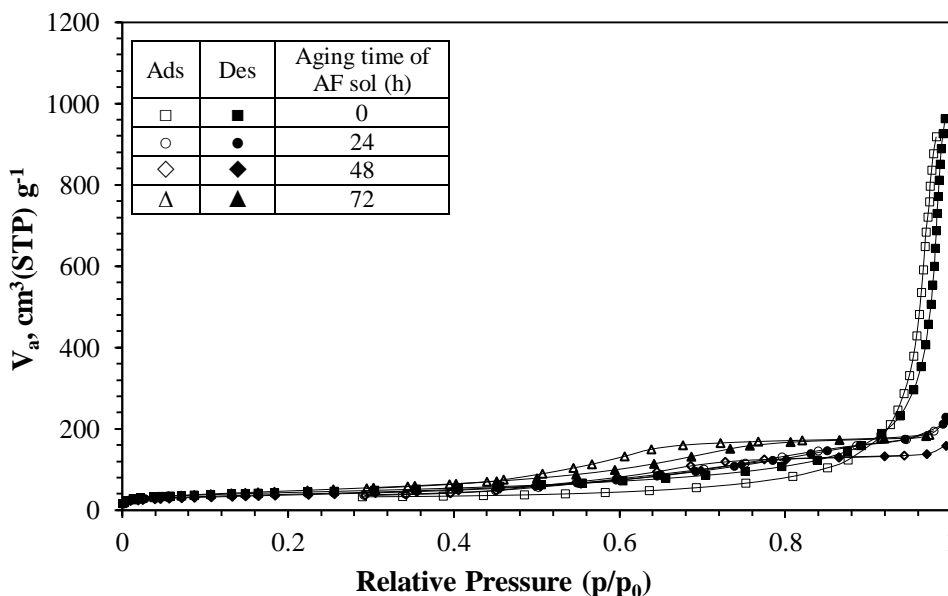
Figure 4.11 N_2 adsorption-desorption isotherm of synthesized alumina with varying aging time of AF sol with aged RF-gel for 21 hours.

With varying aging time of RF-gel, pore size distributions of alumina particles in Figure 4.12 and textural properties in Table 4.2 show that all synthesized alumina are mesoporous particles with the range of pore diameter is between 2 to 70 nm. The pore size peak is similar when changing aging time of RF-gel while pore volume and surface area of products are nearly constant. The average surface area is 140 m^2/g. This can confirm that varying aging time of RF-gel has not an effect on textural properties of the particle.

The case which varies aging time of AF sol, pore size distributions of alumina particles in Figure 4.13 is considered. It shows that the pore distribution is narrower when the aging time of AF sol is increasing. The range of pore diameter is between 2 to 200 nm. Moreover, the pore size peak (as shown in Table 4.2) strongly decreases when aging time of AF sol changes from 0 to 24 hours. This means the sols occur during aging time of AF sol 0 to 24 hours. Interestingly, the broadest and highest pore size peak is at 0-hour-aged AF sol and average pore size diameter is 106 nm. The broad pore distribution and bimodal pore distribution are not appropriate for using as catalyst support because it will be affect on catalyst loading performance.
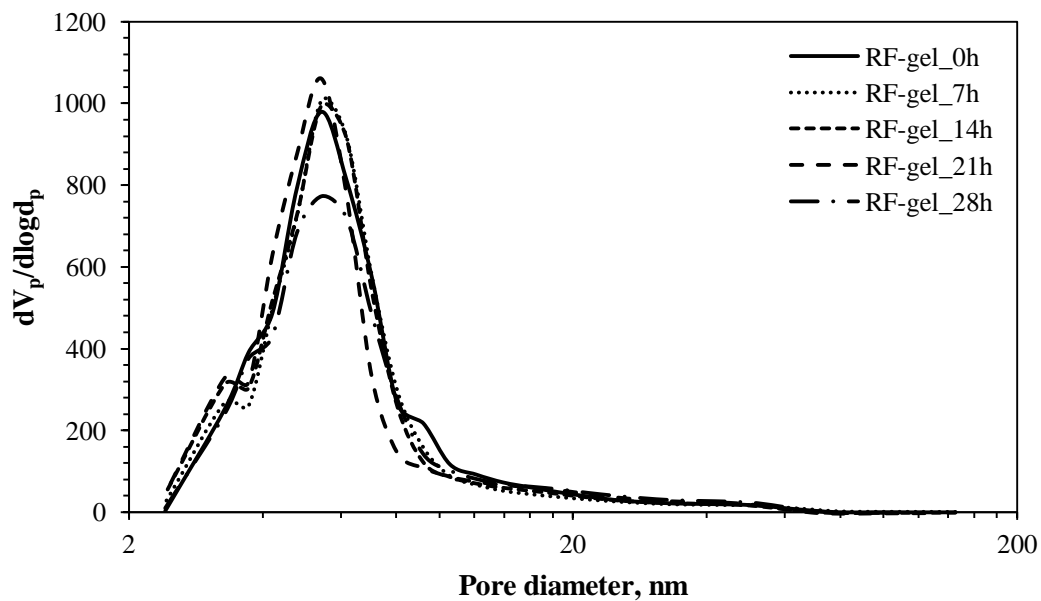
Figure 4.12 Pore size distribution of synthesized alumina with varying aging time of RF-gel with aged AF sol for 3 days.
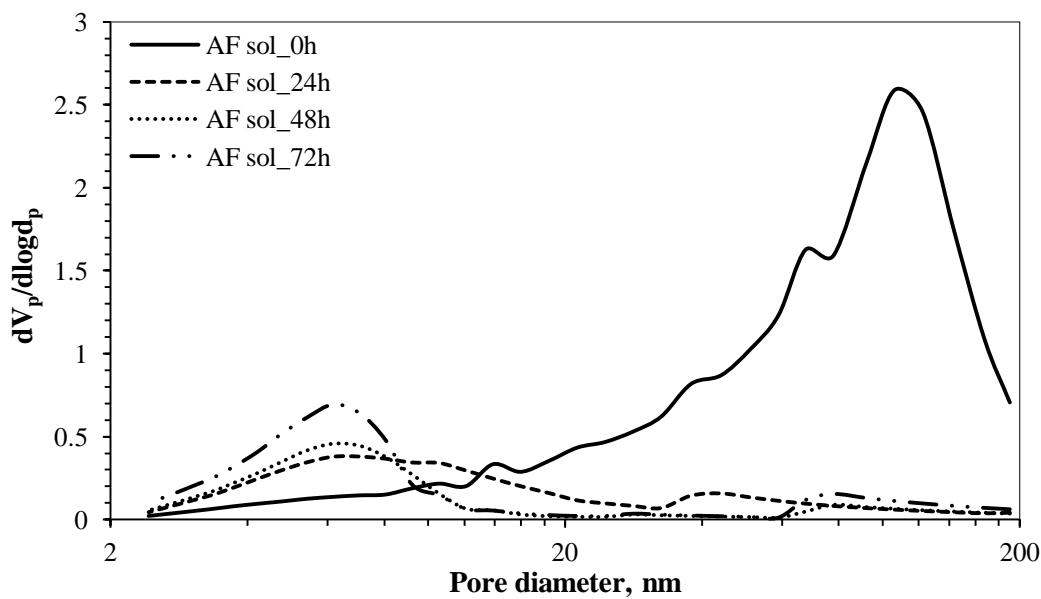
Figure 4.13 Pore size distribution of synthesized alumina with varying aging time of AF sol with aged RF-gel for 21 hours.

Table 4.2 Textural properties of synthesized alumina which studying aging time.

Aging time of RF-gel (h)	Aging time of AF sol (h)	BET surface area $(m^2/g)^a$	Pore size peak $(nm)^b$	Pore volume $(cm^3/g)^b$
0	72	141.98	5.43	0.3103
7	72	137.62	5.43	0.2949
14	72	146.13	5.43	0.2995
21	72	145.03	5.43	0.2960
28	72	130.20	5.43	0.2759
21	0	151.96	106.09	1.4192
21	24	138.22	7.05	0.3254
21	48	129.13	6.18	0.2404
21	72	145.03	5.43	0.2960

[a] The BET surface areas were calculated by using BET equation.
[b] The average pore diameters and pore volumes were calculated by using BJH equation.

From these results, the structure of AF sol/RF-gel composite can be supposed figure below:
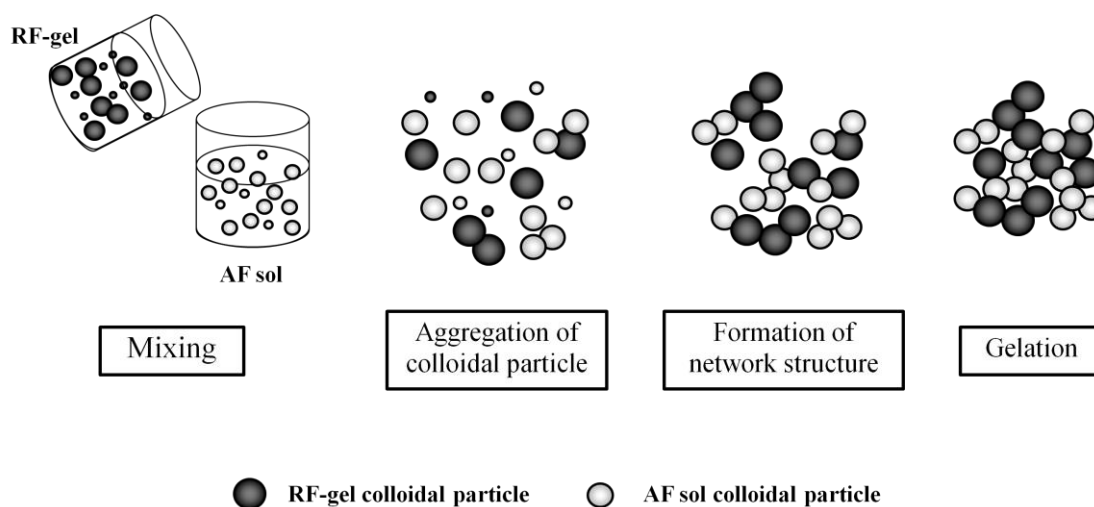
Figure 4.14 Schematic of AF sol/RF-gel composite formation.

Figure 4.14 indicates clusters forming of AF sol/RF-gel composite. The AF sol and RF-gel form to be clusters independently when AF sol was mixed with RF-gel. After that these clusters form to be colloidal particles. This can be explained by when varying aging time of RF-gel then mixed the gel; the pore size of alumina is similar while the pore size distribution is changing when the aging time of AF sol is varying. However, both AF sol and RF-gel colloidal particles can cling together with bonding between aluminium acetylacetonate

and RF-gel as adhesive which was describe in the part of 4.2.1 and 4.2.2 above. The RF particles can be removed by calcination in air to result in carbon combustion. The RF-gel can be used as assisted-template which results pore of alumina particles.

In the case of mixing AF sol aged for 0 hour and RF-gel aged for 21 hours, the AF smaller sols are occurred. The smaller sols can not obstruct growing of the RF-gel clusters. Thus, the bigger RF-gel colloidal particles make larger pore size of alumina product which is shown in Figure 4.13.

4.3 EFFECTS OF CONCENTRATION OF CHEMICALS

Concentration of formaldehyde in the AF sol and resorcinol in the mixed gel were studied. The both chemicals concentrations were calculated as molar ratio comparing with concentration of aluminium acetylacetonate in the system.

4.3.1 VARYING FORMALDEHYDE CONCENTRATION OF THE SOL

This section was studied results from varying formaldehyde in the AF sol. The concentration was calculated as A/F molar ratio. The RF-gel was aged for 21 hours and AF sol was aged for 3 days were considered. The results were described by the synthesized alumina.

Figure 4.15 shows FTIR spectra of the mixed gel with varying A/F molar ratio. The aluminium acetylacetonate which fixed molar quantity was dissolved in different concentration of formaldehyde. In the system, only concentration of formaldehyde was varying while concentration of other chemcals which are aluminium acetylacetonate, resorcinal, water and catalyst were fixed. After the mixed gel was aged for 3 days, the interesting peaks in the spectra of different formaldehyde concentration are not shifted. This also means varying A/F ratio does not affect on partern of FTIR spectra. It can indicates that during the clusters of aluminium preformed sol cross-link with the clusters of RF-gel, formaldehyde molecule in the AF sol does not act as adhesive but the aluminium acetylacetonate in the sol cause cohesion between the clusters.
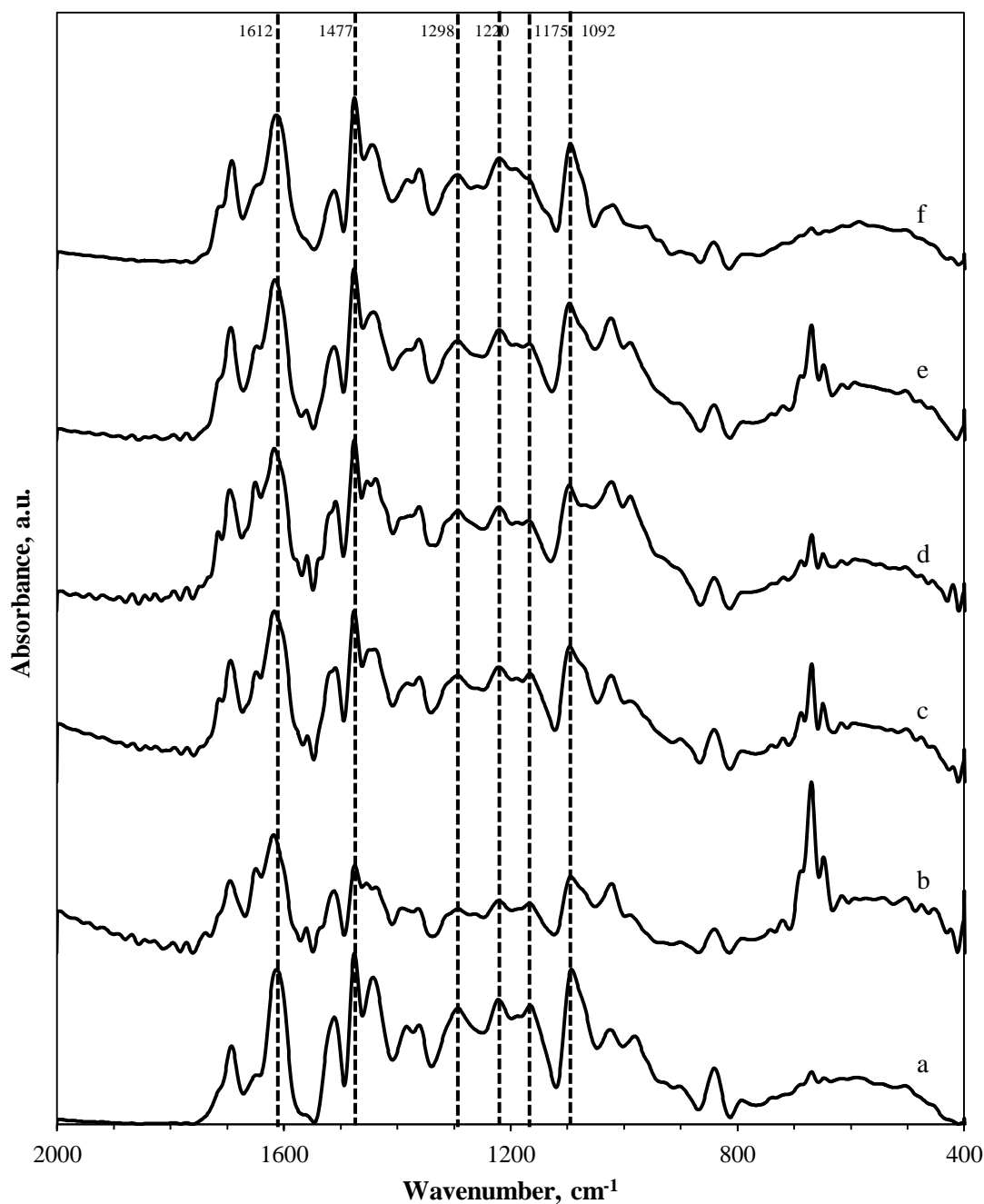
Figure 4.15 FTIR spectra of the mixed gel which were aged for 3 days with varying A/F molar ratio (a) 0.13, (b) 0.10, (c) 0.06, (d) 0.03, (e) 0.02 and (f) 0.01.

Figure 4.16a which shows the methylene and methylene ether bridges ratio of the mixed gel in the beginning of mixing is considered. Increasing concentration of formaldehyde increases methylene ether bridges ratio and slightly increases methylene bridges ratio. Comparison of methylene and methylene ether bridges ratio between RF-gel (the horizontal line and dash line, respectively) and the mixed gel is considered. This means that adding

quantity of formaldehyde is similarly with adding quantity of –C=O- function. The –C=O- function results in methylene ether bridge (-CH₂-O-CH₂-) when condensation reaction of RF-gel occurs.

After the mixed gel was aged for 3 days (as shown in Figure 4.16b), the bridges ratio still increases when A/F molar ratio increases. Increasing formaldehyde slightly affects on RF-gel formation. This means excess formaldehyde work as solvent. It does not concern with the RF-gel formation but only improves dispersion of the RF clusters in the system [10].

(a)   (b)
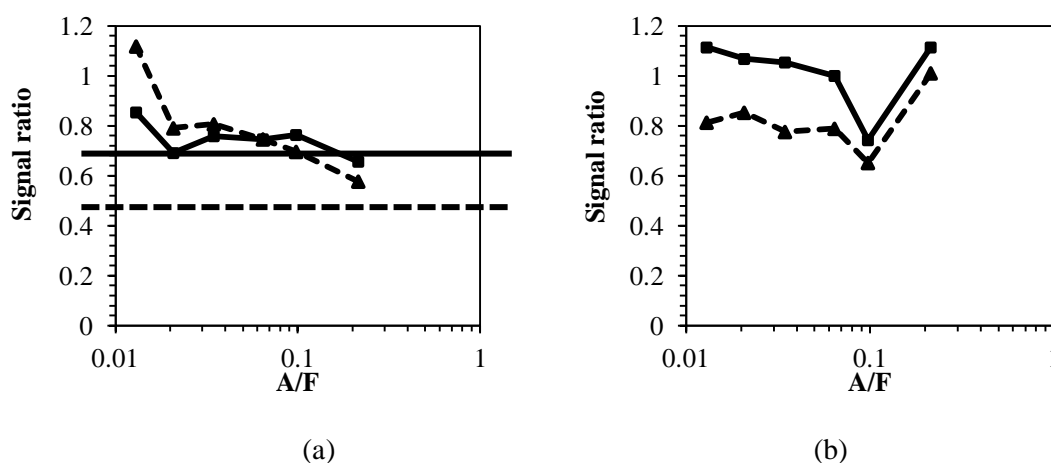
Figure 4.16 FTIR signals ratio of (■) methylene and (▲) methylene ether bridges of the mixed gel with respect to aromatic rings in the gel with varying A/F molar ratio. The mixed gel aged for (a) 0 day and (b) 3 days.

Figure 4.17 shows N₂ adsorption-desorption isotherm of synthesized alumina with varying A/F molar ratio. The isotherms are type IV with hysteresis loop which indicates the particle with mesoporous structure. From the IUPAC classification of pore structure, this hysteresis loop indicates geometry pore shapes like tubular [32].
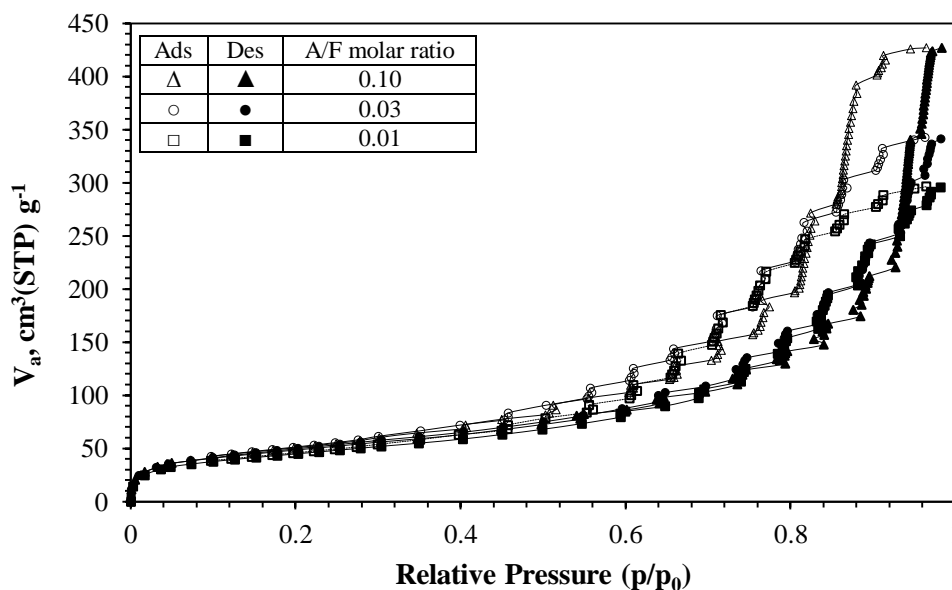
Figure 4.17 N_2 adsorption-desorption isotherm of synthesized alumina with varying A/F molar ratio.

Table 4.3 shows the surface area of synthesized alumina and pore diameter of the particles which analyzed from Nitrogen adsorption-desorption technique. Formaldehyde concentrations affect the surface area of particles with no pattern. However, formaldehyde concentration increases (decreasing A/F), average pore size diameter and pore volume of the particles also increase. This mean formaldehyde concentration has a significant effect on textural properties of alumina particles.

Table 4.3 Textural properties of synthesized alumina with varying A/F molar ratio.

A/F	BET surface area $(m^2/g)^a$	pore size peak $(nm)^b$	pore volume $(cm^3/g)^b$
0.10	148.95	4.79	0.2677
0.06	144.02	4.72	0.2470
0.03	158.77	5.29	0.2918
0.02	151.01	10.18	0.4912
0.01	175.66	13.05	0.7236

[a] The BET surface areas were calculated by using BET equation.
[b] The average pore diameters and pore volumes were calculated by using BJH equation.

Pore size distributions of alumina particles in Figure 4.18 shows products are mesoporous particles with the range of pore diameter is between 2 to 55 nm. Increasing

concentration of formaldehyde in the preformed sol causes broader pore size distribution. Interestingly, increasing formaldehyde concentration (decreasing A/F molar ratio) causes bimodal pore distribution. This graph confirms that formaldehyde concentration in the AF sol has a significant effect on pore size distribution. The results are explained by excess formaldehyde from AF sol reacted with RF-gel called 'dilution effect'. This effect (excess F) causes larger particles of RF-gel carbon structure [10, 43]. This result affects pore size of the alumina directly. The larger RF-gel colloidal particles obstruct growing of AF sol particles. Thus, the particles of AF sol will be small with large pore size. The SEM images shown below confirm occurring dilute effect.
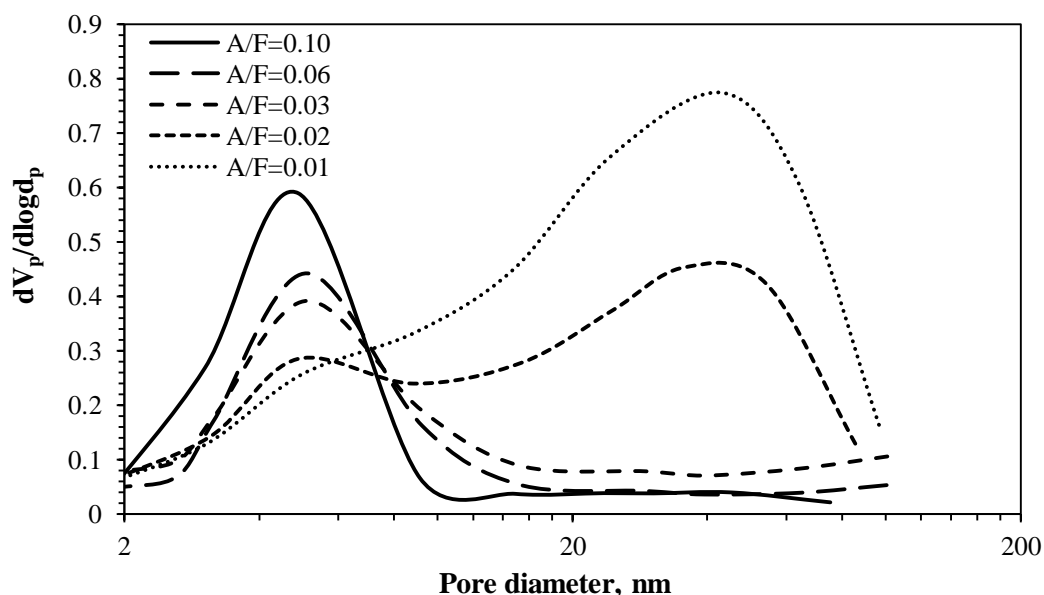
Figure 4.18 Pore size distribution of alumina with varying A/F molar ratio.

The alumina cluster size decreases when A/F molar ratio decrease (Increasing formaldehyde concentration). The bimodal pore size distribution is indecated in the SEM images (as shown in Figure 4.19c1 and Figure 4.19c2) at A/F = 0.01. Bimodal pore size distribution consists of pores originate from the inter-particular void between alumina particles and the pore causes from RF-gel colloidal particles which are already removed after calcination. The results are explained by excess formaldehyde from AF sol reacted with RF-gel called 'dilution effect' (explained previously).
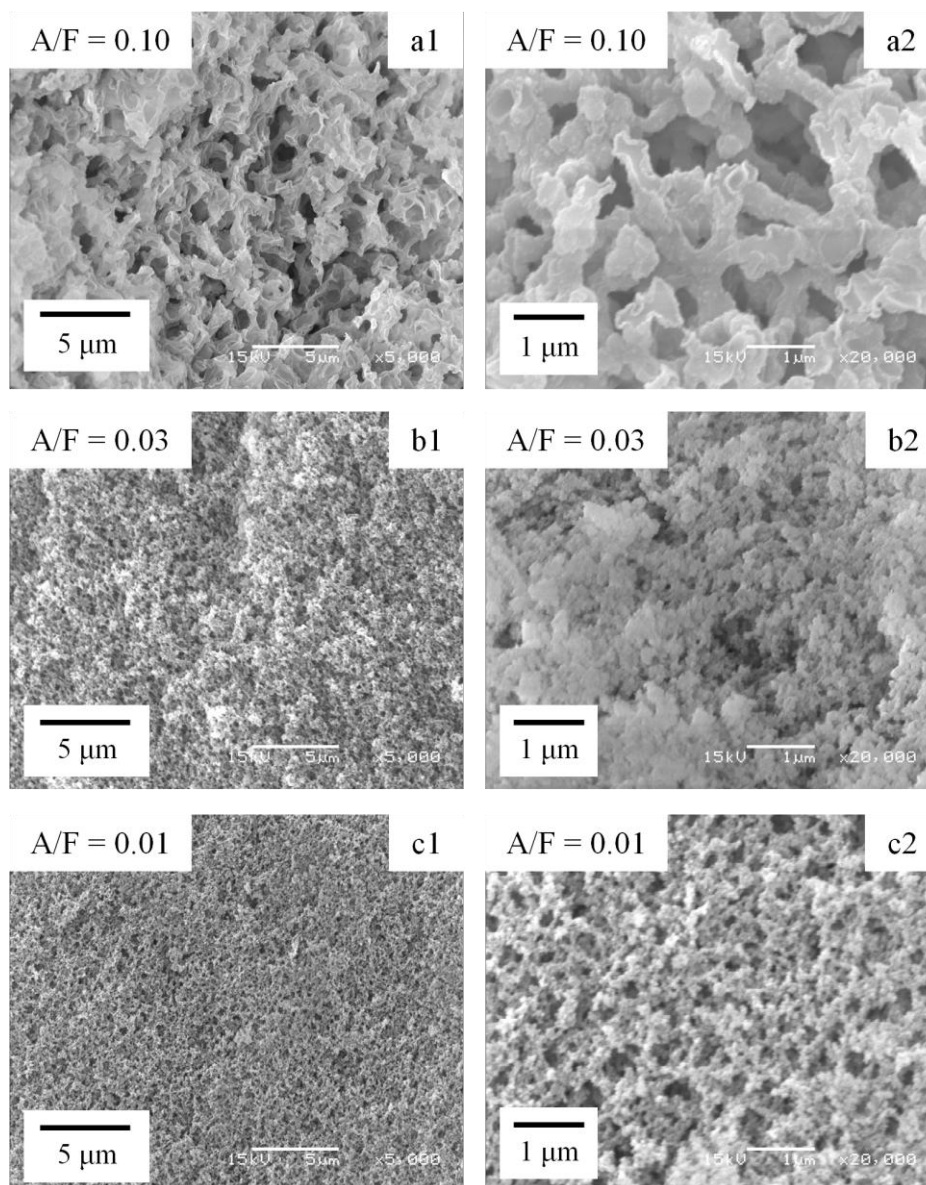
Figure 4.19 SEM images of synthesized alumina in different A/F molar ratio (a) 0.10, (b) 0.03 and (c) 0.01 with magnification (1) 5,000x and (2) 20,000x.

The schematic of particles structure explaining dilution effect is shown below. The dilution effect (excess F) causes larger particles of RF-gel carbon structure [10, 43]. The larger RF-gel colloidal particles obstruct growing of AF sol particles. Thus, the particles of AF sol will be small with large pore size. In the case of low concentration of formaldehyde, the large colloidal particles of AF sol are occurred.

Low F
concentration
(High A/F)

High F
concentration
(low A/F)

| Aggregation of colloidal particle | Formation of network structure | Gelation |

⬤ RF-gel colloidal particle ○ AF sol colloidal particle
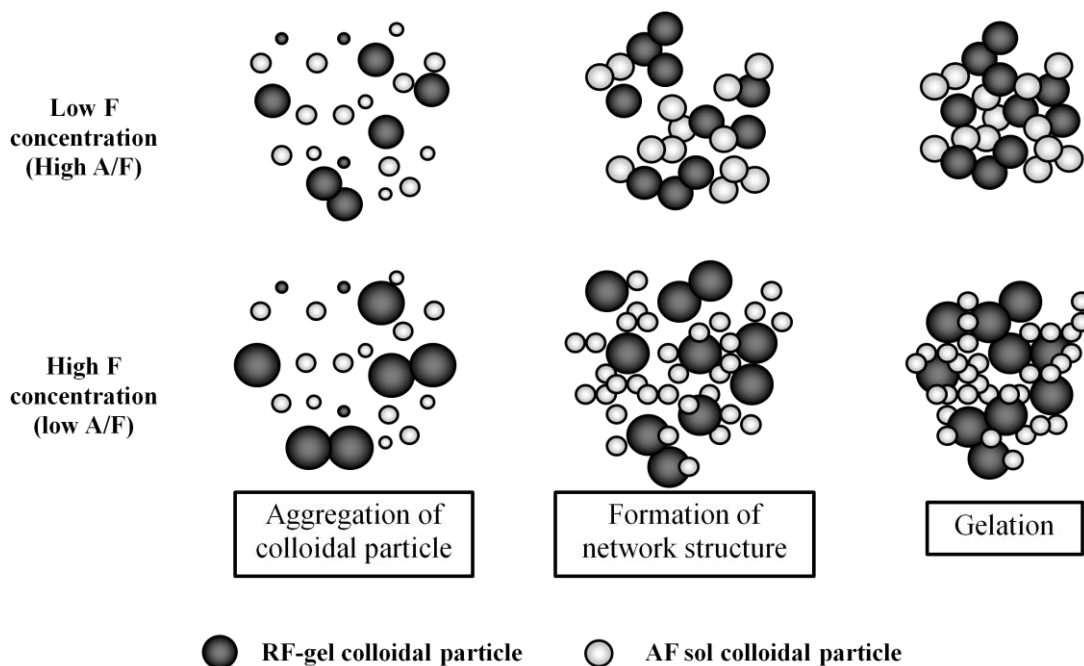
Figure 4.20 Schematic of synthesized particles structure.

4.3.2 VARYING RESORCINOL-FORMALDEHYDE GEL (RF-GEL) CONCENTRATION

This section was studied in varying of RF-gel concentration in the process. The concentration was calculated as molar ratio of aluminium acetylacetonate to resorcinol (A/R). The RF-gel was aged for 21 hours and AF sol was aged for 3 days were considered. The results were described by the synthesized alumina.

Figure 4.21 shows FTIR spectra of the mixed gel with varying A/R molar ratio. In the experiment, changing A/R molar ratio means adding various RF-gel into the aluminium preformed sol. This means that the concentrations of both resorcinal and formaldehyde in the system are varied. When A/R ratio changes, the partern of FTIR spectra is changed and methylene ether ($-CH_2-O-CH_2-$) bridges which represent to wavenumber of 1092 cm^{-1} are shifted as well. These results can confirm that AF sol reacts with RF-gel. Interestingly, this indicates that the aluminium acetylacetonate concentration has a significant effect on FTIR spectra which is stronger than formaldehyde concentration's. The concentration of aluminium acetylacetonate affects on condensation reaction of RF-gel. This result summarizes aluminium acetylacetonate in the AF sol certainly reacts with RF-gel.
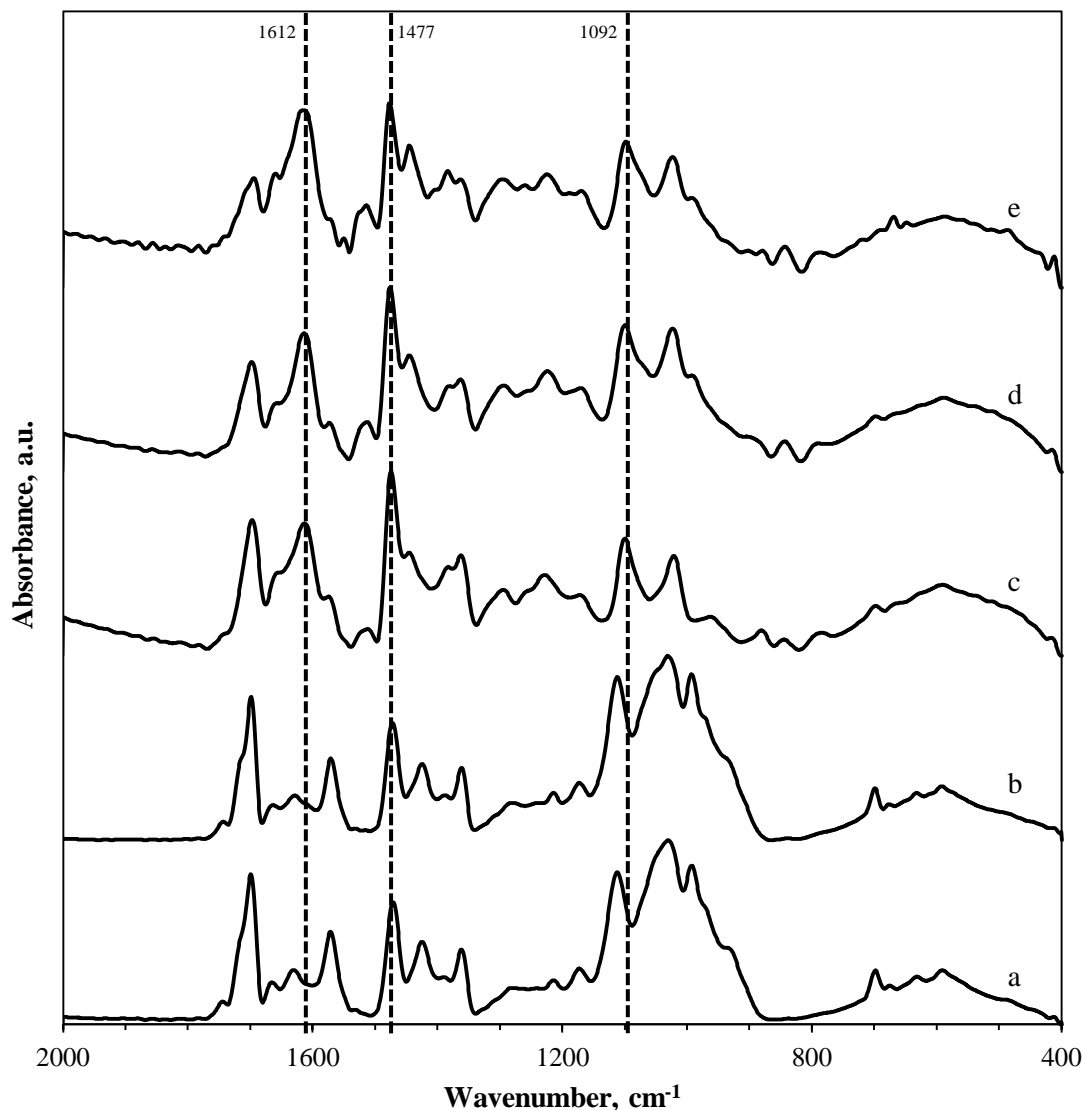
Figure 4.21 FTIR spectra of the mixed gel aged for 3 days with varying A/R molar ratio (a) 13.75, (b) 1.38, (c) 0.18, (d) 0.09 and (e) 0.05.

Figure 4.22a which shows the methylene and methylene ether bridges ratio of the mixed gel in the beginning of mixing are considered. The bridges ratio extremely increases when RF solution decreases (also means increasing aluminium acetylacetonate in the system). This can describe aluminium acetylacetonate accelerates condensation reaction of RF-gel. Moreover, the results can confirm that the effect from aluminium acetylacetonate concentration on RF-gel formation is stronger than effect from formaldehyde. After the mixed gel was aged for 3 days (as shown in Figure 4.22b), the bridges ratio is nearly constant when varying A/R molar ratio while the bridges ratio still increases when A/F molar ratio increases. The results can describes that in the case of varying A/R, aluminium acetylacetonate

accelerate the condensation reaction of RF-gel since the beginning of mixing. After leaving the gel, formation of RF-gel is very slowly because excess concentration of RF-gel obstructs acceleration from aluminium acetylacetonate.

(a)   (b)
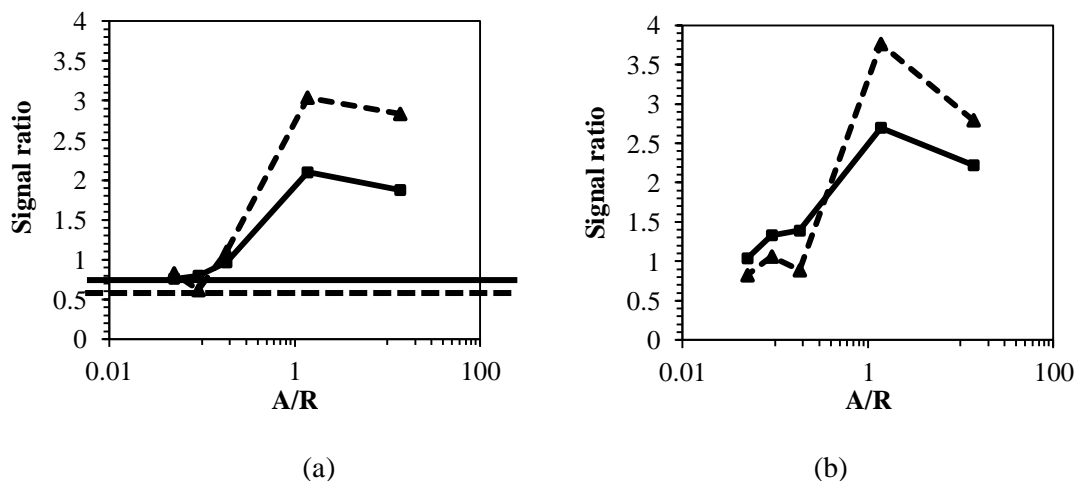
Figure 4.22   FTIR signals ratio of (■) methylene and (▲) methylene ether bridges of the mixed gel with respect to aromatic rings in the gel with varying A/R molar ratio. The mixed gel aged for (a) 0 day and (b) 3 days.

Figure 4.23 shows N_2 adsorption-desorption isotherm of synthesized alumina with varying concentration of RF-gel in the system. The all-condition isotherms are type IV which indicates the particle with mesoporous structure. Interestingly, the hysteresis loops which A/R molar ratios are 13.75, 0.18, 0.05 are H2, H1, H1 respectively. From the IUPAC classification of pore structure, H1 hysteresis loop indicates geometry pore shapes like tubular and H2 loop indicates geometry pore shapes with narrow pore size distribution [32]. This result shows the influent of RF-gel concentration on alumina pore structure.
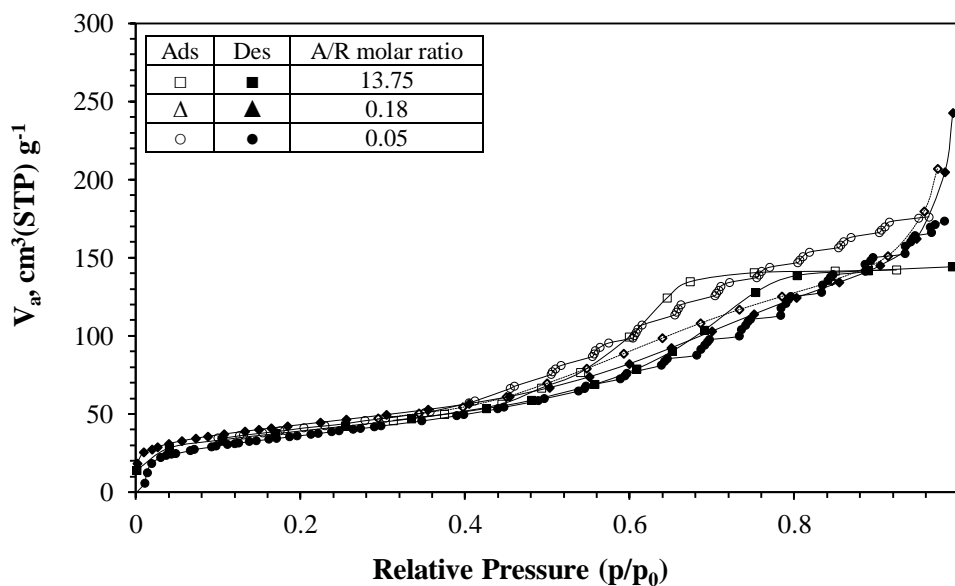
Figure 4.23 N_2 adsorption-desorption isotherm of synthesized alumina with varying A/R molar ratio.

In Figure 4.24, the pore size distribution shows all particles are mesoporous. It can be seen that the pore distribution range increases when the A/R molar ratio increases. The range of pore size distribution is narrowed when increase A/R molar ratio (decreasing concentration of RF-gel in the system). Moreover, Table 4.4 shows surface area of alumina increase when AF sol concentration decreases which optimum point is at A/R = 0.18. This confirms that RF-gel is used as template which increases surface area of alumina. Nevertheless, adding high concentration of RF-gel causes bimodal pore size distribution. The two node pore distribution can describes that there are two types of pore. These are the primary pore size which is from inter-particular void between alumina colloidal particles and secondary pore size which is from removal RF-gel carbon assisted template particles by calcination. The secondary type of pore is caused by adding excess RF-gel.
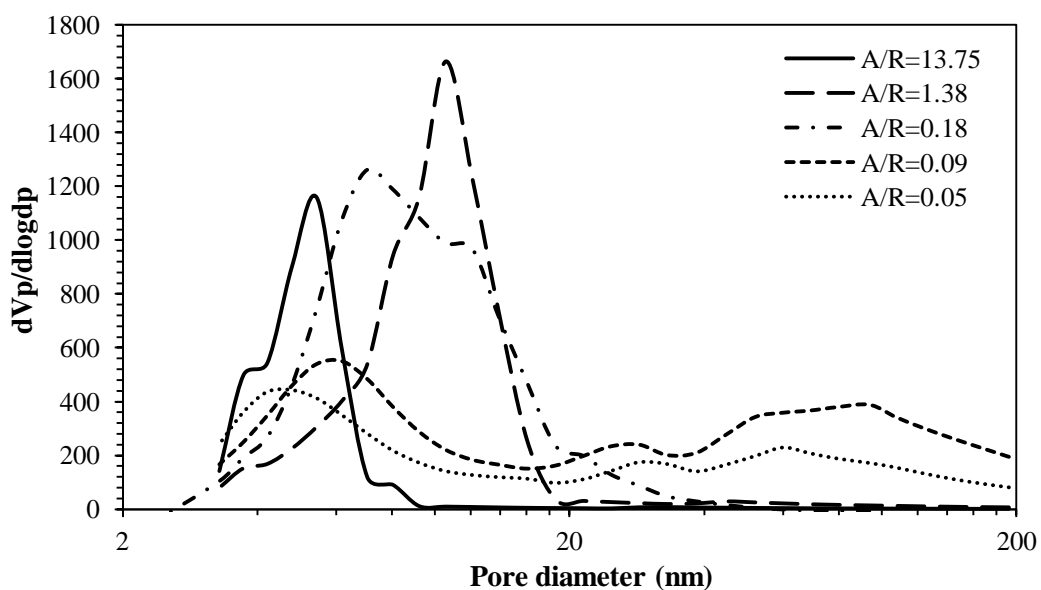
Figure 4.24 Pore size distribution of synthesized alumina with varying A/R molar ratio.

Table 4.4 Textural properties of synthesized alumina with varying A/R molar ratio.

A/R	BET surface area $(m^2/g)^a$	Average pore size $(nm)^b$	Pore volume $(cm^3/g)^b$
13.75	138.34	5.43	0.2307
1.38	164.39	10.55	0.4800
0.18	173.37	12.86	0.5574
0.09	168.84	12.44	0.5250
0.05	153.46	9.35	0.3588

[a] The BET surface areas were calculated by using BET equation.
[b] The average pore diameters and pore volumes were calculated by using BJH equation.

The schematic of particles structure which is shown below indicates the effect of RF-gel concentration on the particles forming. At the high concentration of RF-gel (low A/R), there are possibility of more aggregation between RF-gel particles. After calcination, the products have larger pore size which cause from RF-gel particles aggregation void.
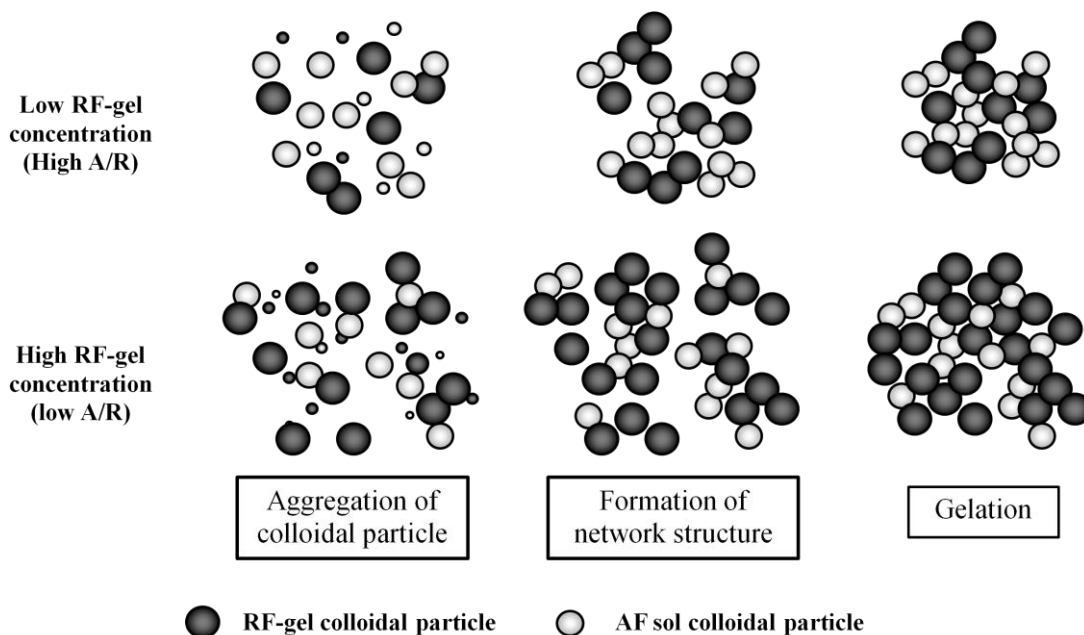
Figure 4.25 Schematic of synthesized particles structure.

4.4 EFFECTS OF ETHANOL ON SYNTHESIZED ALUMINA

Ethanol was added into the mixed gel for extending the gelation time of the mixed gel [13]. The bonds which occur in the gel were studied by FTIR spectra. The mixed gel with ethanol adding which was aged for 3 days was sampled. Finally, the textural properties of products were studied.

Absolute ethanol was used as solvent. It made the mixed gel to be dissolves with no reaction between them. This can be confirmed by FTIR spectra of Ethanol, the mixed gel and the mixed gel with ethanol in Figure 4.26. Comparing between the mixed gel with ethanol and without ethanol, there are new peaks in absorbance band of the gel with ethanol which are shown as bold lines. The peaks in wavenumber 688 and 1150 cm^{-1} correspond to O-H and C-O alcohol stretching vibration, respectively. The absorbance peaks in the interest wavenumber 1612, 1298, 1220 and 1175 cm^{-1} of the mixed gel with ethanol in the beginning of mixing and after the mixed gel was aged for 3 days remain similarly with the peak of the mixed gel without ethanol in the system. FTIR spectra of the mixed gel and the mixed gel with ethanol are considered, wavenumber 1612 and 1220 cm^{-1} show the C=C and C-H vibration of aromatic ring of resorcinol. Moreover, the wavenumber 1477 and 1092 cm^{-1} indicate methylene bridges (-CH$_2$-) and methyl ether (-CH$_2$-O-CH$_2$-) bridges of RF-gel respectively are not shifted [41, 42, 44].
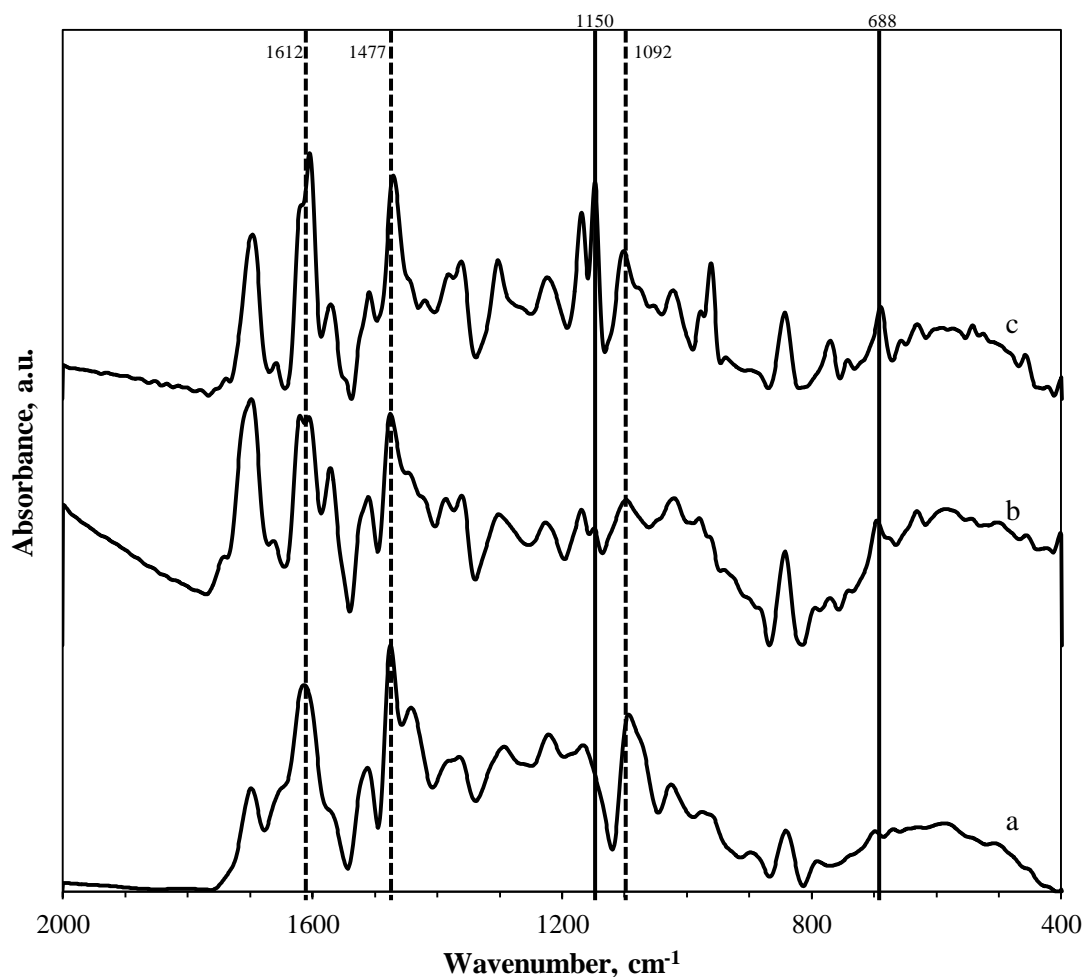
Figure 4.26 FTIR spectra of the mixed gel which were aged for 3 days (a) without adding ethanol, (b) with adding ethanol (E/R = 5.67) and (c) with adding ethanol (E/R = 28.34).

Figure 4.27 which shows comparison of the methylene and methylene ether bridges ratio between the mixed gel without ethanol and with ethanol at E/R molar ratio (at 5.67 and 28.34) is considered. In the beginning of mixing, the bridges ratios slightly change. The bridges ratios slightly decrease after the mixed gel was aged for 3 days. Interestingly, in Figure 4.27a which E/R at E/R=5.67, the bridges ratio increase at low A/F molar ratio. This means ethanol can not accelerate the condensation reaction of RF-gel. Ethanol which used as solvent only improves dispersion of the clusters. However, adding too much ethanol (E/R=28.34) obstructs formation of the bridges.
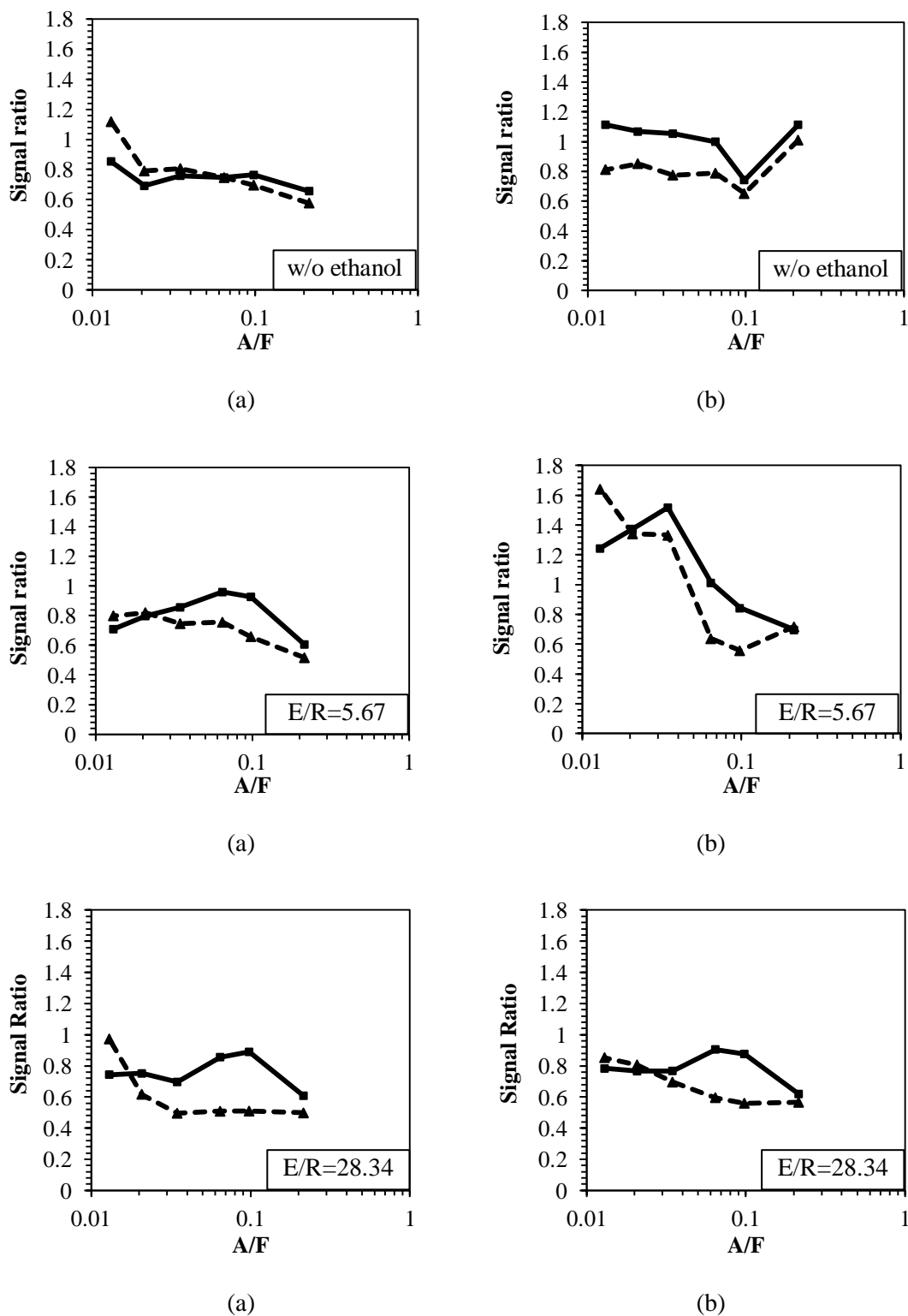
Figure 4.27 FTIR signals ratio of (■) methylene and (▲) methylene ether bridges of the mixed gel with respect to aromatic rings in the gel with varying A/F molar ratio. The mixed gel aged for (a) 0 day and (b) 3 days.

Figure 4.28 shows N_2 adsorption-desorption isotherm of synthesized alumina with varying A/F molar ratio and adding ethanol as solvent. The isotherms are still type IV with hysteresis loop which indicates the particle with mesoporous structure. From the IUPAC classification of pore structure, this hysteresis loop indicates geometry pore shapes like tubular [32].
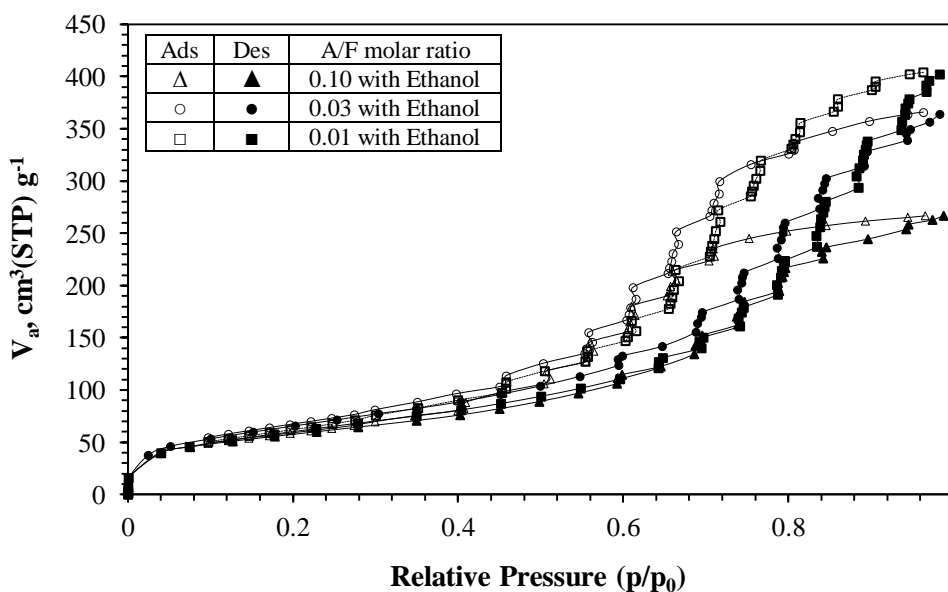
Figure 4.28 N_2 adsorption-desorption isotherm of synthesized alumina with varying A/F molar ratio in AF sol at fixed E/R molar ratio at 5.67.

Figure 4.29 shows all particles are mesoporous. From Table 4.5, the surface area of the alumina increase when ethanol is existed in the system. Pore distribution of synthesizes alumina in Figure 4.29 narrower than pore distribution without ethanol in Figure 4.18. This can confirm that ethanol can be used as solvent. Using ethanol also improves dispersion clusters in the solution. Furthermore, adding ethanol can extend the gelation time of the mixed gel [13]. This effect is appropriable for spray drying condition because the low viscous gel can be pumped into the feed stream by peristaltic pump. However, the pore distribution is bimodal at low A/F molar ratio (high formaldehyde concentration). This result can be described previously by excess formaldehyde reacting with RF-gel.

Table 4.5 Textural properties of synthesized alumina.

A/F	E/R	BET surface area $(m^2/g)^a$	pore size peak $(nm)^b$	pore volume $(cm^3/g)^b$
0.13	5.67	212.50	5.43	0.4624
0.1	5.67	207.72	5.43	0.4443
0.06	5.67	214.92	5.43	0.4676
0.03	5.67	242.21	6.18	0.6102
0.02	5.67	223.21	6.18	0.6116
0.01	5.67	223.23	7.05	0.6704
0.13	28.34	216.72	4.78	0.4438
0.10	28.34	203.62	6.18	0.4854
0.06	28.34	213.27	6.18	0.4813
0.03	28.34	326.74	6.18	0.7686
0.02	28.34	240.08	6.18	0.5959
0.01	28.34	225.83	6.18	0.5425
0.13	28.34 (after 5h aging)	225.16	4.78	0.3999
0.10	28.34 (after 5h aging)	205.63	3.29	0.3617
0.06	28.34 (after 5h aging)	225.11	5.43	0.4812
0.03	28.34 (after 5h aging)	229.01	5.43	0.5314
0.02	28.34 (after 5h aging)	230.36	5.43	0.5539
0.01	28.34 (after 5h aging)	257.52	5.43	0.5433

[a] The BET surface areas were calculated by using BET equation.
[b] The average pore diameters and pore volumes were calculated by using BJH equation.
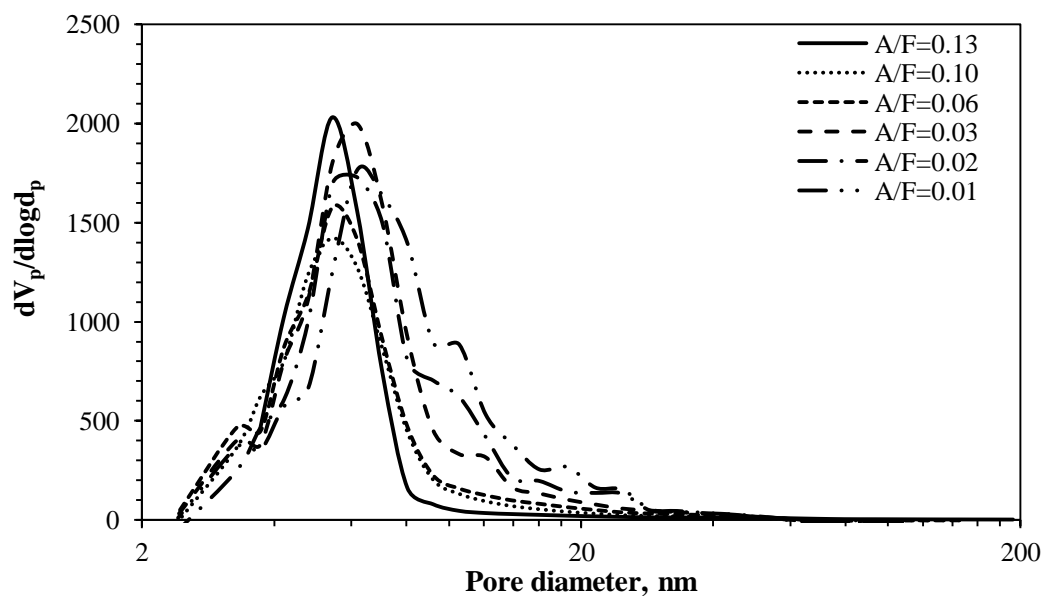
Figure 4.29 Pore size distribution of synthesized alumina with varying A/F molar ratio in AF sol and adding ethanol (E/R=5.67).

From Figure 4.30, the mixed gel with ethanol makes products overcrowd with colloidal particles comparing with the mixed gel without ethanol. This result means ethanol causes colloidal particle is able to close to neighbors more. The products have narrow pore size distribution. However, in the experiments, the mixed gel with adding ethanol can result in precipitation of the gel after the gel is aged for a long time (over a month).
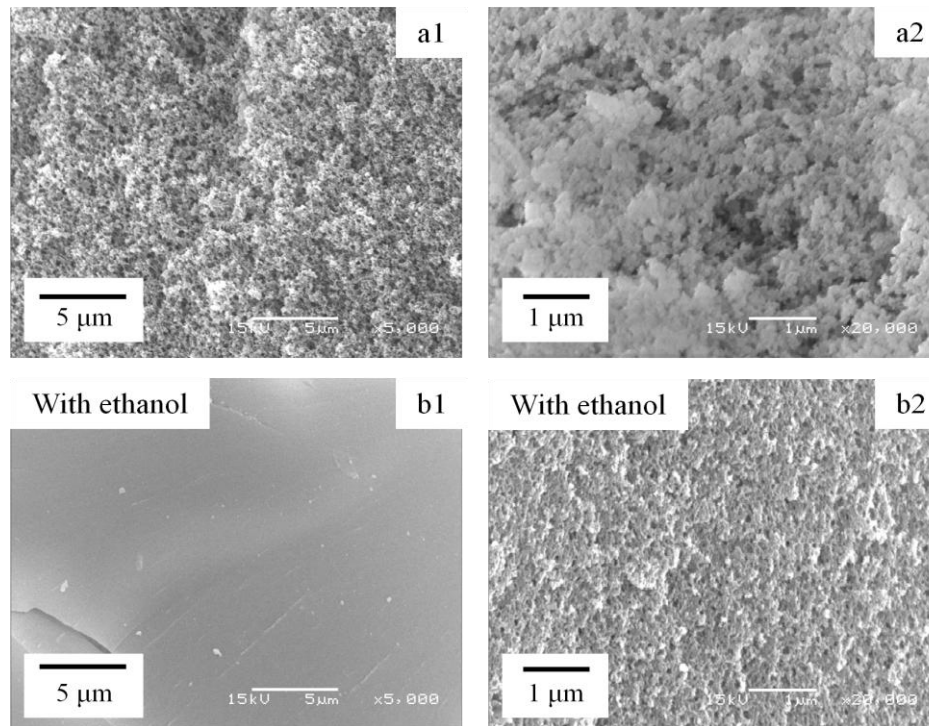
Figure 4.30 SEM images of synthesized alumina at A/F molar ratio = 0.03: (a) without ethanol and (b) with ethanol with magnification (1) 5,000x and (2) 20,000x.

In summary, adding ethanol causes colloidal particle is able to close to neighbors more. The product has uniform pore size. Furthermore, ethanol extend the gelation time of the mixed gel. This effect is appropriable for spray drying condition. The structure of colloidal particles can be described as figure below:
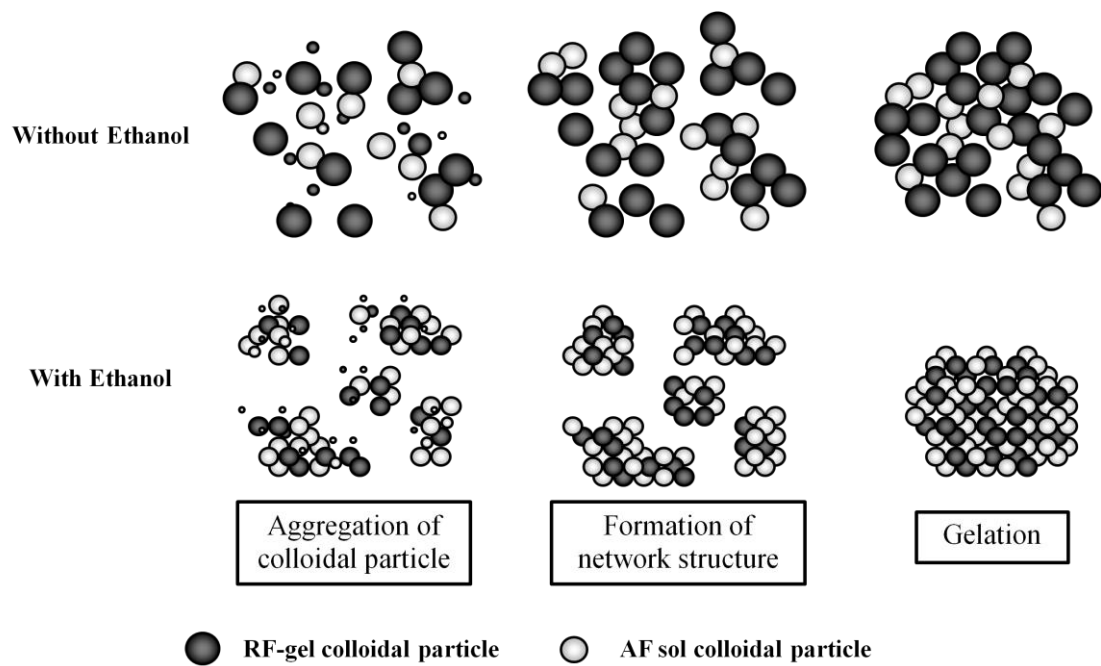
Figure 4.31 Schematic of synthesized particles structure.

From section 4.3 and 4.4, concentration of chemicals which are formaldehyde, RF-gel and Ethanol significantly affect on textural properties of bulk alumina. These effects have an impact on colloidal particles structure of the mixed gel. The structures of colloidal particles which form from the mixed gel can be summarized as figure below:
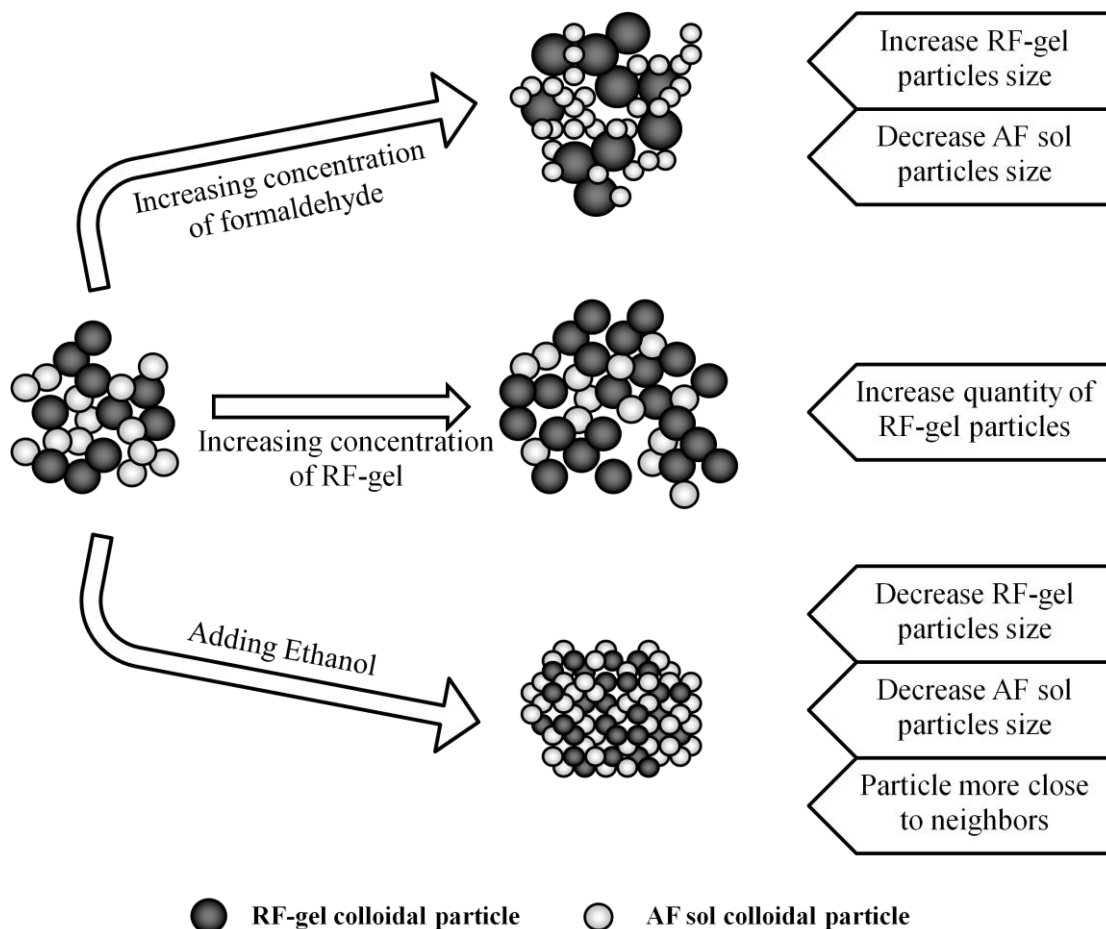
Figure 4.32 Schematic of synthesized particles structure.

4.5 EFFECTS OF SPRAY DRYING PROCESS

This part describes the alumina particles which were synthesized by the mixed gel with adding ethanol and spray dried via spray dryer.

4.5.1 TEXTURAL PROPERTIES OF SYNTHESIZED ALUMINA

All isotherms in Figure 4.33 are type IV with hysteresis loop which indicates the particle with mesoporous structure. Comparing between bulk alumina (drying via conventional dryer) and spray dried alumina; the maximum adsorption volume of bulk alumina is more than the maximum adsorption volume of spray dried alumina. Obviously, the hysteresis loop of spray dried alumina is H2 type from the IUPAC classification of pore structure while bulk alumina products cause H1 type hysteresis loop. The pore structure of H1

type is geometry i.e. tubular shape and H2 type is geometry pore shapes with narrow pore size distribution [32].
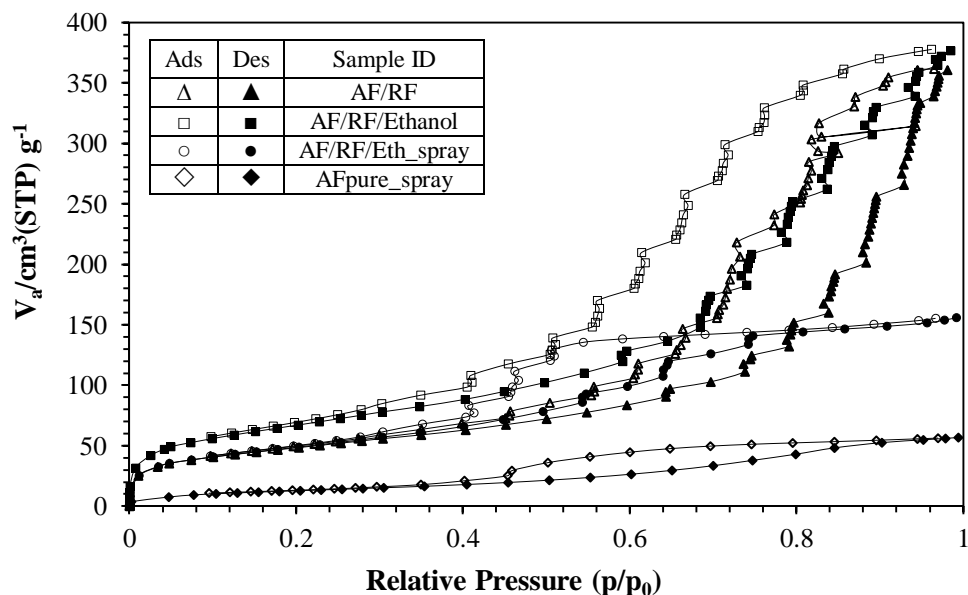
Figure 4.33 N_2 adsorption-desorption isotherm of spray dried alumina comparing with bulk alumina.

Spray drying process extremely affects the pore size distribution of alumina. In Figure 4.34, all products are mesoporous. Furthermore, spray dried alumina has pore distribution in ranges only 2-10 nm while alumina with conventional drying has pore size range 2-50 nm. The pore size distribution of spray dried alumina is narrower than pore size distribution of conventional dried alumina. This means pore size of alumina is uniform. The powders from spray drying are micron size and smaller than particles from conventional drying with grinding. The results can be explained by the drying rate of spray drying process is more than the drying rate of conventional drying. Conventional drying results in growing of colloidal particles during hold the mixed gel in the dryer. In the case of spray drying, the mixed gel is fed and formed to be powders pass through the spray dryer within several seconds. Spray drying causes smaller size of particles. Moreover, increasing drying rate (using spray dryer) increases shrinkage of the dried gel [45].

However, after calcination, the colloidal particles inside spray dried powder occur sintering easily because small powder with shrinkage can contact heat easier than large particle. The sintering makes colloidal particles melt and fuse together. The inter-particular

void between particles is minimized. The pore diameter is also uniform. The spray drying effect can reduce the surface area of particles as well.
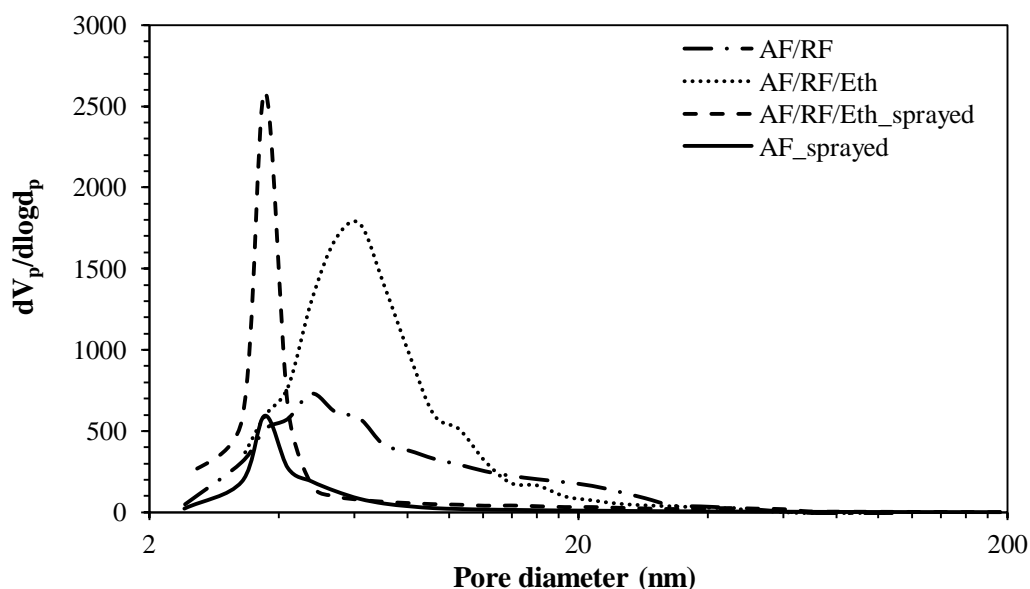
Figure 4.34 Pore size distribution of alumina comparing between spray drying process and conventional drying at A/F = 0.03.

From Table 4.6, the surface area of the alumina is reduced when using spray dryer. These results are described by sintering effect which explained above. Interestingly, the surface area of synthesized alumina which is made from AF sol only (without RF-gel assisted-template) is only 48 m^2/g. These results confirm that RF-gel is used as template which increases surface area of alumina.

Table 4.6 Textural properties of synthesized alumina comparing between conventional drying and spray drying.

Sample ID	BET surface area $(m^2/g)^a$	average pore size $(nm)^b$	pore volume $(cm^3/g)^b$
AF/RF	173.37	5.07	0.587
AF/RF/Ethanol	240.68	6.18	0.632
AF/RF/Eth_sprayed	209.18	3.72	0.315
AF_sprayed	48.46	3.72	0.100

[a] The BET surface areas were calculated by using BET equation.
[b] The average pore diameters and pore volumes were calculated by using BJH equation.

4.5.2 TEXTURAL PROPERTIES OF SYNTHESIZED ALUMINA WITH STUDYING
EFFECT OF FORMALDEHYDE

The isotherms in Figure 4.35 are type IV with hysteresis loop which indicates the particle with mesoporous structure. Obviously, the hysteresis loop of spray dried alumina with A/F 0.10 (low formaldehyde concentration) is clearly H2 type from the IUPAC classification of pore structure. The pore structure of this type is also geometry pore shapes with narrow pore size distribution [32].
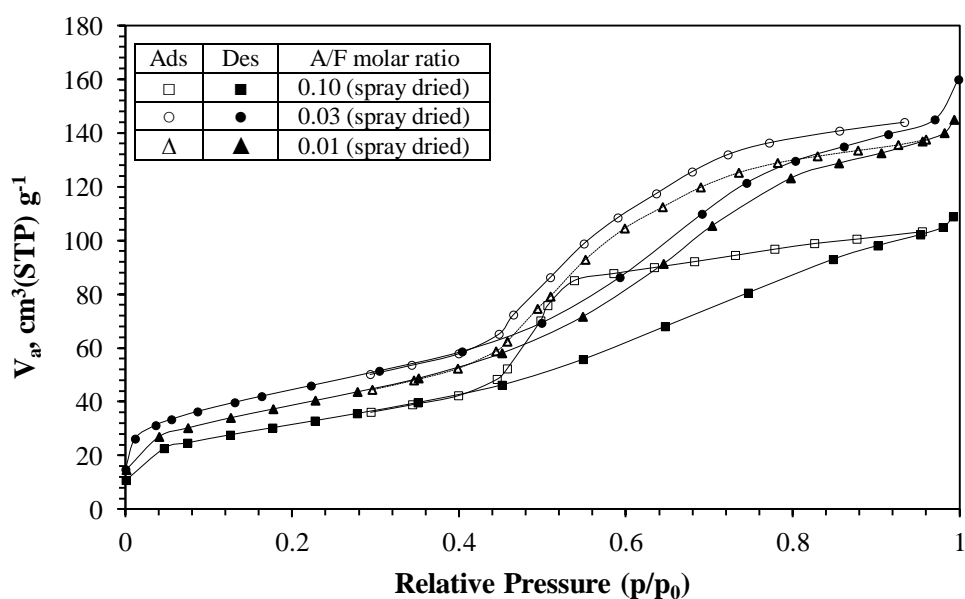
Figure 4.35 N_2 adsorption-desorption isotherm of spray dried alumina with varying A/F molar ratio in AF sol at fixed E/R molar ratio at 28.34.

From Figure 4.36, all alumina are mesoporous with the pore size distribution is narrow at low formaldehyde concentration. The broad pore size distribution also occurs when formaldehyde concentration increases. However, comparing with conventional drying at high formaldehyde concentration, all pore size distributions are narrower. Furthermore, in Table 4.7, the average pore size diameter slightly changes. This means effect from spray drying is stronger than dilute effect from formaldehyde.
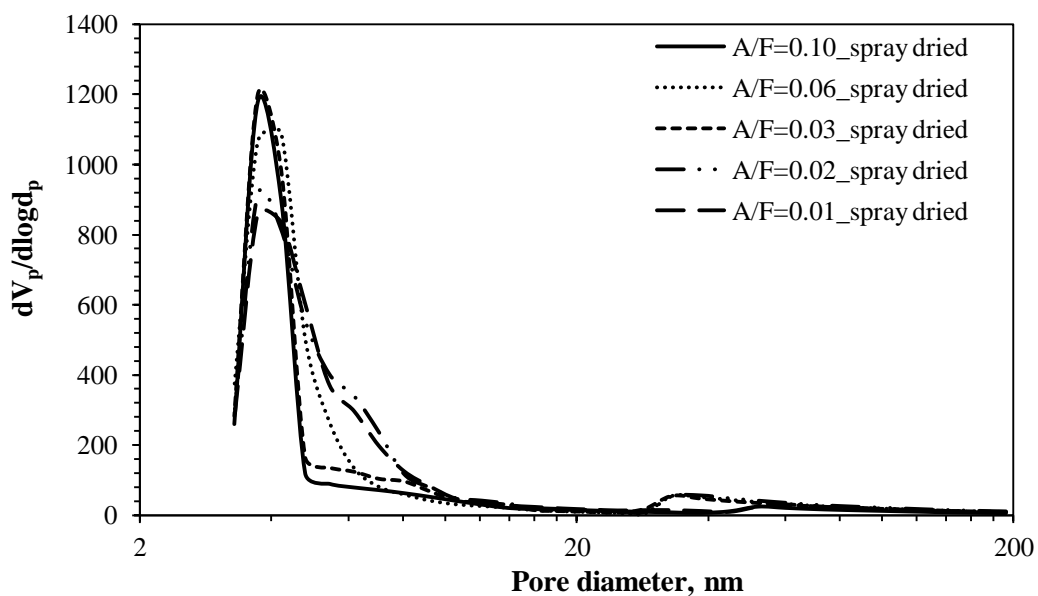
Figure 4.36   Pore size distribution of spray dried alumina with varying A/F molar ratio and with E/R = 28.34.

Table 4.7   Textural properties of synthesized alumina.

A/F	E/R	BET surface area $(m^2/g)^a$	pore size peak $(nm)^b$	pore volume $(cm^3/g)^b$
0.06	5.67	107.39	3.72	0.1722
0.03	5.67	125.5	3.72	0.2002
0.02	5.67	176.07	3.72	0.2508
0.10	28.34	115.45	4.76	0.1645
0.06	28.34	143.32	5.42	0.2145
0.03	28.34	122.80	5.42	0.1833
0.02	28.34	159.95	6.18	0.2359
0.01	28.34	141.60	5.42	0.2255

[a] The BET surface areas were calculated by using BET equation.
[b] The average pore diameters and pore volumes were calculated by using BJH equation.

4.5.3 SCANNING ELECTRON MICROSCOPY (SEM) IMAGES ANALYSIS

Figure 4.37c shows alumina which is sphere while alumina in Figure 4.37a and b cannot identify the shape certainly. The spherical granules cause from the droplets come out from the nozzle of spray dryer and were dried by hot nitrogen gas. The zooming SEM images show colloidal particle form to be granules. Although the alumina with spray drying can not

be seen as colloid particles when the SEM image is zoomed at 20,000x, the transmission electron microscopy (TEM) images in Figure 4.38 show the smaller particles of alumina which dried via spray dryer. The images confirm that spray drying process causes smaller size of particles with shrinkage.
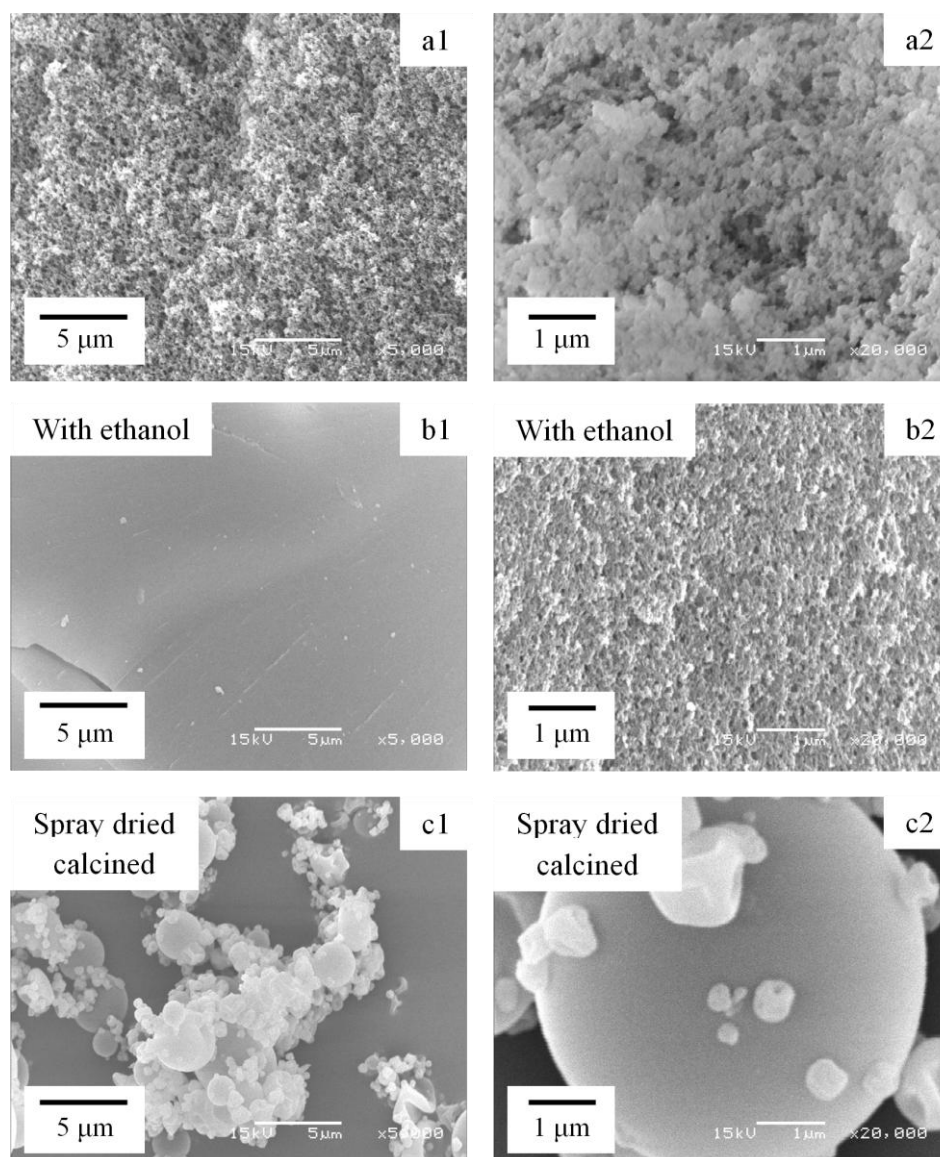

Figure 4.37 SEM images of synthesized alumina at A/F molar ratio = 0.03: (a) without ethanol (b) with ethanol and (c) spray dried/calcined with magnification (1) 5,000x and (2) 20,000x.
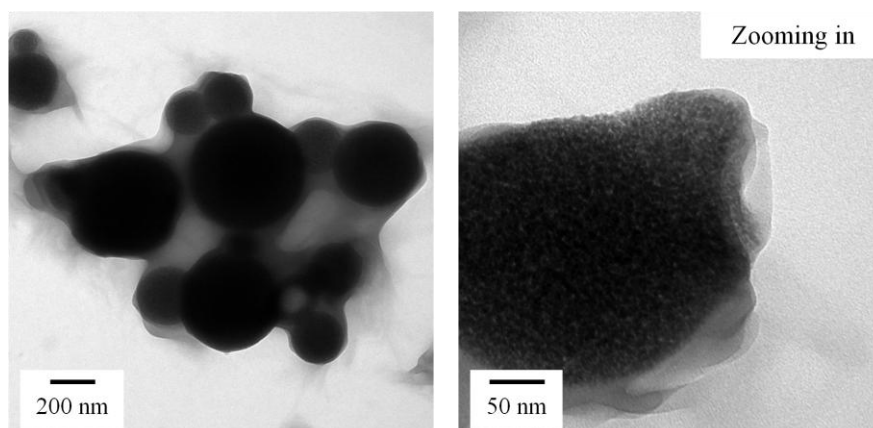
Figure 4.38 TEM images of synthesized alumina which dried via spray dryer.

Figure 4.39b shows alumina particles are sphere while alumina particles in Figure 4.39a cannot identify the shape certainly. This confirms that spray drying cause spherical-shape granules. Interesting, the 10,000x-zooming-in SEM image in Figure 4.39c shows hollow sphere granules. This shape is occurred starting with feeding nitrogen gas, simultaneously with, the mixed gel at two-feed nozzle and form to be droplets. Thus, the droplets contact dry gas within the chamber. The droplets start drying from surface to core by heat and mass transferring. Because the droplets form hard-shell outside, the gas in the droplet can come out difficultly.
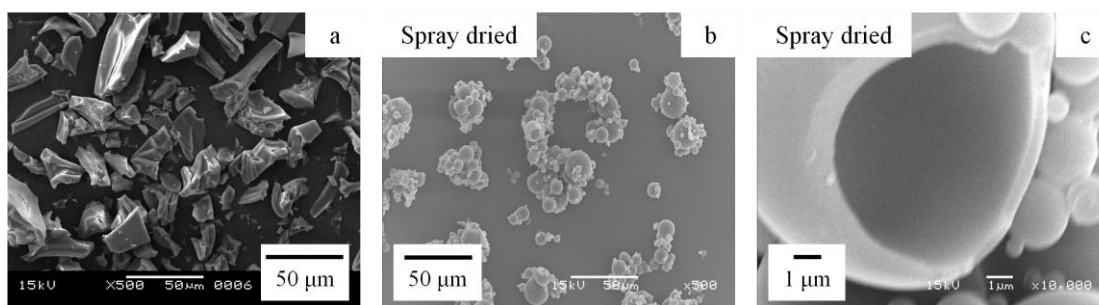
Figure 4.39 SEM images of alumina which synthesized without RF-gel template via (a) conventional drying (b) spray drying and (c) spray drying (zooming in).

In Figure 4.40 and Figure 4.41, the final granules are also smaller than before-calcined granules. This results can describes that synthesized carbon template (RF-gel) was removed after calcining at 800°C. Interestingly, Figure 4.41 can not indicate the colloidal particles size like conventional drying case. This results shows that the sintering effect is stronger than effect from varying A/F molar ratio.
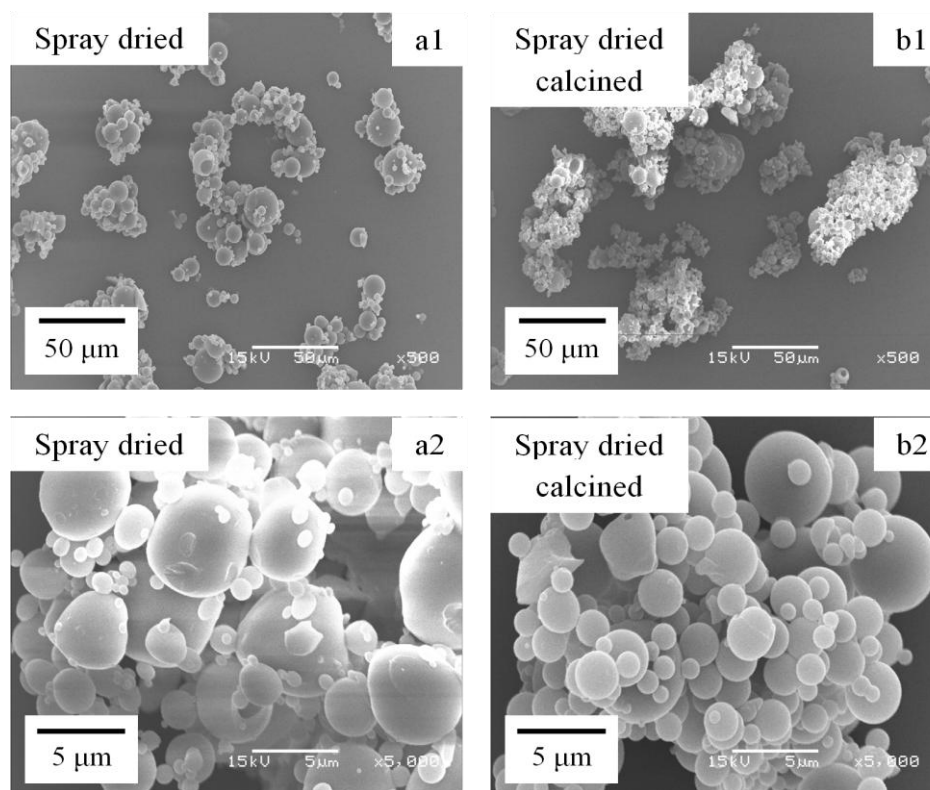
Figure 4.40 SEM images of spray dried particle which synthesized without RF-gel template: (a) before and (b) after calcined with magnification (1) 500x and (2) 5,000x.
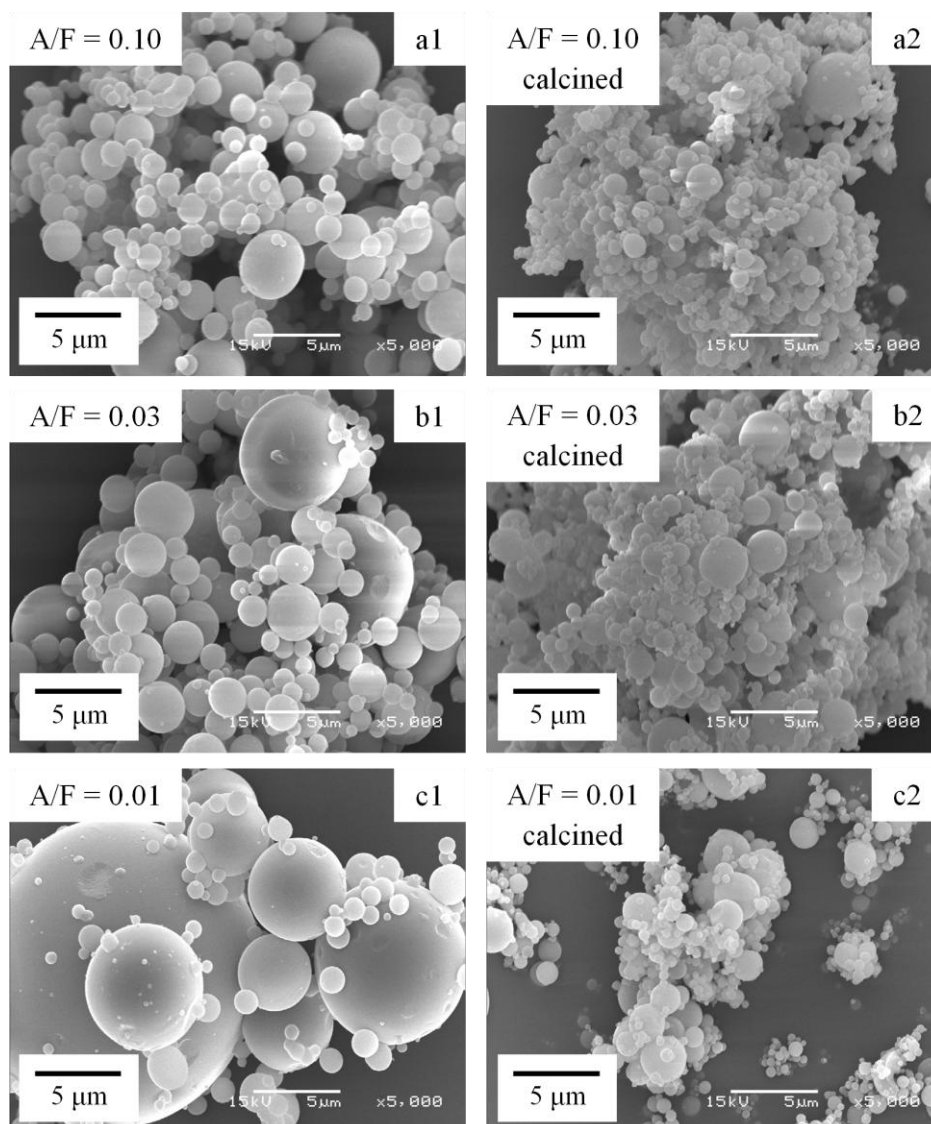
Figure 4.41 SEM images of particle with varying A/F molar ratio (a) 0.10, (b) 0.03 and (c) 0.01 after (1) spray drying and (2) calcination.

4.6 X-RAY DIFFRACTION ANALYSIS

Figure 4.42 to Figure 4.45 shows products XRD patterns. The particles were characterized for phase transformation by using X-ray diffraction analysis. The results indicate all products are alumina. The alumina particles are obtained after calcination the AF sol/RF-gel composite at 800 ℃ for 4 hours. The particles are transformed from amorphous to crystalline γ-alumina during calcination. All alumina products are in γ-phase at 800°C. This can be summarized that aluminium acetylacetonate can be used as precursor in aluminium

preformed sol process with using RF-gel as template. In Table 4.8, the crystallite sizes of synthesized alumina particles are calculated from Scherrer's equation. The crystallite sizes of products are in range 3.65 to 7.12 nm and the average crystallite size is 4.86 nm. Varying concentration of chemicals, aging time of RF-gel and AF sol and drying process have not an effect on phase transformation of alumina.
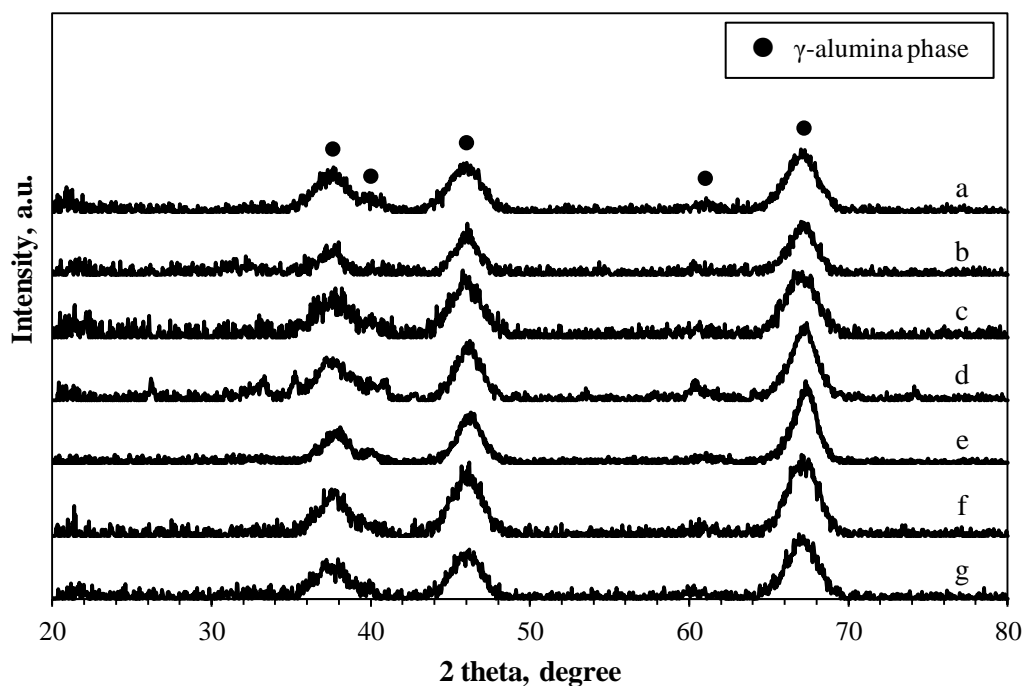
Figure 4.42 XRD patterns of the synthesized alumina with varying aging time of AF sol (a) 0 h, (b) 12 h, (C) 24 h, (d) 36 h, (e) 48 h, (f) 60 h and (g) 72 h.
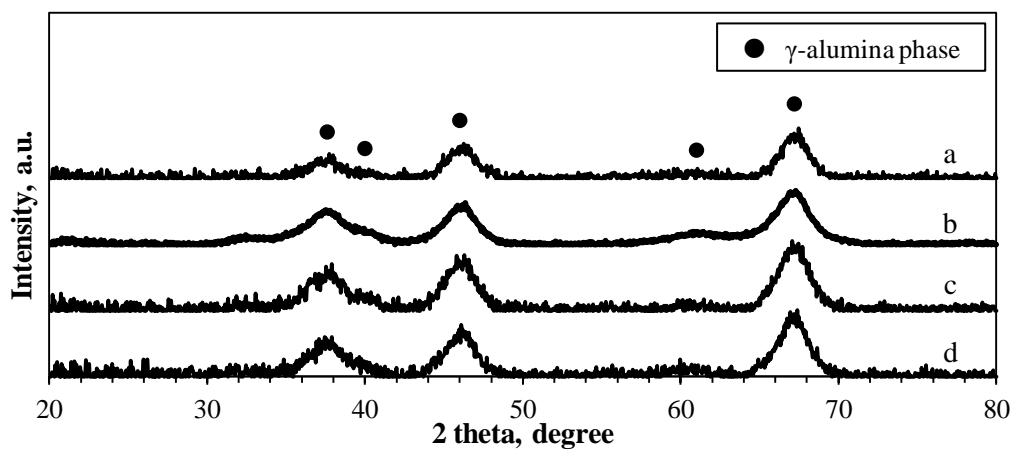
Figure 4.43 XRD patterns of the synthesized alumina with varying aging time of RF-gel (a) 0 h, (b) 7 h, (C) 14 h and (d) 21 h.

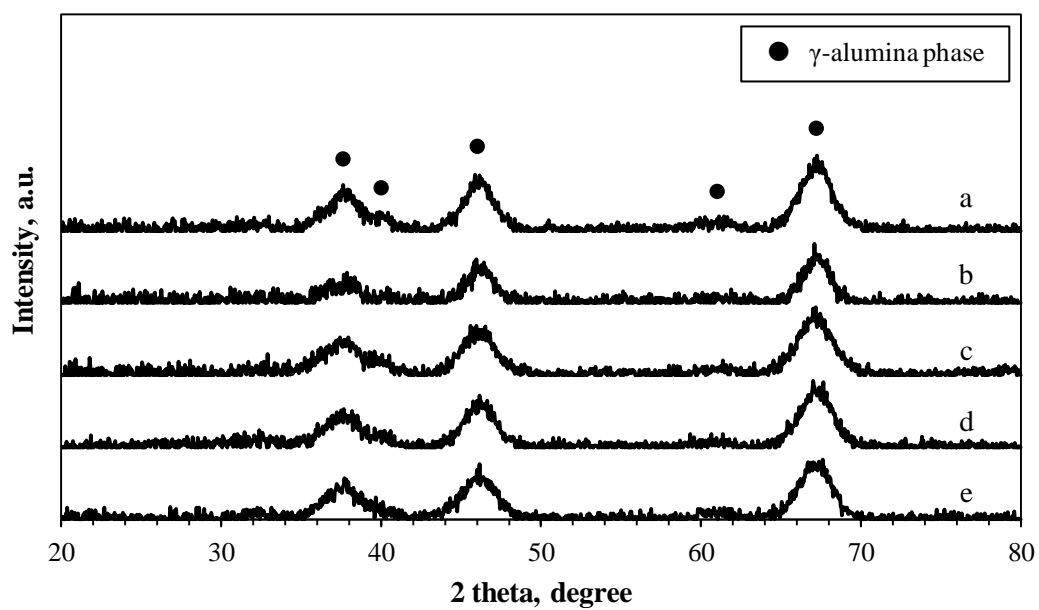**Figure 4.44** XRD patterns of the synthesized alumina with varying A/F molar ratio (a) 0.10, (b) 0.06, (C) 0.03, (d) 0.02 and (e) 0.01.
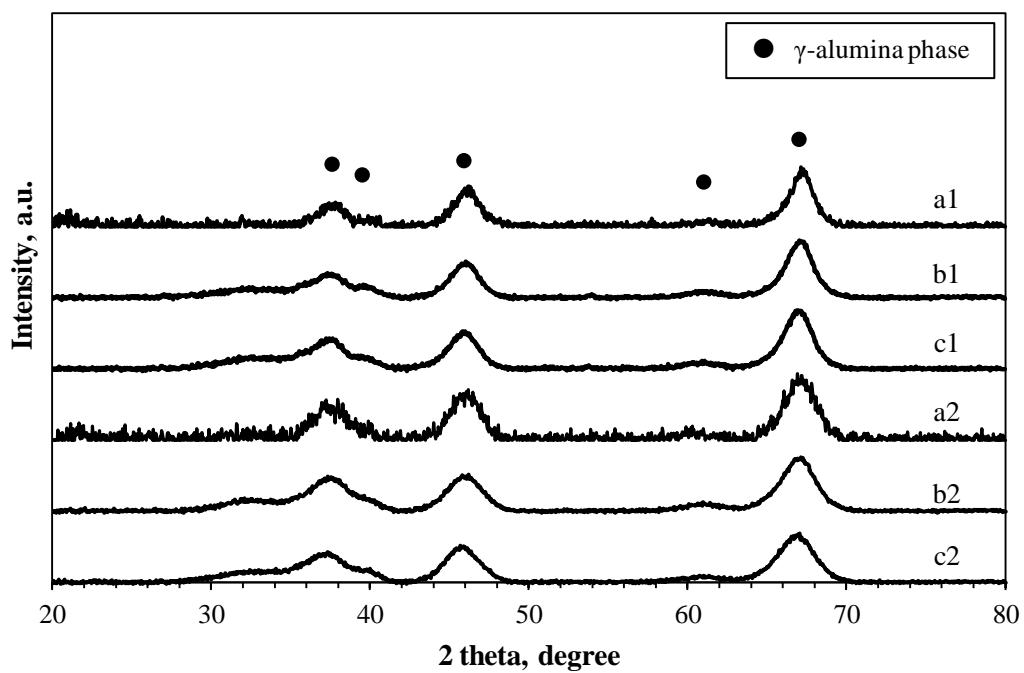
Figure 4.45 XRD patterns of the alumina which are synthesized (1) without RF-gel template and (2) with RF-gel template, (a) without ethanol, (b) with ethanol and (C) sprayed particles.

Table 4.8 Crystallite size of synthesized alumina.

A/F	Aging time of RF-gel (h)	Aging time of AF sol (h)	Crystallite Size (nm)	Remarks
0.03	-	72	5.02	Without RF-gel
0.03	-	72	5.19	With ethanol
0.03	-	72	4.60	Sprayed
0.1	21	0	4.72	-
0.1	21	12	5.57	-
0.1	21	24	4.29	-
0.1	21	36	5.89	-
0.1	21	48	7.12	-
0.1	21	60	5.01	-
0.1	0	72	6.12	-
0.1	7	72	3.76	-
0.1	14	72	4.92	-
0.1	21	72	4.61	-
0.06	21	72	4.33	-
0.03	21	72	4.14	-
0.02	21	72	4.70	-
0.01	21	72	4.21	-
0.03	21	72	4.58	With ethanol
0.03	21	72	3.65	Sprayed

Figure 4.46 shows particles which calcined in different temperature from 800 to 1200°C. These products were synthesized from the AF sol mixed with RF-gel same as this work. The alumina particles are obtained with γ-phase and stable α-phase. When the calcination temperature increases, the particles are transformed alumina phase from γ-phase to alumina α-stable phase. The temperature starts this transformation at 1100°C, approximately.

From these results, the calcination temperature is the strongest parameter that influences on phase transformation of alumina comparing with effects of drying process, aging time and concentration of chemicals [20].

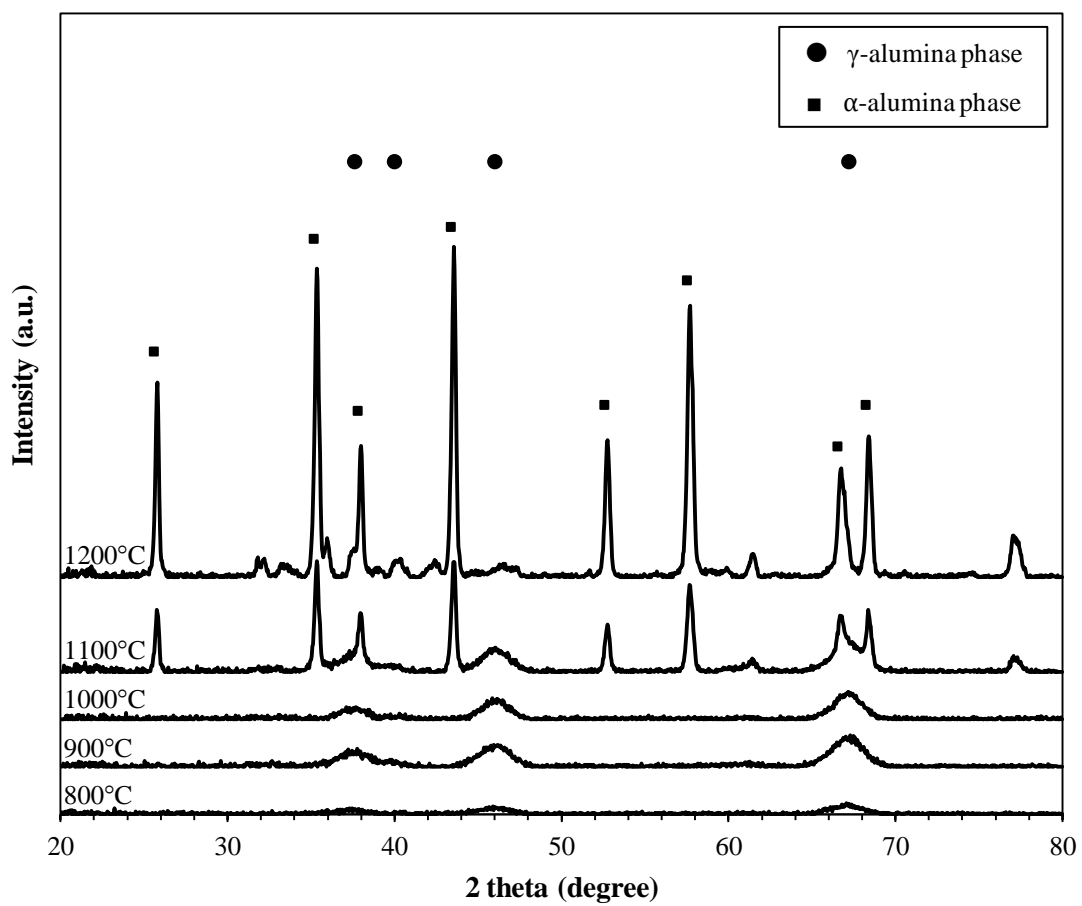**Figure 4.46** XRD patterns of the alumina products which are calcined at different temperature.

CHAPTER V

CONCLUSIONS AND RECOMMENDATIONS

5.1 SUMMARY OF THE RESULTS

The conclusions of the present research are the following:

1. Aluminium acetylacetonate can be used as precursor for synthesis of mesoporous alumina by sol-gel process with using RF-gel as synthesized carbon assisted-template.

2. Aluminium preformed sol (AF sol) accelerates the condensation reaction of resorcinol-formaldehyde gel (RF-gel) by cross-linking between aluminium acetylacetonate in the AF sol and the RF-gel.

3. All products are γ-alumina when the dried gel is calcined at 800°C. The calcination temperature is strongest effect which affects on phase transformation of the synthesized alumina.

4. Morphology and size distribution of synthesized alumina particles can be controlled by controlling aging time of RF-gel and concentration of chemicals which are formaldehyde, resorcinol and ethanol.

5. Ethanol extends the gelation time of the mixed gel which is reduced its viscosity.

6. Spray drying can be used for drying the mixed gel which is AF sol/RF-gel composite. The products have uniform pore size because of sintering in calcination.

5.2 CONCLUSION

Porous alumina can be synthesized from aluminium preformed sol using aluminium acetylacetonate as precursor. Moreover, resorcinol-Formaldehyde gel (RF-gel) can be used as assisted template to control the porosity of the synthesized alumina. All of the studied effects (i.e., aging time of the AF sol and RF-gel, concentration of chemicals and drying techniques) enhance the textural properties of alumina in difference. The aging time of RF-gel does not affect on pore size distribution of alumina particles while the results which are investigate aging time of AF sol are different. Effects from concentration of chemicals which are formaldehyde in the AF sol, RF-gel and ethanol have an impact on porosity of the product. Interestingly, effect of spray drying on porosity of the product is stronger than effects of concentration of chemicals. Spray drying makes alumina has uniform pore size. All products synthesized in the work are γ-alumina.

5.3 RECOMMENDATIONS FOR THE FUTURE STUDIES

In this studied effects of aging time, concentration of chemicals and drying process were investigated. Some recommendations for future work are listed as follows:

1. The cross-linking between aluminium acetylacetonate and formaldehyde in AF sol should be studied.

2. For product which prepared without RF-gel, the alumina is quite black. This result shows incompletely calcination. However, XRD pattern of this product is γ-alumina.

3. Although the mixed gel can be dried via spray dryer, the viscosity of the mixed gel should be investigated.

4. The different of drying temperature and drying gas between conventional drying and spray drying should be investigated.

REFERENCES

[1]   Blachou, V., Goula, D. and Philippopoulos, C. Wet milling of alumina and preparation of slurries for monolithic structures impregnation. Industrial & Engineering Chemistry Research 31 (1992): 364-369.

[2]   Keshavarz, A. R., Rezaei, M. and Yaripour, F. Preparation of nanocrystalline γ-Al$_2$O$_3$ catalyst using different procedures for methanol dehydration to dimethyl ether. Journal of Natural Gas Chemistry 20 (2011): 334-338.

[3]   Kanti, N. M. Soft solution processing for the synthesis of alumina nanoparticles in the presence of glucose. Journal of the American Ceramic Society 93 (2010): 1260-1263.

[4]   Liu, Q., et al. Synthesis, characterization and catalytic applications of mesoporous γ-alumina from boehmite sol. Microporous and Mesoporous Materials 111 (2008): 323-333.

[5]   Parida, K., Pradhan, A., Das, J. and Sahu, N. Synthesis and characterization of nano-sized porous gamma-alumina by control precipitation method. Materials Chemistry and Physics 113 (2009): 244-248.

[6]   Zhang, Z. and Pinnavaia, T. J. Mesostructured γ-Al$_2$O$_3$ with a lathlike framework morphology. Journal of the American Chemical Society 124 (2002): 12294-12301.

[7]   Xu, B., et al. Synthesis of mesoporous alumina with highly thermal stability using glucose template in aqueous system. Microporous and Mesoporous Materials 91 (2006): 293-295.

[8]   Bosco, R., et al. Alumina through sol-gel route, Influence of preparation parameters. Advances in Basic and Applied Aspects of Industrial Catalysis Studies in Surface Science and Catalysis 113 (1998): 591-598.

[9]   Sharbatdaran, M., Amini, M. M. and Majdabadi, A. Effect of aluminium alkoxide with donor-functionalized group on texture and morphology of the alumina prepared by sol–gel processing. Materials Letters 64 (2010): 503-505.

[10]   Ritter, J. A. and Al-Muhtaseb, S. A. Preparation and properties of resorcinol-formaldehyde organic and carbon gels. Advanced Materials 15 (2003): 101-114.

[11]   Anu, P. M. U. and Rajendra, S. Synthesis of nanoporous metal oxides through the self-assembly of phloroglucinol–formaldehyde resol and tri-block copolymer. Journal of Colloid and Interface Science 358 (2011): 399-408.

[12]   Masters, K. Spray drying handbook. Longman Scientific and Technical,1991.

[13]   Qin, G. and Guo, S. Preparation of RF organic aerogels and carbon aerogels by alcoholic sol–gel process. Carbon 39 (2001): 1929 –1941.

[14]   Pekala, R. W. Organic aerogels from the polycondensation of resorcinol with formaldehyde. Journal of Materials Science 24 (1989): 3221-3227.

[15]   Bertrand, G., et al. Influence of slurry characteristics on the morphology of spray-dried alumina powders. Journal of the European Ceramic Society 23 (2003): 263-271.

[16]   Ivanov, V., Boehme, R. and Schumacher, G. Dynamic compaction of nanosized ceramic oxide powders. Material Science Forum 225 (1996): 623 - 628.

[17]   Duran, P. Processing of nanocrystalline ceramic powders. Boletin de la Sociedad Espanola de Ceramica 5 (1999): 403 - 415.

[18]   Ruihong, Z., Fen, G., Hu Yongqui, Z. and Huanqi. Self-assembly synthesis of organized mesoporous alumina by precipitation method in aqueous solution. Microporous and Mesoporous Materials 93 (2006): 212.

[19]   Cain, M. and Morrell, R. Nanostructured ceramics: a review of their potential. Applied Organometallic Chemistry - A European Journal 15 (2001): 321 - 330.

[20]   Venkatesh, R. and Ramanan, S. R. Influence of processing variables on the microstructure of sol-gel spun alumina fibres. Materials Letters 55 (2002): 189-195.

[21]   Santos, P. S., Santos, H. S. and Toledo, S. P. Standard transition aluminas. electron microscopy studies. Materials Research 3 (2000): 104-114.

[22]   Paglia, G., et al. The boehmite-derived γ-alumina system I: structural evolution with temperature, with the identification and structural determination of a new transition phase, γ-alumina. Chemistry of Materials 16 (2004): 220-236.

[23]   Maĉedo, M. I. F. Sol-gel synthesis of transparent alumina gel and pure gamma alumina by urea hydrolysis of aluminum nitrate. Journal of Sol-Gel Science and Technology 30 (2004): 135-140.

[24]   Wang, S., Li, X., Li, Y. and Zhai, Y. Synthesis of γ-alumina via precipitation in ethanol. Materials Letters 62 (2008): 3552-3554.

[25]   O'Donoghue, M. A guide to man-made gemstones. Great Britain: Van Nostrand Reinhold Company,1983.

[26]   Kung, H. H. and Ko, E. I. Preparation of oxide catalysts and catalyst supports-a review of recent advances. The Chemical Engineering Journal 64 (1996): 203-214.

[27]   Ruben, G. C., Pekala, R. W., Tillotson, T. M. and Hrubesh, L. W. Imaging aerogels at the molecular level. Journal of Materials Science 27 (1992): 4341-4349.

[28]   Lin, C. and Ritter, J. A. Novel synthesis of porous carbons with tunable pore size by surfactant-templated sol–gel process and carbonisation. Carbon 35 (1997): 1271.

[29]   Patel, R. P., Patel, M. P. and Suthar, A. M. Spray drying technology: an overview. Indian Journal of Science and Technology 2 (2009): 44-47.

[30] Kimura, T., Suzuki, N., Gupta, P. and Yamauchi, Y. Effective mesopore tuning using aromatic compounds in the aerosol-assisted system of aluminium organophosphonate spherical particles. Dalton Transactions 39 (2010): 5139.

[31] Pitchumani, R., Heiszwolf, J. J., Schmidt-Ott, A. and Coppens, M. O. Continuous synthesis by spray drying of highly stable mesoporous silica and silica–alumina catalysts using industrial raw materials. Microporous and Mesoporous Materials 120 (2009): 39-46.

[32] Kaneko, K. Determination of pore size and pore size distribution 1. Adsorbents and catalysts. Journal of Membrane Science 96 (1994): 59-89.

[33] Frey, R. G. and Halloran, J. W. Compaction behavior of spray-dried alumina. Journal of the American Ceramic Society 67 (1984): 199-203.

[34] Bruinsma, P. J., Kim, A. Y., Liu, J. and Baskaran, S. Mesoporous silica synthesized by solvent evaporation: spun fibers and spray-dried hollow spheres. Chemistry of Materials 9 (1997): 2507-2512.

[35] Lind, A., et al. Spherical silica agglomerates possessing hierarchical porosity prepared by spray drying of MCM-41 and MCM-48 nanospheres. Microporous and Mesoporous Materials 66 (2003): 219-227.

[36] Klug, H. P. and Alexander, L. E. X-Ray diffraction procedures: for polycrystalline and amorphous materials. Wiley-VCH,1974.

[37] Caballero, F. P. and Koel, M. Preparation of nanostructured carbon materials. Proceedings of the Estonian Academy of Sciences 57 (2008): 48-53.

[38] Elsayed, M. A. and Heslop, M. J. Preparation and structure characterization of carbons prepared from resorcinol-formaldehyde resin by CO2 activation. Adsorption 13 (2007): 299-306.

[39] Li, W. C. and Guo, S. C. Characterization of the microstructures of organic and carbon aerogels based upon mixed cresol-formaldehyde. Carbon 39 (2001): 1989-1994.

[40]   Czarnecki, A. Determination of integrated intensities of overlapped IR bands by curve-fitting, Fourier self-deconvolution and a combination of both methods. Spectrochimica Acta - Part A Molecular Spectroscopy 52 (1996): 1593-1601.

[41]   Poljanšek, I. and Krajnc, M. Characterization of phenol-formaldehyde prepolymer resins by in line FT-IR spectroscopy. Acta Chimica Slovenica (2005): 238-244.

[42]   Coates, J. Interpretation of infrared spectra, a practical approach. Encyclopedia of Analytical Chemistry (2000): 10815-10837.

[43]   Petricevic, R., Glora, M. and Fricke, J. Planar fibre reinforced carbon aerogels for application in PEM fuel cells. Carbon 39 (2001): 857-867.

[44]   Lia, W. C., Lub, A. H. and Guoa, S. C. Characterization of the microstructures of organic and carbon aerogels based upon mixed cresol–formaldehyde. Carbon 39 (2001): 1989-1994.

[45]   Tamon, H., Ishizaka, H., Yamamoto, T. and Suzuki, T. Influence of freeze-drying conditions on the mesoporosity of organic gels as carbon precursors. Carbon 38 (2000): 1099.

APPENDICES

APPENDIX A

FTIR SPECTRA OF THE MIXED GEL

From section 4.2.1, FTIR spectra of the mixed gel combined with varying aging time of AF sol and RF-gel was studied. All spectra are shown in these figures as follow:
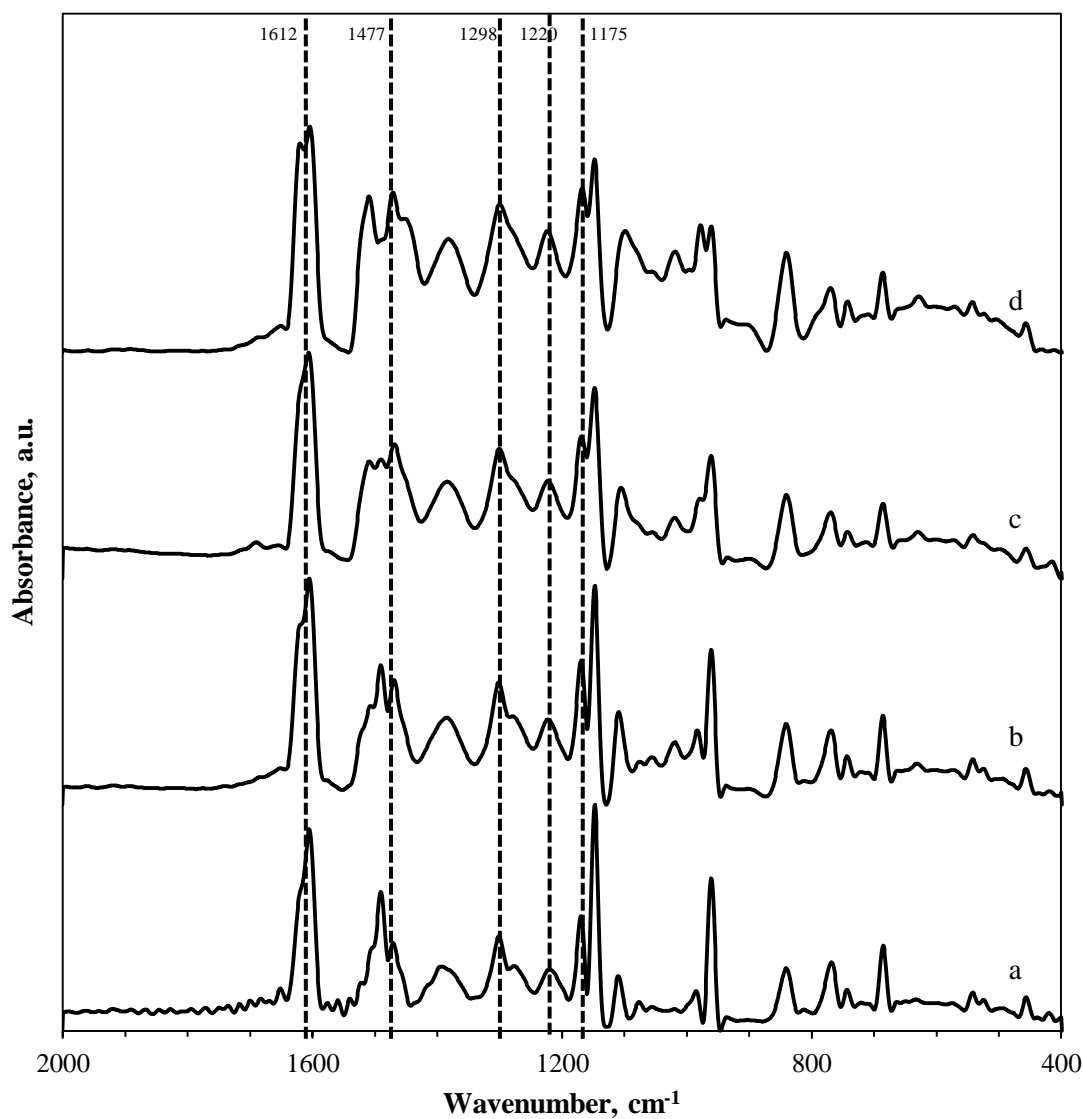

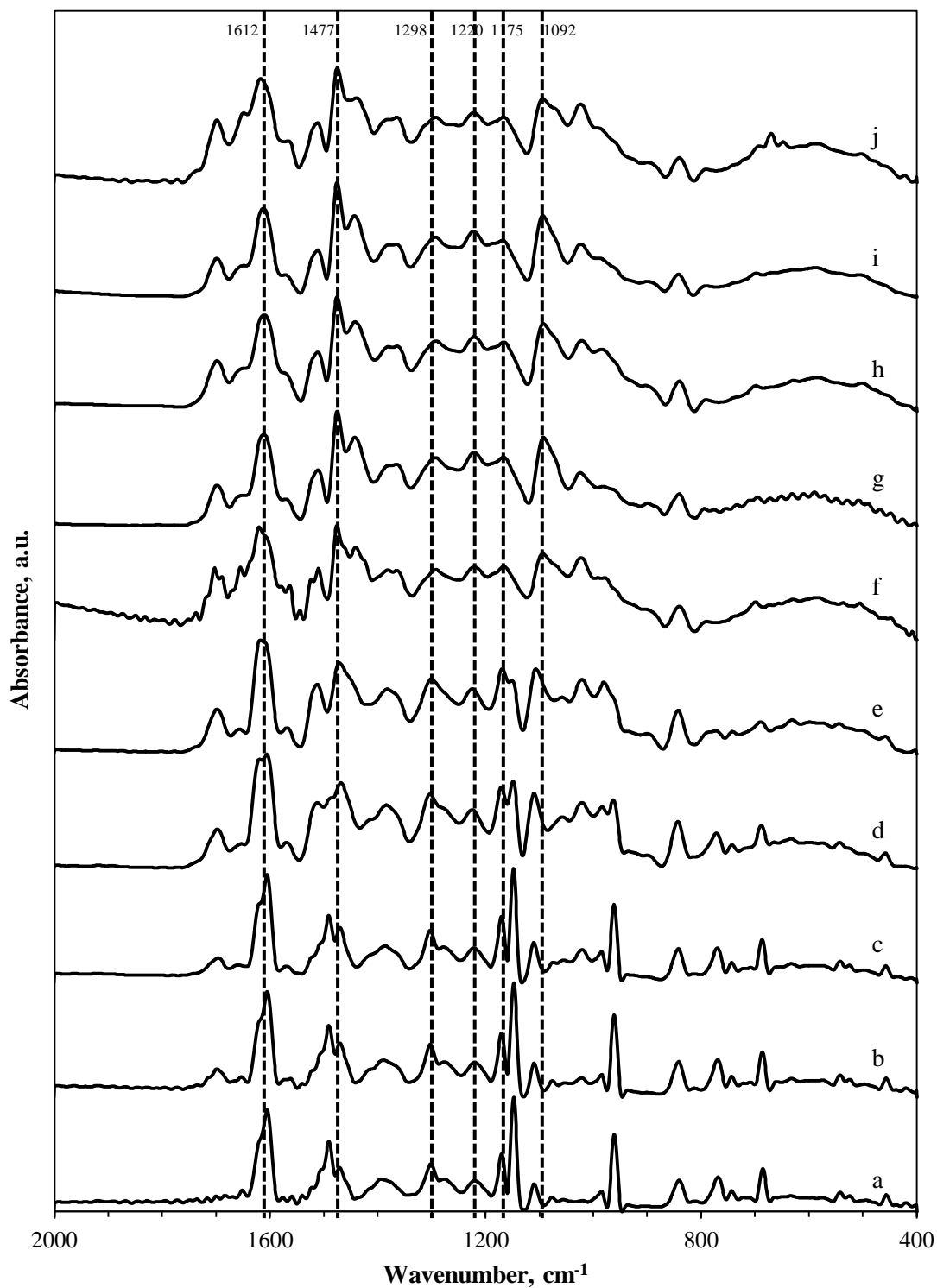**Figure A.1** FTIR spectra of the RF-gel aged for (a) 0 h, (b) 7 h, (c) 14 h and (d) 21 h.

Figure A.2 FTIR spectra of the 0-hour-aged RF-gel combined with 3-day-aged AF sol (a) before mixing (b) after mixing and aged for (c) 4 h, (d) 7 h, (e) 15 h, (f) 25 h, (g) 40 h, (h) 50 h, (i) 60 h and (j) 72 h.
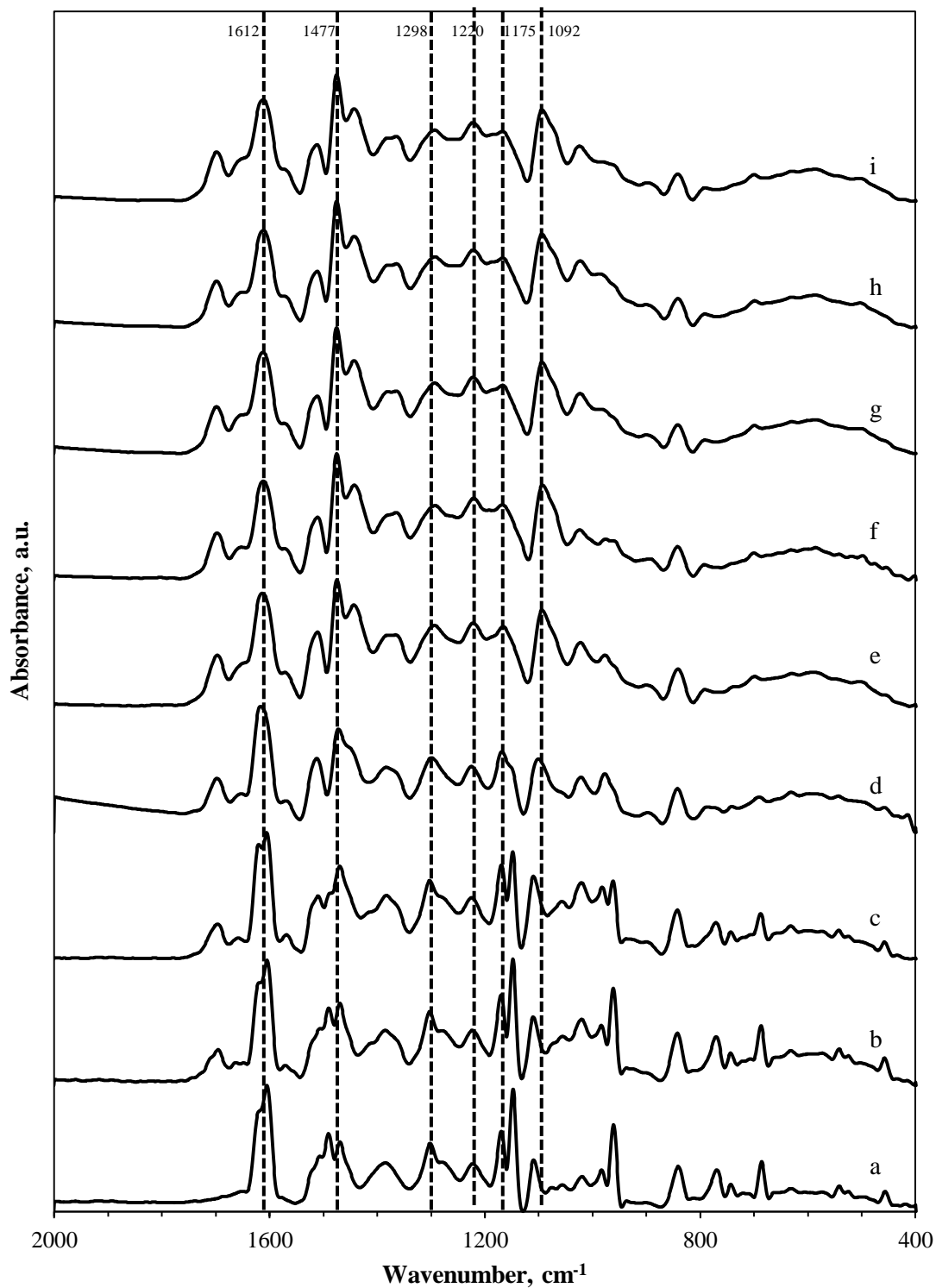
Figure A.3 FTIR spectra of the 7-hour-aged RF-gel combined with 3-day-aged AF sol (a) before mixing (b) after mixing and aged for (c) 10 h, (d) 15 h, (e) 25 h, (f) 40 h, (g) 50 h, (h) 60 h and (i) 72 h.
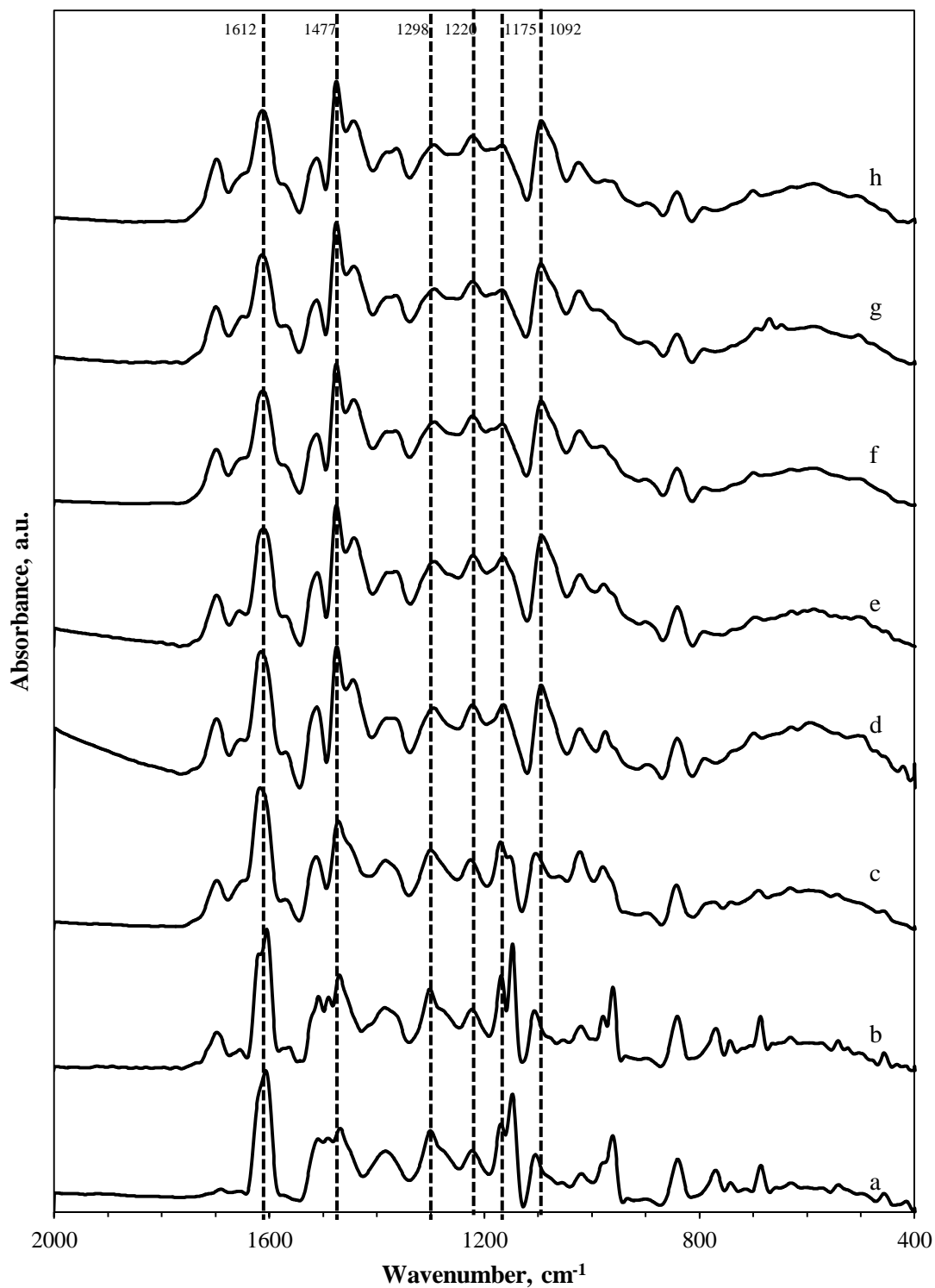
Figure A.4 FTIR spectra of the 14-hour-aged RF-gel combined with 3-day-aged AF sol (a) before mixing (b) after mixing and aged for (c) 15 h, (d) 25 h, (e) 40 h, (f) 50 h, (g) 60 h and (h) 72 h.
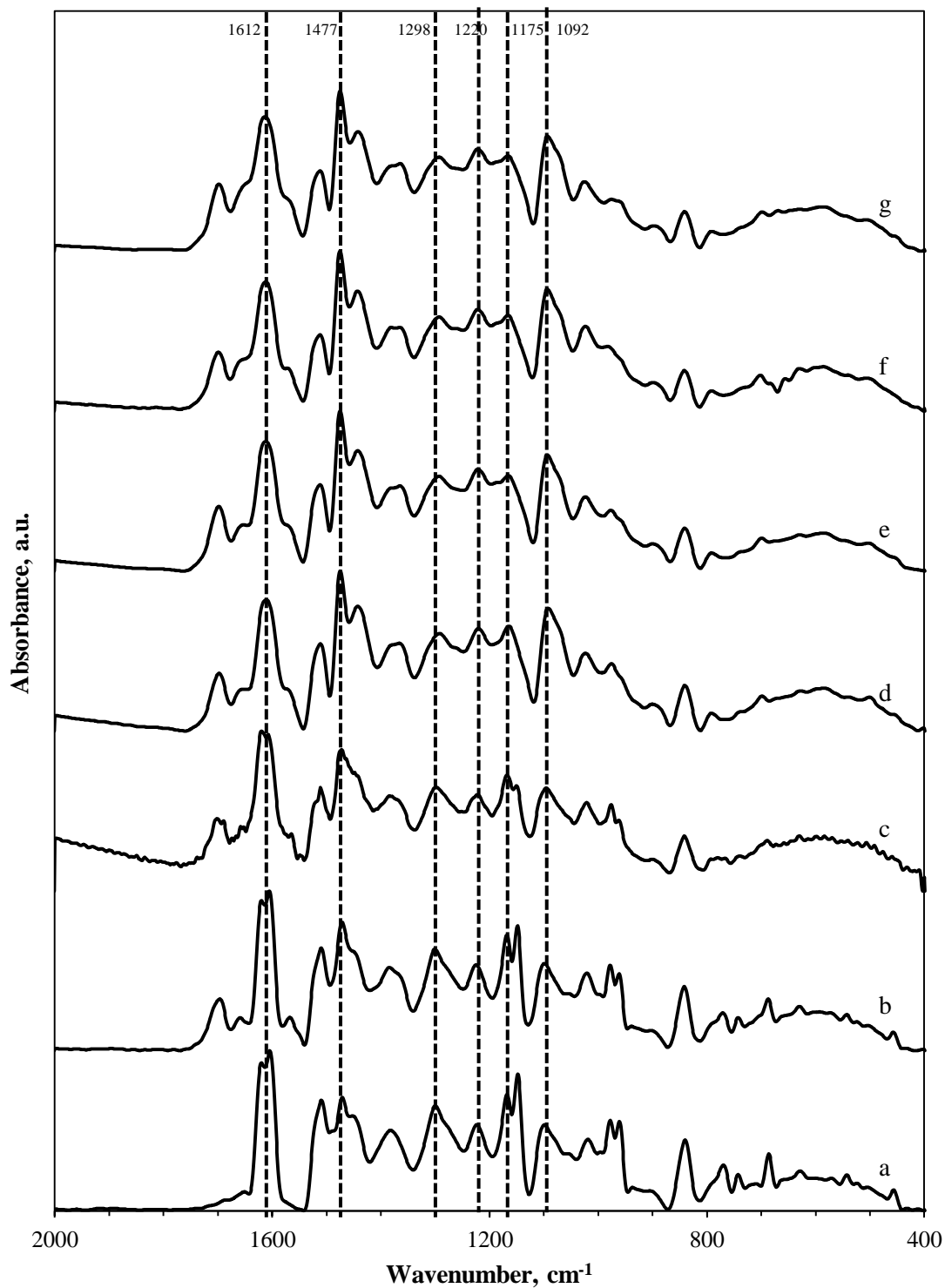
Figure A.5 FTIR spectra of the 21-hour-aged RF-gel combined with 3-day-aged AF sol (a) before mixing (b) after mixing and aged for (c) 25 h, (d) 40 h, (e) 50 h, (f) 60 h and (g) 72 h.
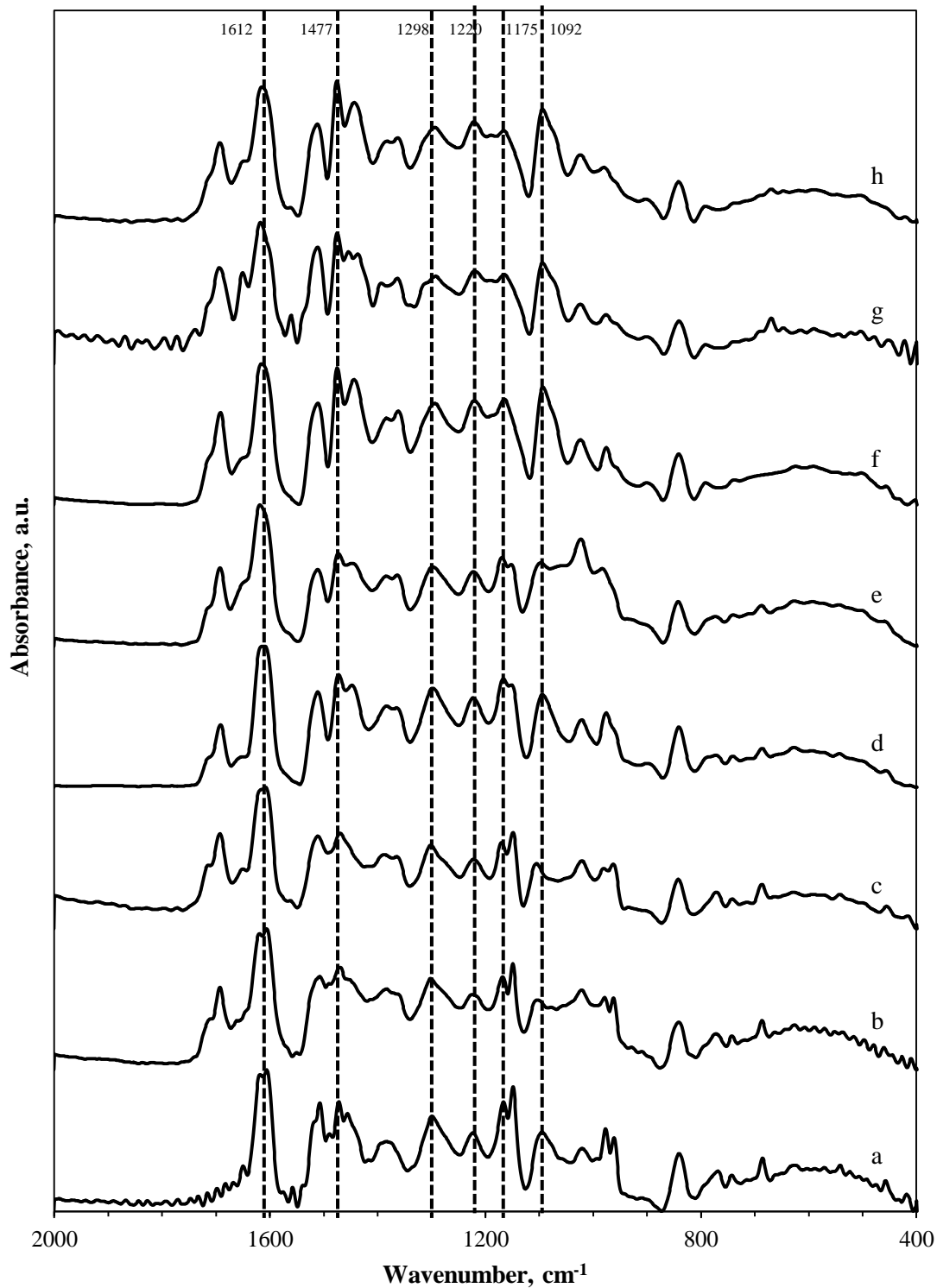
Figure A.6 FTIR spectra of the 21-hour-aged RF-gel combined with 0-day-aged AF sol
(a) before mixing (b) after mixing and aged for (c) 25 h, (d) 30 h, (e) 36 h, (f)
48 h, (g) 60 h and (h) 72 h.

Figure A.7 FTIR spectra of the 21-hour-aged RF-gel combined with 1-day-aged AF sol (a) before mixing (b) after mixing and aged for (c) 25 h, (d) 30 h, (e) 36 h, (f) 48 h, (g) 60 h and (h) 72 h.

Figure A.8 FTIR spectra of the 21-hour-aged RF-gel combined with 2-day-aged AF sol (a) before mixing (b) after mixing and aged for (c) 25 h, (d) 30 h, (e) 36 h, (f) 48 h, (g) 60 h and (h) 72 h.
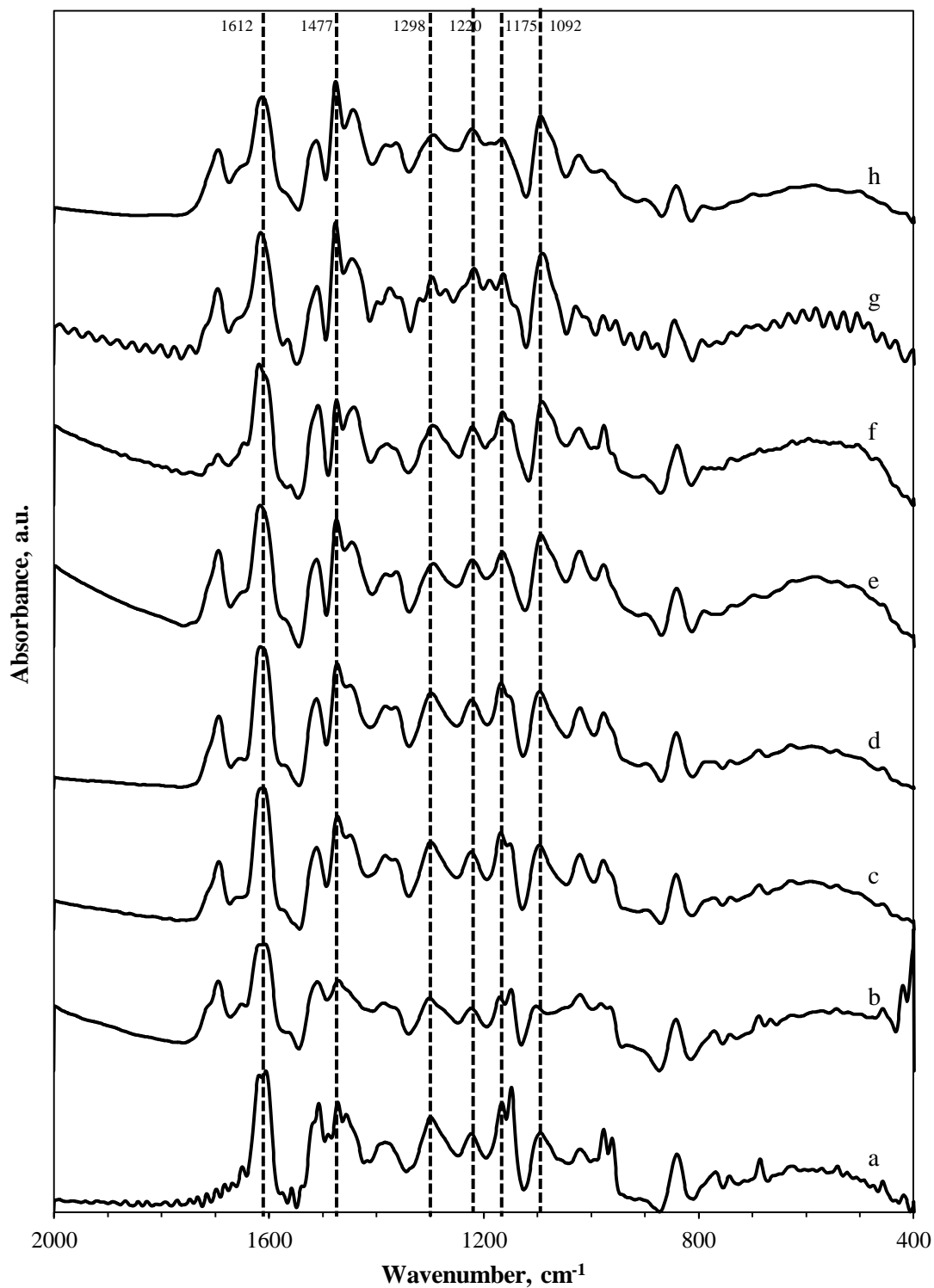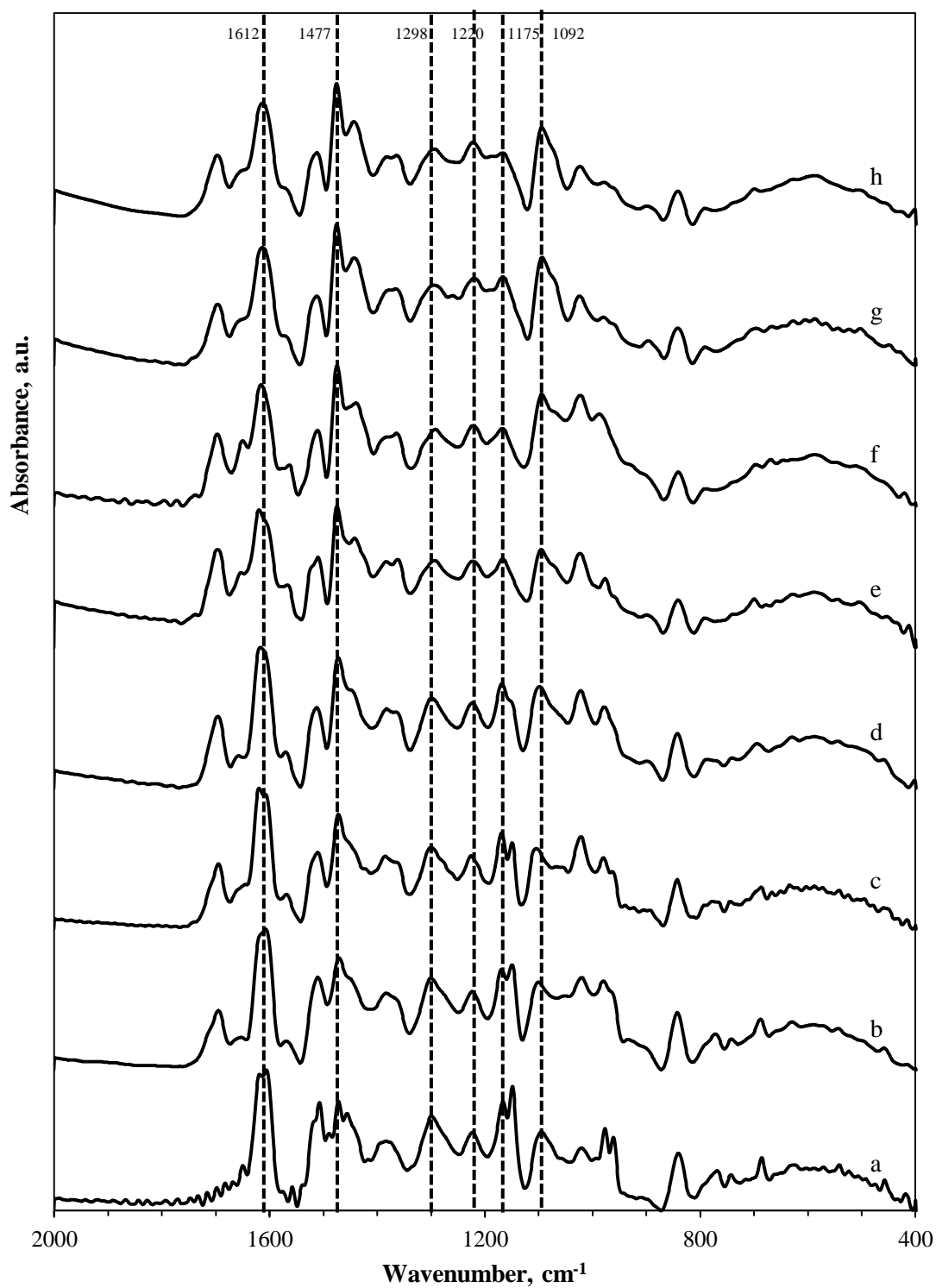
APPENDIX B

MASS LOSING OF AF SOL/RF-GEL COMPOSITE

B.1 THERMAL GRAVIMETRIC ANALYSIS (TGA) AND SCANNING ELECTRON MICROSCOPE

In this part, the aluminium preformed sol/RF-gel composite was studied the thermal decomposition by thermal gravimetric analysis in oxygen atmosphere. The dried mixed gel was studied the mass losing by calcining at 25°C until 800°C.

Figure B.1 shows mass losing of the dried mixed gel by calcining until 800°C from thermal gravimetric analyzer. During the composite particles was heating until 450°C, mass of particles was extremely decreased. Moreover, the weight of synthesized alumina which is shown in Table B.1 was slightly changed between process occured. The lossing weight indicates the carbon was removed from the particles. Carbon was clearly removed from the particle after calcination at 800°C.
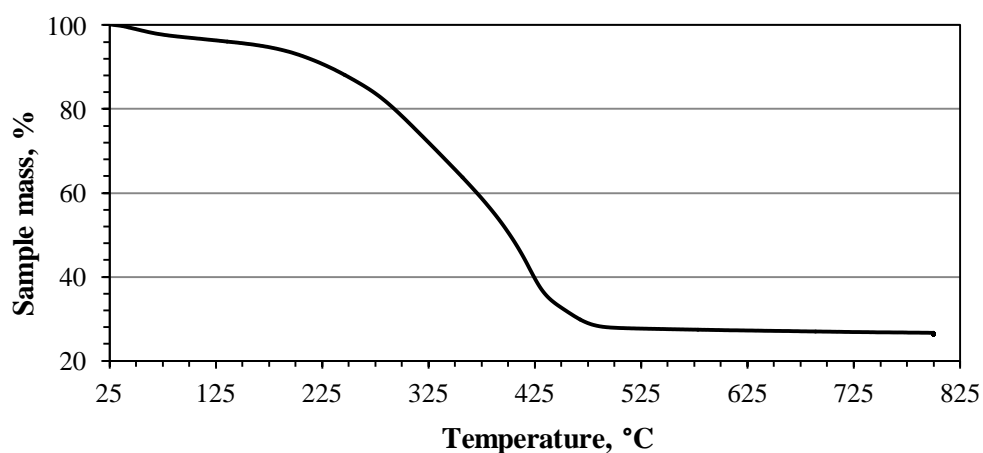

Figure B.1 Results from TGA analysis for the aluminium preformed sol/RF-gel composite.

Table B.1 Mass losing of the dried mixed gel and synthesized alumina.

Sample ID	Mass loss (%)
AF sol/RF-gel composite	70.28
Alumina (after calcined)	0.92

B.2 ENERGY DISPERSIVE X-RAY SPECTROMETER (SEM/EDX) QUANTITATIVE ANALYSIS

SEM/EDX quantitative analysis which obtained from shooting the SEM sample by X-ray can confirm that the products are alumina particles after calcination at 800°C. In Table B.2, the quantities of carbon atom (C) are about 4% which is less than sample before calcination which C atom over 40%.

Table B.2 EDX quantitative analysis of the example particles before and after calcination.

Sample ID	Atom count (%)		
	C	O	Al
AF sol/RF-gel composite	45.38	45.52	9.10
Alumina (after calcined)	3.57	47.29	49.15

VITA

Miss Sukruthai Sapniwat was born on April 29th, 1988 in Patumthani Province, Thailand. She received the Bachelor's Degree of Engineering with major in Chemical Engineering from Chulalongkorn University, Bangkok, Thailand in April 2010. She entered the master of Engineering in Chemical Engineering at Chulalongkorn University, Bangkok, Thailand in May 2010.

LIST OF PUBLICATION

1. Sukruthai Sapniwat, Apinan Soottitantawat, Varong Pavarajarn, Wiyong Kangwansupamonkon "SYNTHESIS OF SPHERICAL POROUS ALUMINA WITH PREFORMED SOL AND ASSISTED-TEMPLATE VIA SPRAY DRYING", Pure and Applied Chemistry International Conference (PACCON2012), Chiang Mai, Thailand, January 11-13, 2012.

2. Sukruthai Sapniwat, Apinan Soottitantawat, Varong Pavarajarn, Wiyong Kangwansupamonkon "SYNTHESIS OF POROUS γ-ALUMINA ASSISTED BY RESORCINOL-FORMALDEHYDE GEL", Nanothailand 2012, Khon Kaen, Thailand, April 9-12, 2012.